

BINARY VAPOR-LIQUID PHASE EQUILIBRIUM  
FOR METHANE AND CARBON MONOXIDE IN  
SELECTED HYDROCARBONS

By

SRINIVASA SRIVATSAN

Bachelor of Engineering (Honors)

Birla Institute of Technology  
and Science

Pilani, India

1985

Submitted to the Faculty of the  
Graduate College of the  
Oklahoma State University  
in partial fulfillment of  
the requirements for  
the Degree of  
MASTER OF SCIENCE  
December, 1991

BINARY VAPOR-LIQUID PHASE EQUILIBRIUM  
FOR METHANE AND CARBON MONOXIDE IN  
SELECTED HYDROCARBONS

Thesis Approved:

*K. M. Gassm*

Thesis Adviser

*Robert Robinson*

*David A. Lee*

*Thomas C. Collins*

Dean of the Graduate College

## PREFACE

This study details the binary vapor-liquid phase equilibrium for methane and carbon monoxide in selected hydrocarbons. The solubilities of methane and carbon monoxide were measured at temperatures from 104 to 302 °F and pressures to 104 bar in selected hydrocarbons. Binary interaction parameters have been obtained using the Soave-Redlich-Kwong and Peng-Robinson equations of state for each of the systems studied.

I extend my sincere thanks to my adviser, Dr. K. A. M. Gasem, for introducing me to this area of work and for his guidance during all stages of it. Dr. Gasem's dedication to teaching and research, his patience and understanding and enthusiasm have been an inspiration to all graduate students.

I would like to thank Dr. R. L. Robinson, Jr., for critical assessment of this work and for the time spent in explaining the subtleties of experimental and theoretical thermodynamics.

Dr. D. A. Tree, as the third member of my committee, has reviewed this work and his comments are greatly appreciated.

My friend, Dr. Naif Darwish deserves special thanks

for explaining me so very patiently the operation of the equipment and the various software packages used.

My greatest appreciation goes to my wife for her total understanding because of which I was able to devote so much time, which was rightfully hers, in the lab. My parents and parents-in-law have given me the moral encouragement at times when needed most. All of them have made my master's education one really worth achieving.

Finally, I would like to acknowledge the financial support received from the United States Department of Energy.

## TABLE OF CONTENTS

Chapter	Page
I. INTRODUCTION.....	1
II. LITERATURE REVIEW.....	3
Experimental Data.....	3
Experimental Apparatus.....	5
III. THERMODYNAMIC PRINCIPLES OF VAPOR-LIQUID EQUILIBRIUM.....	9
Phase Equilibrium Problem.....	9
SRK and PR Equations of State.....	12
IV. EXPERIMENTAL APPARATUS AND OPERATING PROCEDURE.....	14
Equilibrium Cell.....	14
Injection Pumps.....	16
Constant Temperature Baths.....	16
Pressure Measurements.....	17
Vacuum System.....	17
Storage Vessels.....	19
Fittings, Tubings and Valves.....	19
Chemicals.....	19
Experimental Procedure.....	19
V. ERROR ANALYSIS.....	22
Expected Uncertainty in Mole Fraction.....	31
Expected Uncertainty in Bubble Point Pressure.....	33
VI. BINARY VAPOR-LIQUID PHASE EQUILIBRIUM FOR METHANE + 1) TOLUENE, 2) N-HEXANE AND 3) N-DODECANE - RESULTS AND DISCUSSION.....	37
VII. BINARY VAPOR-LIQUID PHASE EQUILIBRIUM FOR CARBON MONOXIDE + HEAVY NORMAL PARAFFINS - RESULTS AND DISCUSSION.....	59
Effect of Carbon Number on Soave Interaction Parameters.....	81

Chapter	Page
Effect of Temperature on Soave Interaction Parameters.....	85
Predictions using EOS-Specific Critical Properties.....	88
VIII. CORRELATION OF CARBON MONOXIDE SOLUBILITIES IN NORMAL PARAFFINS.....	92
Model Evaluation.....	94
Generalization of Interaction Parameters....	100
IX. CONCLUSIONS AND RECOMMENDATIONS.....	106
Conclusions.....	106
Recommendations.....	107
BIBLIOGRAPHY.....	108
APPENDIXES.....	113
APPENDIX A - DENSITIES OF SOLVENTS USED IN THIS STUDY.....	114
APPENDIX B - TYPICAL OUTPUT OF PRESSURE CALIBRATION TEST.....	115
APPENDIX C - CRITICAL PROPERTIES AND ACENTRIC FACTORS OF NORMAL PARAFFINS SPECIFIC TO THE SRK EOS.....	116
APPENDIX D - SRK EOS REPRESENTATION OF CARBON MONOXIDE SOLUBILITY IN N-PARAFFINS USING EOS SPECIFIC CRITICAL PROPERTIES.....	117

## LIST OF TABLES

Table	Page
I. Literature References for Methane / Carbon Monoxide + Hydrocarbon Systems Used in This Study.....	4
II. Purities and Sources of Chemicals Used in This Study.....	20
III. Solubility Data for Carbon Dioxide + Benzene and Carbon Dioxide + n-Dodecane.....	24
IV. Solubility Data for Methane + n-Decane.....	25
V. Typical Volume of Solute Injected to Yield the Average Mole Fraction at the Selected Isotherm, along with the Uncertainty in Mole Fraction ( $\sigma_{x1}$ ).....	34
VI. Uncertainty in Bubble Point Pressure of the Binary Systems in This Study Estimated at the Average Composition of the Corresponding Isotherm.....	36
VII. Solubility Data for Methane + Toluene.....	38
VIII. Solubility Data for Methane + n-Hexane.....	40
IX. Solubility Data for Methane + n-Dodecane.....	42
X. Critical Properties and Acentric Factors Used in the SRK and PR Equations of State....	43
XI. SRK and PR Equation of State Representations of Solubility of Methane in Toluene.....	48
XII. SRK and PR Equation of State Representations of Solubility of Methane in n-Hexane.....	49
XIII. SRK and PR Equation of State Representations of Solubility of Methane in n-Dodecane.....	50
XIV. Solubility Data for Carbon Monoxide + n-Eicosane.....	60

Table	Page
XV. Solubility Data for Carbon Monoxide + n-Octacosane.....	61
XVI. Solubility Data for Carbon Monoxide + n-Hexatriacontane.....	62
XVII. Critical Properties and Acentric Factors Used in the SRK and PR Equations of State....	63
XVIII. SRK and PR Equation of State Representations of Carbon Monoxide Solubility in n-Eicosane. ....	71
XIX. SRK and PR Equation of State Representations of Carbon Monoxide Solubility in n-Octacosane.....	72
XX. SRK and PR Equation of State Representations of Carbon Monoxide Solubility in n-Hexatriacontane.....	73
XXI. Experimental Data for Carbon Monoxide + n-Paraffins Used in This Study.....	93
XXII. Specific Cases Used in EOS Model Evaluation....	95
XXIII. Critical Properties and Acentric Factors Used in Model Evaluation and Generalization.....	96
XXIV. Results of Model Evaluation for Carbon Monoxide + n-Paraffins using the SRK EOS.....	98
XXV. SRK EOS Optimum Interaction Parameters for Carbon Monoxide + n-Paraffins - Model Evaluation.....	99
XXVI. Specific Cases for Generalization of Interaction Parameters Using SRK EOS.....	101
XXVII. Results of Model Generalization Using SRK EOS for Carbon Monoxide + n-Paraffins .....	103
XXVIII. SRK EOS Optimum Interaction Parameters for Carbon Monoxide + n-Paraffins - Model Generalization.....	104

## LIST OF FIGURES

Figure	Page
1. Schematic Diagram of the Experimental Apparatus....	15
2. Details of Vacuum System.....	18
3. Comparison of Carbon Dioxide Solubilities in Benzene at 104 °F.....	26
4. Comparison of Methane Solubilities in n-Decane at 100 °F.....	27
5. Comparison of Methane Solubilities in n-Decane at 160 °F.....	28
6. Comparison of Methane Solubilities in n-Decane at 220 °F.....	29
7. Comparison of Carbon Dioxide Solubilities in n-Dodecane at 122 °F.....	30
8. Bubble Point Pressure Data for Methane + Toluene.....	44
9. Bubble Point Pressure Data for Methane + n-Hexane.....	45
10. Bubble Point Pressure Data for Methane + n-Dodecane.....	46
11. Comparison of Methane Solubilities in Toluene at 150 °F.....	52
12. Comparison of Methane Solubilities in Toluene at 302 °F.....	53
13. Comparison of Methane Solubilities in n-Hexane at 100 °F.....	54
14. Comparison of Methane Solubilities in n-Hexane at 160 °F.....	55
15. Comparison of Methane Solubilities in n-Hexane at 220 °F.....	56

Figure	Page
16. Comparison of Methane Solubilities in n-Dodecane.....	58
17. Bubble Point Pressure Data for Carbon Monoxide + n-Eicosane.....	65
18. Bubble Point Pressure Data for Carbon Monoxide + n-Octacosane.....	66
19. Bubble Point Pressure Data for Carbon Monoxide + n-Hexatriacontane.....	67
20. Bubble Point Pressure Data for Carbon Monoxide + n-Paraffins at 212 °F.....	69
21. Comparison of Carbon Monoxide Solubilities in n-Eicosane.....	75
22. Comparison of Carbon Monoxide Solubilities in n-Eicosane Using Lumped $C_{ij}$ and $D_{ij}$ .....	76
23. Comparison of Carbon Monoxide Solubilities in n-Octacosane.....	77
24. Comparison of Carbon Monoxide Solubilities in n-Octacosane Using Lumped $C_{ij}$ and $D_{ij}$ .....	78
25. Comparison of Carbon Monoxide Solubilities in n-Hexatriacontane.....	79
26. Comparison of Carbon Monoxide Solubilities in n-Hexatriacontane Using Lumped $C_{ij}$ and $D_{ij}$ ....	80
27. Soave Interaction Parameters $C_{ij}$ and $D_{ij}$ for Carbon Monoxide + n-Paraffins at 212 °F.....	82
28. Generalized Soave Interaction Parameters $C_{ij}$ and $D_{ij}$ for Carbon Monoxide + n-Paraffins at 212 °F.....	84
29. Soave Interaction Parameters $C_{ij}$ and $D_{ij}$ and Corresponding RMS Errors for Carbon Monoxide + n-Octacosane at 212 °F.....	86
30. Soave Interaction Parameter, $C_{ij}$ , and Corresponding RMS Errors for Carbon Monoxide + n-Paraffins at 212 °F.....	87
31. Soave Interaction Parameters $C_{ij}$ and $D_{ij}$ for Carbon Monoxide + n-Paraffins.....	89

Figure	Page
32. Soave Interaction Parameter, $C_{ij}$ , for Carbon Monoxide + n-Paraffins.....	90

## NOMENCLATURE

a	equation of state cohesive energy parameter
AAD	arithmetic average of the absolute values of the deviations of n observations about the mean
b	equation of state covolume parameter
BIAS	arithmetic average of deviations of n observations
CN	paraffin carbon number
$C_1, C_2, C_3$	correlation constants for $C_{ij}$
$C_{ij}$	equation of state binary interaction parameter
DEV	deviation of calculated value from experimental value, $X_{calc} - X_{exp}$
$D_1, D_2, D_3$	correlation constants for $D_{ij}$
$D_{ij}$	equation of state binary interaction parameter
$\hat{f}$	fugacity of a component in solution
$\bar{h}$	partial molar enthalpy
MAX	maximum absolute deviation
N	number of components in a system (phase rule)
n	moles of component or number of experimental observations
p	system pressure
R	universal gas constant
RMSE	root mean square error, $[\sum DEV^2/n]^{1/2}$
SS	objective function defined in Chapter III
$\bar{s}$	partial molar entropy
T	system temperature

$V$	system volume
$x$	liquid mole fraction
$y$	vapor mole fraction

#### Greek Symbols

$\gamma$	activity coefficient of component
$\Delta$	change in property
$\rho$	density of component
$\sigma$	standard error
$\hat{\phi}$	fugacity coefficient of component in solution
$w$	acentric factor

#### Subscripts

calc	calculated
exp	experimental
$i$	component or data point index
$l, L$	liquid
$v, V$	vapor

#### Superscripts

$l$	liquid
$v$	vapor
$o$	pure component

## CHAPTER I

### INTRODUCTION

Study of phase behavior of mixtures is important in the design and development of separation processes such as those encountered in petroleum refining, coal conversion and supercritical extraction. Since multiple phases occur in almost all stages involved in such processes, the proper description of phase behavior is important in each step of these processes.

This study deals with the experimental determination of the solubility of methane and carbon monoxide in selected hydrocarbons, i.e., given the pressure and temperature of a binary mixture (involving a solute gas and hydrocarbon solvent), the objective is to find the concentration (mole fraction) of the solute gas dissolved in the liquid phase. The solubilities of  $\text{CH}_4$  /  $\text{CO}$  have been studied over the temperature range 100–302 °F and pressures to 1504 psia for the following systems:

Methane: Toluene, n-Hexane, and n-Dodecane

Carbon monoxide: n-Eicosane ( $n\text{-C}_{20}$ ), n-Octacosane ( $n\text{-C}_{28}$ ),  
and n-Hexatriacontane ( $n\text{-C}_{36}$ )

The experimental data of this work together with the data

available in the literature for the same systems were analyzed using the Soave-Redlich-Kwong (SRK) and Peng-Robinson (PR) cubic equations of state. The ability of the cubic equations of state in representing these systems was evaluated and binary interaction parameters obtained for each of the systems studied.

The choice of methane and carbon monoxide as the solute gases was based on the important binary mixtures encountered in coal liquefaction processes and partly by the scarcity of vapor-liquid equilibrium data of carbon monoxide with heavy normal paraffins. In addition, carbon monoxide is one of the main constituents of synthesis gas and plays an important role in water-gas shift reactions.

Only binary mixture solubilities have been studied because of the usefulness of binary data in correlation development and testing. In general, all state-of-the-art models for vapor-liquid equilibrium describe the unlike molecule interactions using one to three parameters. The mixing rules in such models describe the unlike molecule interactions solely in terms of parameters that reflect pairwise interactions and which are obtained from data on binary mixtures. Therefore, a systematic study of a series of carefully selected binary systems will allow the resultant model parameters to be generalized and permit estimation of parameters for systems which have not been measured.

## CHAPTER II

### LITERATURE REVIEW

A comprehensive literature survey including Chemical Abstracts, major data compilations (such as Wichterle, et al. [1]), and several specialized journals was conducted concerning the solubility of methane and carbon monoxide in hydrocarbons. The search was focused mainly on two areas concerning this study: (1) experimental vapor-liquid equilibrium (VLE) data involving binary mixtures of methane and carbon monoxide with hydrocarbons and (2) experimental methods which have been used in VLE data acquisition for the last ten years.

#### Experimental Data

While several investigators have compiled references for VLE data on methane + light hydrocarbons [1-5], no data relevant to this study are available on the solubility of methane in n-dodecane. Further, data on the solubility of carbon monoxide in heavy normal paraffins at temperatures of interest to this work are limited to a solitary article [6]. Literature sources available on binary systems investigated in this study and suitable for comparison purposes are presented in Table I.

TABLE I  
LITERATURE REFERENCES FOR METHANE /  
CARBON MONOXIDE + HYDROCARBON  
SYSTEMS USED IN THIS STUDY

System	Temperature Range, °F	CH <sub>4</sub> / CO Mole Fraction Range	Reference Number
CH <sub>4</sub> + n-C <sub>6</sub>	100 - 220	0.16 - 0.30	37
	100 - 220	0.12 - 0.29	38
	122 - 212	0.03 - 0.35	39
	100 - 220	0.19	40
CH <sub>4</sub> + Toluene	150	0.02 - 0.25	35
	302	0.04 - 0.19	36
CO + n-C <sub>20</sub>	212 - 392	0.02 - 0.12	6
CO + n-C <sub>28</sub>	212 - 392	0.02 - 0.13	6
CO + n-C <sub>36</sub>	212 - 392	0.03 - 0.17	6

## Experimental Apparatus

The constant demand by industry for phase equilibrium data at elevated pressures needed for the proper design, operation and optimization of various processes has prompted the continued development of experimental techniques in VLE determination. In the last few years, several methods for experimental investigation of high pressure phase equilibria have been proposed. A review covering the 1970's is given by Eubank [7] and more recent reviews are given by Fornari [4] and Deiters [8].

The experimental techniques used to evaluate multiphase equilibria can be classified by:

- 1) the method employed to determine equilibrium compositions,
- 2) techniques used to achieve equilibrium conditions,
- and 3) methods employed to find points of phase transitions such as bubble and dew point conditions.

Methods employed to determine compositions include analytical or direct sampling methods (DSM) and synthetic or indirect methods. Sampling of the coexisting phases following attainment of equilibrium is necessary when using the analytical methods. Among the difficulties in using analytical methods while studying high pressure phase equilibria is sample preservation. Care should be taken so that the sample withdrawn for analysis closely represents the equilibrium state since separation of components may

result from a small change in temperature or pressure during sampling. The sampling methods, however, are used extensively for phase equilibrium analysis [8-24].

Synthetic methods involve an indirect determination of equilibrium compositions using stoichiometry. The overall compositions are known since specific amounts of the chemical species of interest are mixed, and hence no sampling is necessary. The method is relatively inexpensive and is widely used in phase equilibria investigations [25-32], especially when one of the components is low in volatility like the heavy hydrocarbons. Fontalba, et al. [27] have used an in-situ determination of fluid volumes to determine equilibrium mole fractions.

Equilibrium conditions are achieved either by using a static cell [9-12,16,21,23-29,31,32] or a dynamic method like continuous flow (CF) [18-20] or fluid recirculation [13-17,22,33,34]. Static methods use constant [9,10-12,23,24] or variable volume cells [9,16,21,25-29,31,32]. The mixture volume in the equilibrium cell can be varied either by using a piston cylinder assembly or by using mercury as an incompressible, involatile fluid piston. The use of mercury also enhances the mixing during agitation of the cell. Sometimes bellows are used to vary the volume in the equilibrium cell [9,28].

In a continuous flow apparatus, the solute gas and the solvent are first compressed and mixed. The mixture is then heated to the desired temperature before being injected into

the equilibrium cell where phase separation occurs. Sampling of the coexisting phases is done following phase separation. The time needed to reach steady state with constant effluent stream compositions depends on the system. This method has been in use extensively in the last few years.

Recirculation methods involve passing of a vapor or a liquid stream or both through a recirculation loop and measuring the vapor and liquid compositions by flashing the mixture to be sampled. A detailed reference to articles which provide information about equipment and methods used in the different experimental techniques is given by Fornari [4].

Bubble point determinations use either a visual [30-32,19,21-24] or a graphical technique [9,21,25-28,31]. In a visual cell, phase separations can be observed directly, eliminating the possibility of overlooking the formation of multiple equilibrium phases. The graphical technique uses the discontinuity in a pressure-volume curve as the system passes from a two-phase to an all-liquid condition.

The experimental technique used in this study is a synthetic one involving a variable-volume static cell. The bubble point pressure of a synthetically prepared binary mixture is identified graphically utilizing the discontinuity in compressibility of the mixture as it crosses the liquid-two phase boundary. This method, thus,

consists of the introduction of known amounts of well degassed pure components into a variable-volume thermostated equilibrium cell. The volume of the cell is varied by the introduction or withdrawal of mercury. Mechanical agitation of the equilibrium cell, required to ensure attainment of equilibrium is accomplished by rocking the cell from 45 degrees below horizontal level to 45 degrees above horizontal. Attainment of equilibrium in a reasonable time was ensured by the introduction of steel balls (slightly smaller in diameter than that of the equilibrium cell) into the cell.

## CHAPTER III

### THERMODYNAMIC PRINCIPLES OF VAPOR-LIQUID EQUILIBRIUM

This chapter gives a brief overview of the vapor-liquid phase equilibrium problem. The main emphasis is on the use of a single equation of state for both phases. For a more detailed review, the reader is referred to fundamental texts on phase equilibria [41-46].

#### Phase Equilibrium Problem

The phase equilibrium problem as typically applied to separation processes deals with a multicomponent system of  $N$  non-reacting chemical species for which the phase rule variables are  $T$ ,  $P$ ,  $N-1$  liquid mole fractions and  $N-1$  vapor mole fractions. Application of the phase rule indicates the availability of  $N$  degrees of freedom. Therefore, at equilibrium only  $N$  of the  $2N$  variables are independent. Once  $N$  phase rule variables are specified, the remaining variables can be determined, in principle, by simultaneous solution of the  $N$  equilibrium relations of the form

$$\hat{f}_i^v = \hat{f}_i^l \quad (i = 1, \dots, N) \quad (1)$$

where the superscripts  $v$  and  $l$  denote the vapor and liquid

phases.

In practice, one usually specifies  $T$  or  $p$  and either the liquid phase or the vapor phase composition, fixing  $N$  phase rule variables. For the solution of the remaining  $N$  variables, Equation (1) is rewritten to relate the fugacity of each component to the temperature, pressure and composition.

The defining expression for the fugacity is written as

$$\hat{f}_i^V = py_i\hat{\phi}_i^V \quad i = 1, N \quad (2)$$

$$\hat{f}_i^L = px_i\hat{\phi}_i^L \quad i = 1, N \quad (3)$$

for vapor and liquid phase, respectively. Thus Equation (1) becomes

$$y_i\hat{\phi}_i^V = x_i\hat{\phi}_i^L \quad (4)$$

Neither  $y_i$  nor  $x_i$ , which appear in the equilibrium relation are explicit, because the  $\hat{\phi}_i$ 's are functions of composition as well as  $T$  and  $p$ . To express  $\hat{\phi}_i$ 's analytically as functions of  $T$ ,  $p$  and composition requires an equation of state which adequately represents the volumetric properties of both the liquid and vapor phases throughout the range of temperatures, pressures and composition of interest.

Given an equation of state, the following expression [41], provides for the fugacity coefficients,  $\hat{\phi}_i$ 's in terms of  $T$ ,  $V$  and composition:

$$\ln \hat{\phi}_i = (1/RT) \int_V^{\infty} [(\partial p / \partial n_i)_{T,V,n_j} - (RT/V)] dV - \ln Z \quad (5)$$

where  $n_i$  signifies the number of moles of component  $i$ ,  $V$  is the total volume of either liquid or vapor mixture and  $Z$  is the compressibility factor of the mixture. The subscript  $n_j$  in Equation (5) signifies that all mole numbers except  $n_i$  must be held constant.

Sometimes, for mixtures containing polar fluids or electrolytes, the equation of state is used for the vapor phase only and the activity coefficient,  $\gamma_i$ , is used in the liquid phase to express deviations from ideal liquid solution behavior:

$$\frac{\hat{f}_i^l}{x_i f_i^o} = \gamma_i \quad (6)$$

or alternately,

$$\hat{f}_i^l = \gamma_i x_i f_i^o \quad (7)$$

where  $f_i^o$  is the standard state fugacity of species  $i$  at the system temperature and pressure.

Although the use of either method has certain advantages and disadvantages, the use of a single equation of state is considered thermodynamically more efficient, especially when dealing with supercritical fluids. Further, restricting the predictive capabilities to non-polar, non-associative fluids, the use of a single equation of state method becomes an attractive alternative for phase

behavior predictions.

### SRK and PR Equations of State

Two equations of state used widely in industry are the Soave-Redlich-Kwong (SRK) [47] and Peng-Robinson (PR) [48] equations of state.

The pressure-explicit form of the SRK equation is:

$$P = \frac{R T}{V - b} - \frac{a(T)}{V (V + b)} \quad (8)$$

where:

$$a(T) = a_C \alpha(T) \quad (9)$$

$$a_C = 0.42747 R^2 T_C^2 / P_C \quad (10)$$

$$b = 0.08664 R T_C / P_C \quad (11)$$

$$\alpha = [1 + k (1 - T_r^{0.5})]^2 \quad (12)$$

$$k = 0.48508 + 1.55171 w - 0.15613 w^2 \quad (13)$$

The pressure-explicit form of the PR equation of state is:

$$P = \frac{R T}{V - b} - \frac{a(T)}{V^2 + 2 b V - b^2} \quad (14)$$

where:

$$a(T) = a_C \alpha(T) \quad (15)$$

$$a_C = 0.45724 R^2 T_C^2 / P_C \quad (16)$$

$$b = 0.07780 R T_C / P_C \quad (17)$$

$$\alpha = [1 + k (1 - T_r^{0.5})]^2 \quad (18)$$

$$k = 0.37464 + 1.54226 w - 0.26992 w^2 \quad (19)$$

To apply the SRK or PR equations of state to mixtures the values of "a" and "b" are determined using the mixing rules

$$a_m = \sum \sum z_i z_j (1 - C_{ij}) (a_i a_j)^{0.5} \quad (20)$$

$$b_m = 0.5 \sum \sum z_i z_j (1 + D_{ij}) (b_i + b_j) \quad (21)$$

In Equations (20) and (21),  $C_{ij}$  and  $D_{ij}$  are empirical binary interaction parameters characterizing the binary interactions between components 'i' and 'j'. Values of these parameters are typically determined by fitting experimental binary solubility data to minimize the objective function, SS, which is the weighted-sum-of-squared errors in predicted bubble point pressures

$$SS = \sum \frac{(p_{i \text{ exp}} - p_{i \text{ calc.}})^2}{\sigma_{ip}^2} \quad (22)$$

where  $\sigma_{ip}$  is the uncertainty in the measured pressure (see Error Analysis, Chapter V) and the summation is over the number of data points. Further details of the data reduction techniques employed in this study are given by Gasem [26].

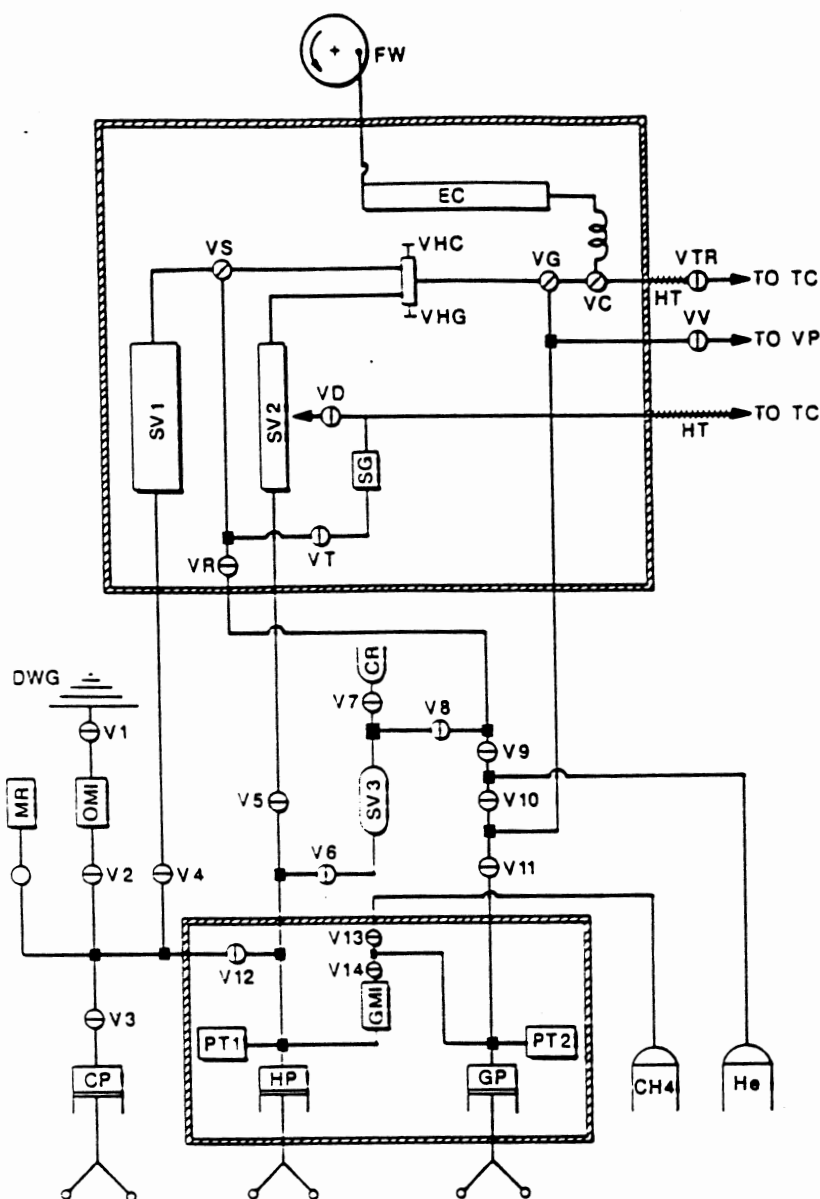
## CHAPTER IV

### EXPERIMENTAL APPARATUS AND OPERATING PROCEDURE

The experimental apparatus used in this study employs a variable-volume, static type blind equilibrium cell for determination of bubble point pressure for synthetically prepared mixtures of the solute gas and the respective solvents, which are in some cases solids at room temperature. An extensive description of the apparatus and a step-by-step procedure for the operation is given by Darwish [49]. No modifications have been made to this apparatus during the course of this study. The identification of the bubble point pressure is achieved by following the compressibility of the mixture as it changes abruptly across the liquid phase boundary. The general schematic of the apparatus is shown in Figure 1 and a brief description of the main components is given below.

#### Equilibrium Cell

This is the principal component of the apparatus and is a variable-volume, rocking type cell (EC). It is a 316 SS tubular reactor with an internal volume of 12.5 cc, length of 10 in, ID of 5/16 in and OD of 9/16 in. One end of the



CP : Cleaning Pump	OMI: Oil-Mercury Interface
CR : Cleaning Reservoir	PT1: Pressure Transducer
DWG: Dead Weight Gauge	PT2: Pressure Transducer
EC : Equilibrium Cell	SG : Sight Glass
FW : Fly Wheel	SV1: Storage Vessel
GMI: Gas-Mercury Interface	SV2: Storage Vessel
GP : Gas Pump	SV3: Storage Vessel
HP : Hydrocarbon Pump	TC : Trash Can
HT : Heating Tape	VP : Vacuum Pump
MR : Mercury Reservoir	

Figure 1. Schematic Diagram of the Experimental Apparatus

equilibrium cell is pivoted and welded to a 1/16 in OD stainless steel tubing through which injections of solvent, solute and mercury are made to the cell. The other end of the cell is plugged and connected to an aluminum drive wheel (FW) which is, in turn, driven by a 1/50 HP variable speed motor, giving the cell a rocking motion. Five steel balls 3/16 in diameter are placed inside the cell to promote mixing between the solute and the solvent. The effective volume of the cell can be varied by the introduction and withdrawal of mercury using a screw pump.

#### Injection Pumps

Three pumps are used in the experimental set up. A 10 cc positive displacement pump (HP) is used for injecting the exact amount of solvent as well as for injecting and withdrawing the mercury from the cell. Solute gas is injected using a 25 cc positive displacement pump (GP). Each of these pumps is rated to 10000 psi and has a resolution of 0.005 cc. A third pump, used mainly for cleaning purposes and for operations where accuracy is not crucial is a 500 cc positive displacement pump with a resolution of 0.02 cc.

#### Constant Temperature Baths

Two air baths are used in the operation of this apparatus. One houses the equilibrium cell, storage vessels (SV1 and SV2) and miscellaneous fittings, tubings and

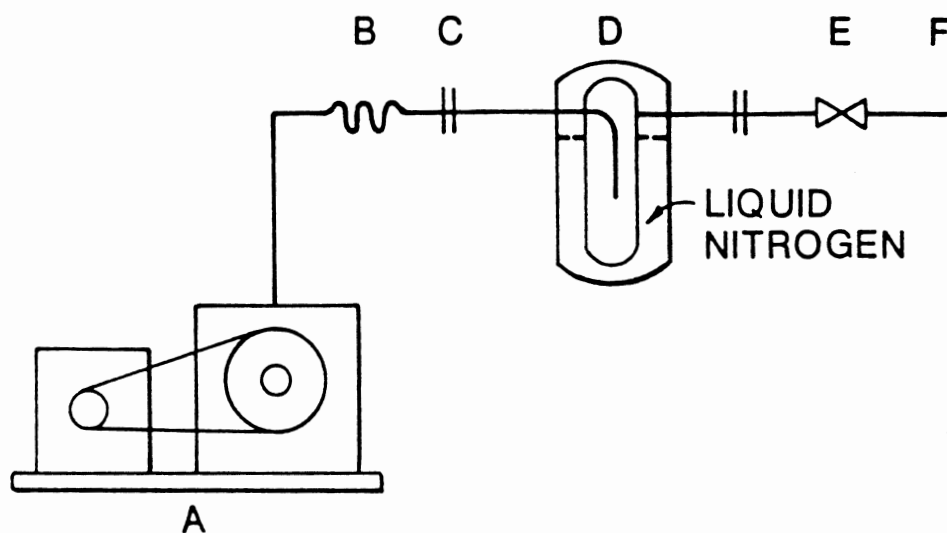
valves. The other bath, made of 1/2 in plywood, houses the two injection pumps (HP and GP) and pressure transducers (PT1 and PT2). The temperature in this bath is kept constant at 50 °C. Two proportional-integral controllers are used (one in each bath) to maintain the temperature within 0.1 °C of the set point temperature. The temperatures in the bath are measured using platinum resistance thermometers connected to a digital readout having a resolution of 0.01 °C.

### Pressure Measurements

The pressure in the equilibrium cell is transmitted to pressure transducer (PT1) through lines filled with mercury. A second transducer (PT2) is used to measure the solute gas pressure directly from the gas injection pump (GP). The pressure transducers have a range from 0 - 3000 psi and are calibrated regularly using a dead weight tester. Pressure measurements are displayed on digital readouts having a resolution of 0.1 psi.

### Vacuum System

The major components of the vacuum system are shown in Figure 2. Pressures down to 50 millitorr are achieved using a mechanical vacuum pump (VP). A glass trap (GT) immersed in liquid nitrogen is used to trap condensable materials and prevent them from reaching the vacuum pump. A vacuum gage (VG) is installed to monitor the vacuum process.



- A. MECHANICAL VACUUM PUMP
- B. CAJON FLEXIBLE BELLOWS TUBING
- C. ULTRA-TORR UNIONS
- D. GLASS COLD TRAP
- E. SHUTOFF VALVE
- F. CONNECTION TO DEGASSING ASSEMBLY

Figure 2. Details of Vacuum System

### Storage Vessels

The most important vessel used is for solvent storage (SV1). This is a high pressure reactor used to store the degassed solvent at the operating temperature of the experiment for several runs. Other vessels used include a 500 cc aluminum vessel (TC1) for solvent disposal, a 250 cc mercury reservoir (MR), an 8 cc stainless steel vessel (SV2) and a 250 cc stainless steel vessel (SV3) used during clean up.

### Fittings, Tubings and Valves

All fittings, tubings and valves used in the apparatus are made of 316 stainless steel supplied by the High Pressure Equipment Company. Sizes of tubings include 1/16, 1/8 and 1/4 in. rated for 15000 psi.

### Chemicals

All chemicals used in this study were provided by commercial suppliers. No further purification of the chemicals was attempted. The chemicals studied in this work, along with their reported purities and suppliers, are presented in Table II.

### Experimental Procedure

Following is a brief description of the procedure used in this study. Injection of degassed solvent into the

TABLE II  
PURITIES AND SOURCES OF CHEMICALS  
USED IN THIS STUDY

Chemicals	Source	Purity (mol%)
Methane	Big 3 Industries, Inc.	99.97+
Carbon Monoxide	Matheson Gas Products	99.99+
Carbon Dioxide	Union Carbide Corpn.	99.99+
Toluene	E.M. Science Company	99.90
n-Hexane	Aldrich Chemical Company	99.00+
n-Dodecane	Alfa Products	99.00
n-Eicosane	Aldrich Chemical Company	99.00+
n-Octacosane	Alfa Products	99.00
n-Hexatriacontane	Aldrich Chemical Company	98.00

equilibrium cell (EC) is done by injecting mercury at the bottom of the solvent cylinder (SV1), thus displacing an equal quantity of solvent into the rocking cell. The solute gas is taken into the gas pump (GP) housed in a constant temperature air bath. The pressure of the solute can be set to the desired pressure of injection. Sequential injections of solute are then made from the gas pump. The injected volumes of solute gas and solvent are metered from the precision screw pumps (HP and GP) maintained at a constant temperature. After each injection of solute into the solvent in the rocking cell, the bubble point pressure of the mixture is determined as follows. Known amounts of mercury are injected sequentially into the equilibrium cell to alter the system volume. After each injection of mercury, the cell is rocked to bring the system to equilibrium and the pressure recorded. The bubble point pressure is located by observing the break point in a pressure-volume curve as the system passes from a two-phase to an all-liquid condition. The typical result of such a static experiment is an isothermal  $p$ - $x$  phase diagram. Good mixing was obtained using the rocking cell, as revealed by the equilibration time. For systems using methane as the solute gas, the equilibration time was less than 5 minutes while systems involving carbon monoxide as the solute gas required about 10 minutes to attain equilibrium.

## CHAPTER V

### ERROR ANALYSIS

Two types of errors commonly encountered during experimental measurements are systematic errors and random errors. Systematic errors are due to flaws in the experimental procedure, erroneous calibration of data recording devices and other such causes. Random errors result from unavoidable small disturbances in the experimental conditions. While random errors can be treated in a statistical fashion, systematic errors must be remedied by eliminating erroneous methods of measurement and identifying other causes, if any. This chapter details the steps taken in this study to minimize the sources of errors. An error propagation study was conducted to estimate the experimental uncertainty in the solute mole fraction and bubble point pressure of the mixture for each of the systems studied.

In this study, systematic errors were minimized by routine calibration of pressure gauges against a dead weight tester and calibrating temperature measuring elements by conducting water ice point and boiling point tests. A typical output of the result of pressure calibration test is shown in Appendix B.

External reproducibility tests were also conducted. Vapor pressure of pure ammonia at a selected temperature was measured and compared with experimental values reported in the literature. The measured vapor pressure of this work and the reported literature value [50] agreed within 0.60 psi at 325 K. In addition, solubility data were measured on three systems for which data exist: carbon dioxide + benzene, methane + n-decane and carbon dioxide + n-dodecane. These systems were chosen as test systems to verify the integrity of the apparatus and procedures employed. Data of this work on these systems are presented in Tables III and IV. Comparison of this work with other investigators appear in Figures 3-7. The comparisons are shown in terms of deviations in solubilities from values predicted using the Soave-Redlich-Kwong (SRK) equation of state. Interaction parameters employed in the equation of state prediction were obtained by minimizing the sum of squares of pressure deviation from the experimental values of this work. Detailed procedure for data reduction is given by Gasem [26].

The data for carbon dioxide + benzene are in good agreement with the data reported by Gasem [26] and Gupta [51] (solubility deviations within the combined uncertainties of the two data sets) and in reasonable agreement with Anderson's [52] data. The methane + n-decane data are in excellent agreement with the earlier work of Darwish [49] and in reasonable agreement with those of

TABLE III  
SOLUBILITY DATA FOR CARBON DIOXIDE + BENZENE  
AND CARBON DIOXIDE + N-DODECANE

Mole Fraction Carbon Dioxide	Bubble Point Pressure bar	Pressure (psia)
CO <sub>2</sub> + Benzene at 313.2 K (40.0 °C, 104.0 °F)		
0.0999	12.8	(185)
0.2254	26.4	(383)
0.3252	36.2	(524)
0.4244	44.1	(640)
CO <sub>2</sub> + n-Dodecane at 323.2 K (50.0 °C, 122.0 °F)		
0.0766	7.8	(113)
0.1153	11.7	(172)
0.2025	21.5	(312)
0.3107	34.2	(497)
0.4059	46.1	(669)

TABLE IV  
SOLUBILITY DATA FOR METHANE + N-DECANE

Mole Fraction Methane	Bubble Point Pressure	
	bar	(psia)
-----310.9 K (37.8 °C, 100.0 °F)-----		
0.0748	16.1	(233)
0.1329	29.7	(430)
0.2086	49.2	(714)
0.2520	61.8	(896)
0.2771	69.5	(1008)
-----344.3 K (71.1 °C, 160.0 °F)-----		
0.0531	13.0	(189)
0.1520	39.2	(569)
0.2113	56.9	(825)
0.2771	77.7	(1126)
-----377.6 K (104.4 °C, 220.0 °F)-----		
0.0568	15.0	(218)
0.1511	42.1	(611)
0.2113	61.0	(885)
0.2384	70.7	(1025)

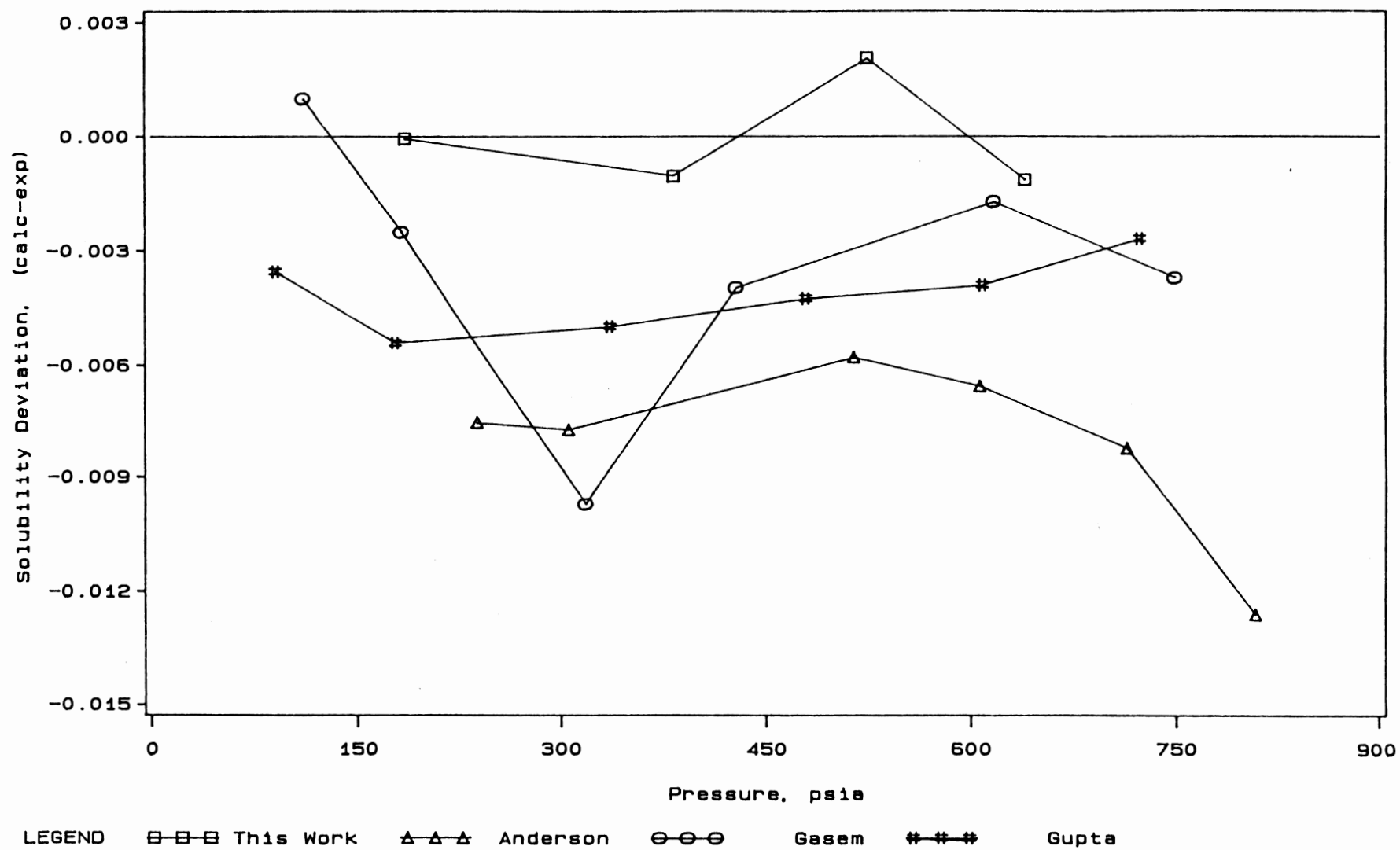


Figure 3. Comparison of Carbon Dioxide Solubilities in Benzene at 104 F

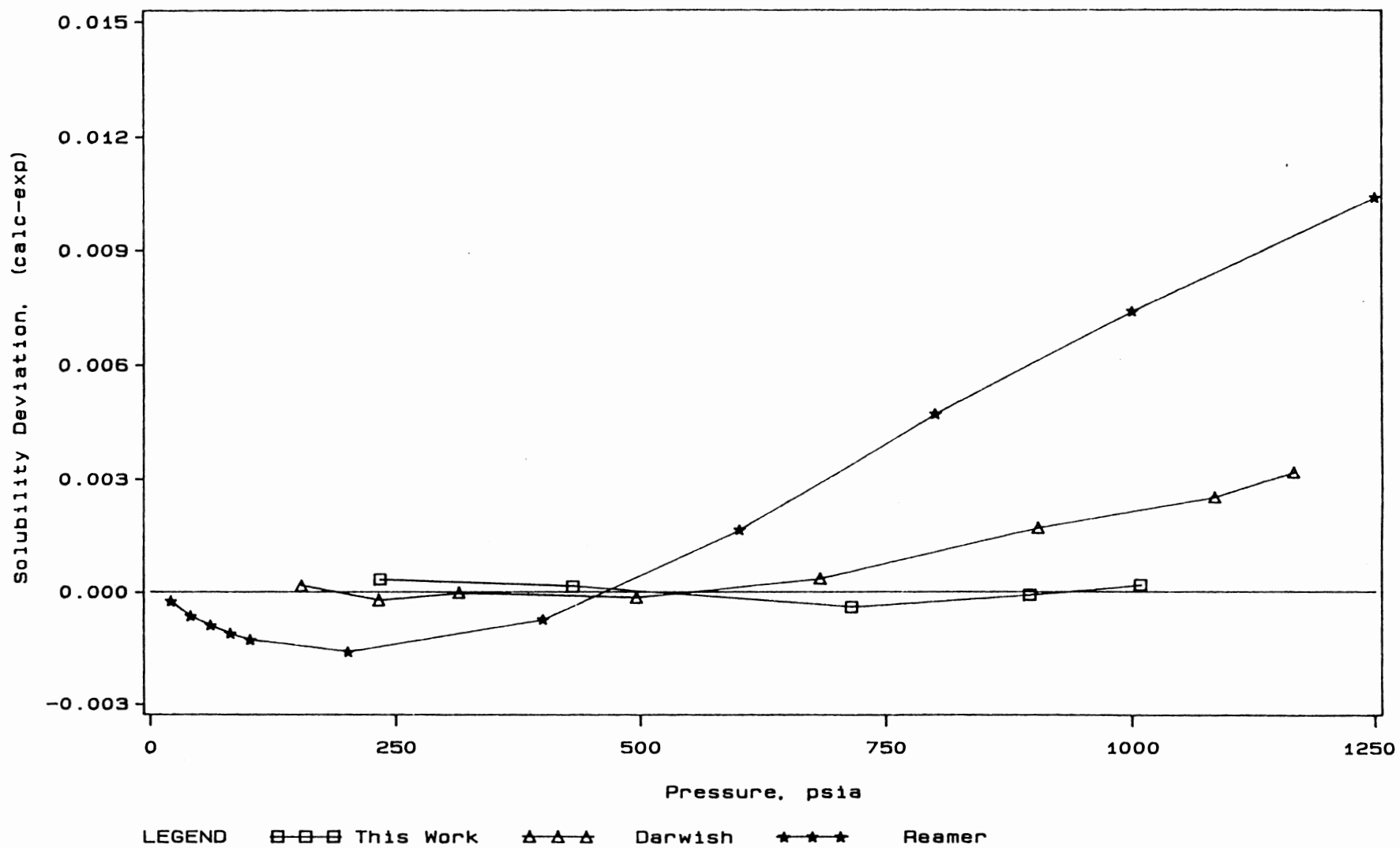


Figure 4. Comparison of Methane Solubilities in n-Decane at 100 F

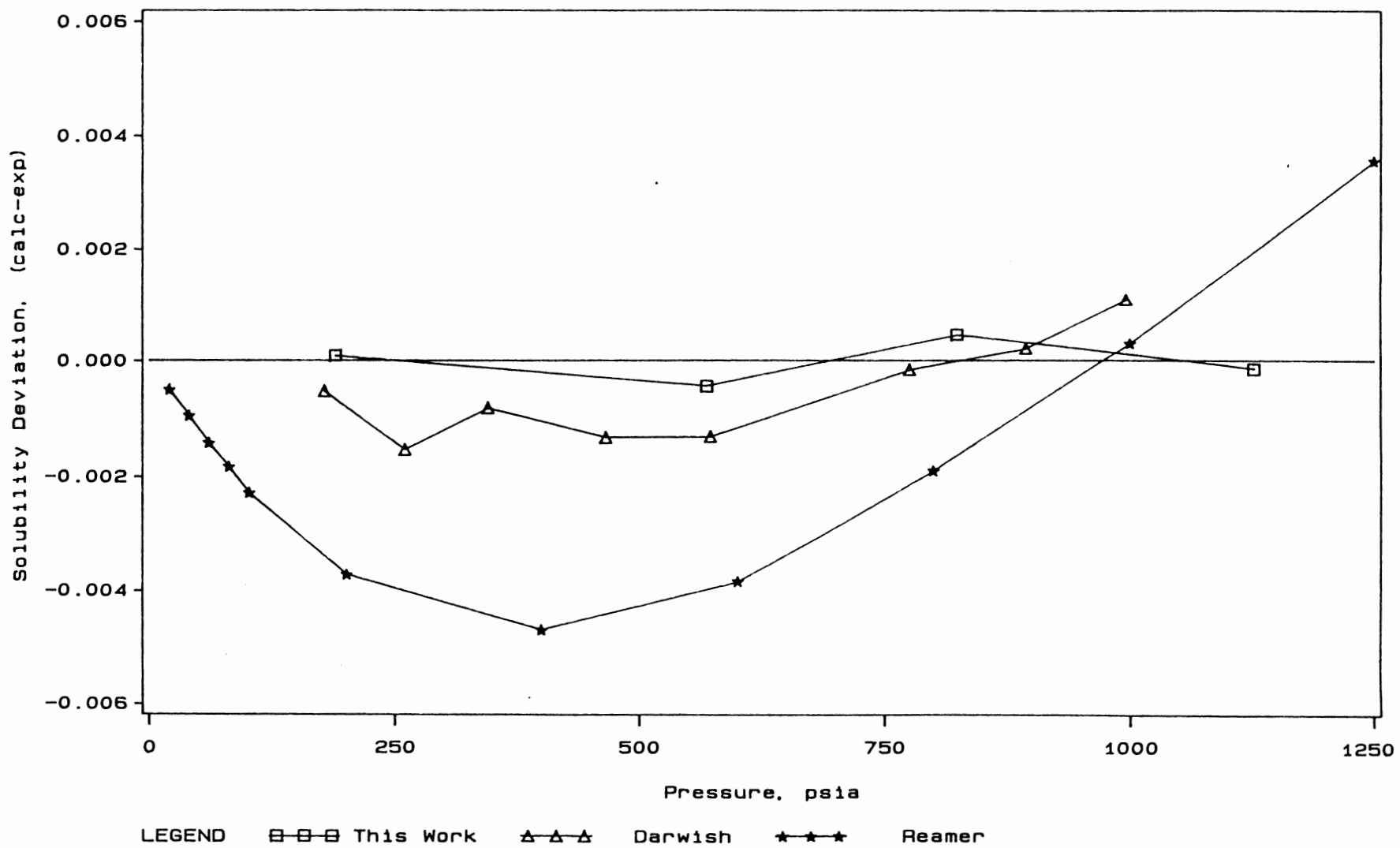


Figure 5. Comparison of Methane Solubilities in n-Decane at 160 F

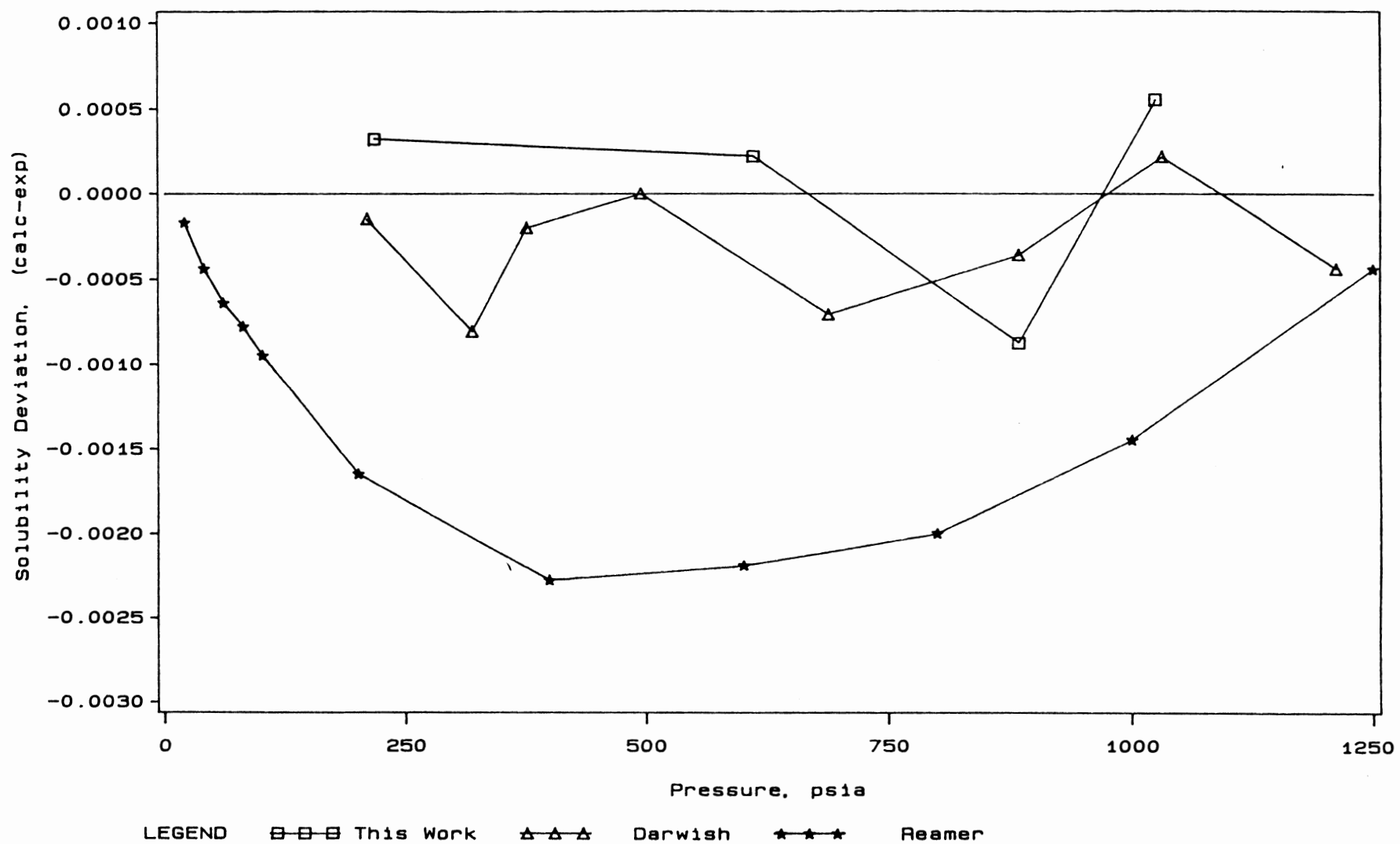


Figure 6. Comparison of Methane Solubilities in n-Decane at 220 F

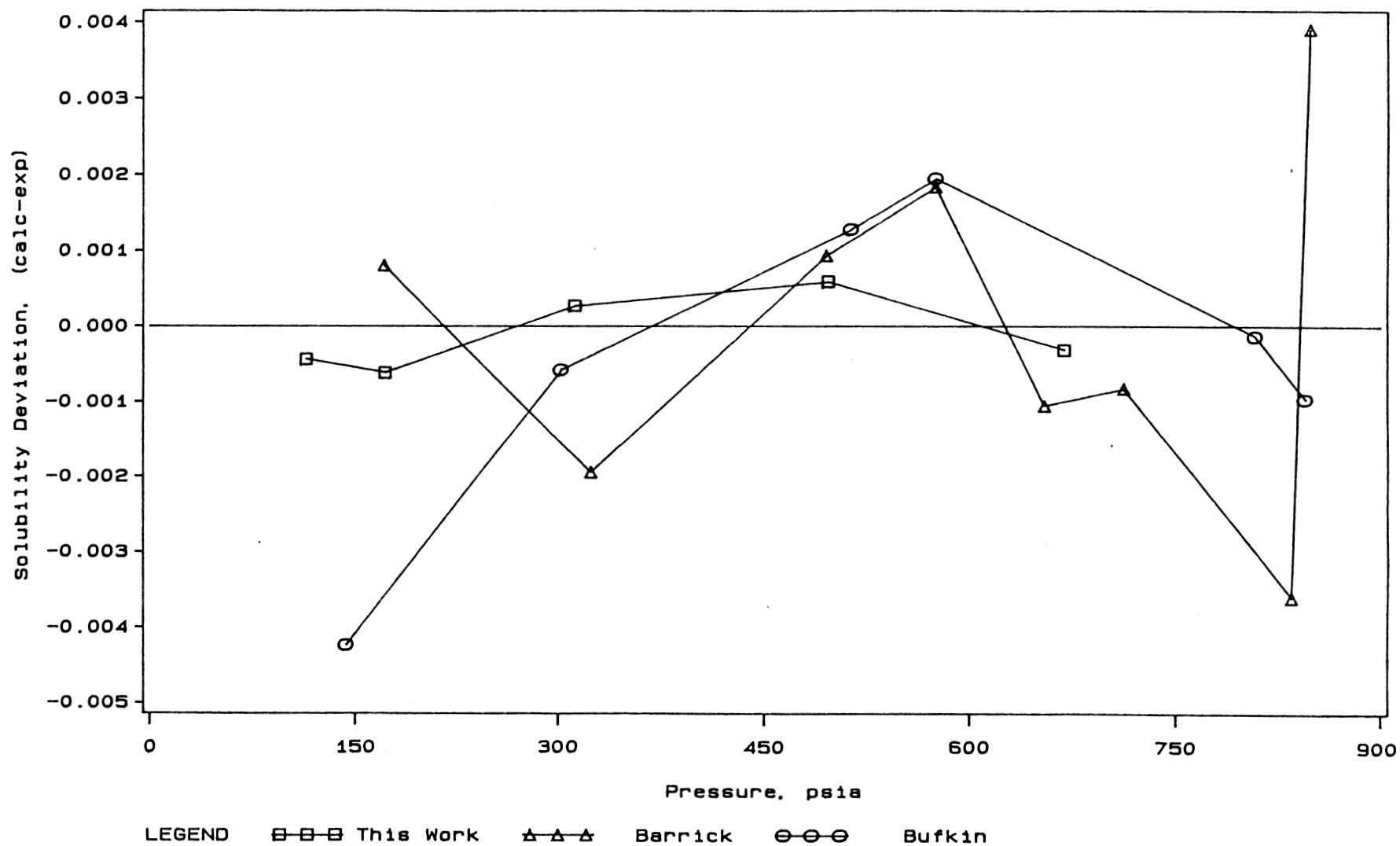


Figure 7. Comparison of Carbon Dioxide Solubilities in n-Dodecane at 122 F

Reamer [53] at all three isotherms of study. Similarly, the comparison of carbon dioxide solubilities in n-dodecane with Barrick [54] and Bufkin [55] confirm the present measurements at 122 °F within the combined uncertainties in the three data sets. The combined comparisons described were taken as confirmation of the proper operation of the present apparatus and procedures.

Random errors give rise to a concept of uncertainty in each measurable variable. Uncertainty is an interval around the measured value of the variable within which the true value could exist. In general, for any observable  $Y$  that depends on the measured independent variables  $X_1, X_2, \dots, X_n$  according to the functional relation

$$Y = f(X_1, X_2, \dots, X_n), \quad (1)$$

the expected uncertainty,  $\sigma_Y$ , assuming (1) absence of any covariance and (2) linear variation for  $\partial Y / \partial X$  ( $\partial Y / \partial X \gg \partial^2 Y / \partial X^2 + \dots$ ), is given by [56]

$$\sigma_Y^2 = (\partial Y / \partial X_1)^2 (\sigma_{X_1})^2 + (\partial Y / \partial X_2)^2 (\sigma_{X_2})^2 + \dots + (\partial Y / \partial X_n)^2 (\sigma_{X_n})^2 \quad (2)$$

If the variable "Y" is also measurable, the square of the instrumental error " $\epsilon_Y$ " must be added to the right side of Equation (2).

#### Expected Uncertainty in Mole Fraction

Mole fraction in a multicomponent mixture is defined as

$$x_i = n_i / \sum n_i \quad (3)$$

where,  $x_i$  is the mole fraction and  $n_i$  is the number of moles of species 'i'. The summation is over all species present in the mixture. For a binary mixture we thus have

$$x_1 = n_1 / (n_1 + n_2) \quad (4)$$

The subscripts 1 and 2 refer to the solute and solvent respectively. Since the number of moles equals the product of molar density and volume injected, Equation (4) can be written as:

$$x_1 = \frac{\sum \rho_{1i} V_{1i}}{\sum \rho_{1i} V_{1i} + \rho_2 V_2} \quad (5)$$

The summation in Equation (5) is over the number of gas injections which produces the mole fraction  $x_1$ . The solvent injection is done only once. If the gas is injected at the same temperature and pressure each time, Equation (5) reduces to

$$x_1 = \frac{\rho_1 \sum V_{1i}}{\rho_1 \sum V_{1i} + \rho_2 V_2} \quad (6)$$

Making use of Equation (2) to define the uncertainty in  $x_1$  and taking derivatives, we get after some rearrangement

$$\sigma_{x_1}^2 = x_1^2 x_2^2 \left[ (\sigma \rho_1 / \rho_1)^2 + (\sigma \rho_2 / \rho_2)^2 + (\sigma V_2 / V_2)^2 + n (\sigma V_{1i} / \sum V_{1i})^2 \right] \quad (7)$$

where  $n$  is the number of gas injections needed to produce a mole fraction  $x_1$ . To estimate the uncertainty of solute mole fraction in each of the solvents considered in this study using Equation (7), values are needed for each term in the parenthesis for a certain mole fraction  $x_1$ .

Conservative estimates are made for the various variables as follows:

$(\sigma_{\rho_1}/\rho_1) = 0.0015$	(Relative uncertainty in the solute densities)
$(\sigma_{\rho_2}/\rho_2) = 0.0015$	(Relative uncertainty in solvent density)
$(\sigma_{V_2}/V_2) = 0.0013$	(Relative uncertainty in solvent volume assuming an uncertainty of 0.0075cc in solvent injection pump and 6 cc of solvent injection)
$\sigma_{V_{1i}} = 0.0075$ cc	(Uncertainty in gas injection pump)

An estimate of the last term in Equation (7) is assumed by calculating the volume of gas needed to give a certain mole fraction of solute  $x_1$ , at any temperature using Equation (6). These data along with the computed uncertainties in mole fraction,  $\sigma_{x_1}$ , are shown in Table V.

#### Expected Uncertainty in Bubble Point Pressure

Bubble point pressure of a given binary mixture is a function of the temperature and composition of the mixture. The uncertainty in pressure ( $\sigma_{bp}$ ) using Equation (2) is given by:

TABLE V

TYPICAL VOLUME OF SOLUTE INJECTED TO YIELD THE  
AVERAGE MOLE FRACTION AT THE SELECTED  
ISOTHERM, ALONG WITH THE UNCERTAINTY  
IN MOLE FRACTION ( $\sigma_{x1}$ )

System (Temperature, °F)	Mole Fraction	Solute Volume, cc	$n(\sigma_V/V)^2$	$\sigma_{x1}^*$ (Eqn. (7))
CH <sub>4</sub> + Toluene (150.0)	0.1204	3.3	1.0E-05	0.0004
CH <sub>4</sub> + n-C <sub>6</sub> (160.0)	0.2216	4.8	7.4E-06	0.0006
CH <sub>4</sub> + n-C <sub>12</sub> (212.0)	0.2020	2.6	1.7E-05	0.0008
CO + n-C <sub>20</sub> (212.0)	0.0899	1.5	4.7E-05	0.0006
CO + n-C <sub>28</sub> (212.0)	0.0876	1.0	1.2E-04	0.0009
CO + n-C <sub>36</sub> (212.0)	0.1190	1.3	6.6E-05	0.0009

\* The uncertainty in mole fraction has been calculated  
assuming an average value of 6cc for solvent injection.

$$(\sigma_{bp})^2 = (\epsilon_p)^2 + (\partial P / \partial x_1)^2 (\sigma_{x_1})^2 + (\partial P / \partial T)^2 (\sigma_T)^2 \quad (8)$$

where,  $\epsilon_p$  is the instrumental error in pressure measurement,  $\sigma_{x_1}$  is the uncertainty in the gas (solute) mole fraction and  $\sigma_T$  is the uncertainty in the temperature measurement. A typical conservative value of  $\sigma_T$  is 0.1 °C.

Darwish [49] has expressed the value of  $\epsilon_p$  due to instrumental and procedural error, as a function of the bubble point pressure by the following relation:

$$\epsilon_p = 0.004 P \quad (9)$$

Combining equations (7) and (8), we get the estimated error in bubble point pressure to be:

$$\sigma_{bp} = [(0.004 P)^2 + (\partial P / \partial x_1)^2 (\sigma_{x_1})^2]^{1/2} \quad (10)$$

The temperature contribution to the uncertainty of pressure, being of a small order ( $\pm 0.1$  psi), has been neglected. To estimate the uncertainty in pressure using Equation (9), values are needed of the change in pressure with respect to the solute mole fraction ( $\partial p / \partial x_1$ ), at the same mole fraction at which  $\sigma_{x_1}$  was determined. A second order polynomial fit of p-x data at each isotherm was used to find this value. The uncertainty estimates for bubble point pressures are given in Table VI.

TABLE VI  
 UNCERTAINTY IN BUBBLE POINT PRESSURE OF THE  
 BINARY SYSTEMS IN THIS STUDY ESTIMATED  
 AT THE AVERAGE COMPOSITION OF  
 THE CORRESPONDING ISOTHERM

System	Temperature °F	$(\partial P / \partial x_1)$ psi	$\sigma_{x1}$	$\sigma_{bp}$ , psia (Eqn. (10))
CH <sub>4</sub> + Toluene	150.0	7.5E+03	0.0004	5
CH <sub>4</sub> + n-C <sub>6</sub>	160.0	4.1E+03	0.0006	4
CH <sub>4</sub> + n-C <sub>12</sub>	212.0	4.8E+03	0.0008	5
CO + n-C <sub>20</sub>	212.0	7.5E+03	0.0006	5
CO + n-C <sub>28</sub>	212.0	7.1E+03	0.0009	7
CO + n-C <sub>36</sub>	212.0	6.8E+03	0.0009	7

## CHAPTER VI

### BINARY VAPOR-LIQUID PHASE EQUILIBRIUM FOR METHANE + 1) TOLUENE, 2) N-HEXANE AND 3) N-DODECANE - RESULTS AND DISCUSSION

The binary vapor-liquid phase equilibrium for methane with heavy hydrocarbons (n-paraffins, naphthenes and aromatics) has been studied by Darwish [49]. The present work complements the earlier study by measuring the solubility of methane in three hydrocarbons, viz. 1) toluene, 2) n-hexane and 3) n-dodecane. Solubilities were measured at temperatures from 311 to 423 K (100 °F to 302 °F) and pressures to 10.4 MPa (1504 psi). The experimental data are presented in Tables VII-IX. These experimental data have been correlated using the SRK and PR equations of state. Optimum binary interaction parameters were obtained by minimizing the sum of squares of pressure deviations from the experimental values. Detailed procedure for data reduction is given by Gasem [26]. The input parameters of the pure components (acentric factors, critical temperatures and critical pressures) required by the SRK and PR equations of state, together with the literature sources, are presented in Table X.

Figures 8-10 show the effect of temperature and

TABLE VII  
SOLUBILITY DATA FOR METHANE + TOLUENE

Mole Fraction Methane	Bubble Point Pressure bar	(psia)
----- 313.2 K (40.0 °C, 104.0 °F) -----		
0.0263	11.7	(170)
0.0547	23.8	(345)
0.0707	31.4	(455)
0.0990	44.4	(644)
0.1203	55.3	(802)
0.1356	63.0	(914)
0.1504	70.8	(1027)
-----338.7 K (65.5 °C, 150.0 °F)-----		
0.0503	23.4	(339)
0.0912	41.9	(608)
0.1071	51.0	(740)
0.1204	57.4	(833)
0.1515	73.6	(1067)
0.1805	89.2	(1294)

TABLE VII (Continued)

Mole Fraction Methane	Bubble Point Pressure bar (psia)
----- 423.2 K (150.0 °C, 302.0 °F) -----	
0.0378	21.1 (306)
0.0524	28.4 (412)
0.0739	38.8 (563)
0.1011	52.5 (761)
0.1143	59.1 (857)
0.1403	72.4 (1050)

TABLE VIII  
SOLUBILITY DATA FOR METHANE + N-HEXANE

Mole Fraction Methane	Bubble Point Pressure bar	(psia)
----- 310.9 K (37.8 °C, 100.0 °F) -----		
0.0496	10.8	(157)
0.0996	21.8	(316)
0.1202	26.5	(384)
0.1493	33.6	(487)
0.1898	43.0	(624)
0.2296	53.0	(769)
0.2494	58.5	(848)
0.2573	60.3	(875)
0.2803	66.3	(962)
0.3234	78.4	(1137)
----- 338.7 K (65.5 °C, 160.0 °F) -----		
0.0623	15.8	(230)
0.0628	15.8	(230)
0.1006	25.7	(373)
0.1498	38.0	(550)
0.1500	38.0	(550)
0.1997	52.3	(758)
0.2216	57.6	(835)
0.2510	66.4	(963)
0.2875	77.8	(1128)

TABLE VIII (CONTINUED)

Mole Fraction Methane	Bubble point bar	Pressure (psia)
----- 377.6 K (104.5 °C, 220 °F)-----		
0.0506	15.5	(225)
0.0509	15.7	(228)
0.0622	19.0	(276)
0.0805	23.5	(341)
0.1004	29.3	(425)
0.1502	42.4	(615)
0.1550	44.0	(638)
0.1708	48.3	(700)
0.2006	57.2	(829)
0.2378	67.6	(980)
0.2499	71.1	(1031)
0.2507	71.3	(1034)
0.2939	84.6	(1227)
0.2972	85.2	(1235)

TABLE IX  
SOLUBILITY DATA FOR METHANE + N-DODECANE

Mole Fraction Methane	Bubble point bar	Pressure (psia)
----- 323.2 K (50 °C, 122 °F)-----		
0.0615	13.3	(193)
0.1023	22.7	(329)
0.1515	35.5	(515)
0.2105	52.1	(755)
0.2530	65.4	(945)
0.3022	82.4	(1194)
0.3566	103.8	(1505)
----- 373.2 K (100.0 °C, 212 °F)-----		
0.0998	25.4	(369)
0.1013	25.9	(375)
0.1817	49.8	(722)
0.2020	56.2	(815)
0.2505	73.2	(1061)
0.3023	92.7	(1344)

TABLE X  
CRITICAL PROPERTIES AND ACENTRIC FACTORS  
USED IN THE SRK AND PR EQUATIONS OF STATE

Component	Pressure bar	Temperature K	Acentric Factor	Reference
Methane	46.60	190.5	0.011	57
Toluene	41.04	591.8	0.263	58
N-Hexane	30.30	507.9	0.298	58
N-Dodecane	18.06	658.3	0.571	58

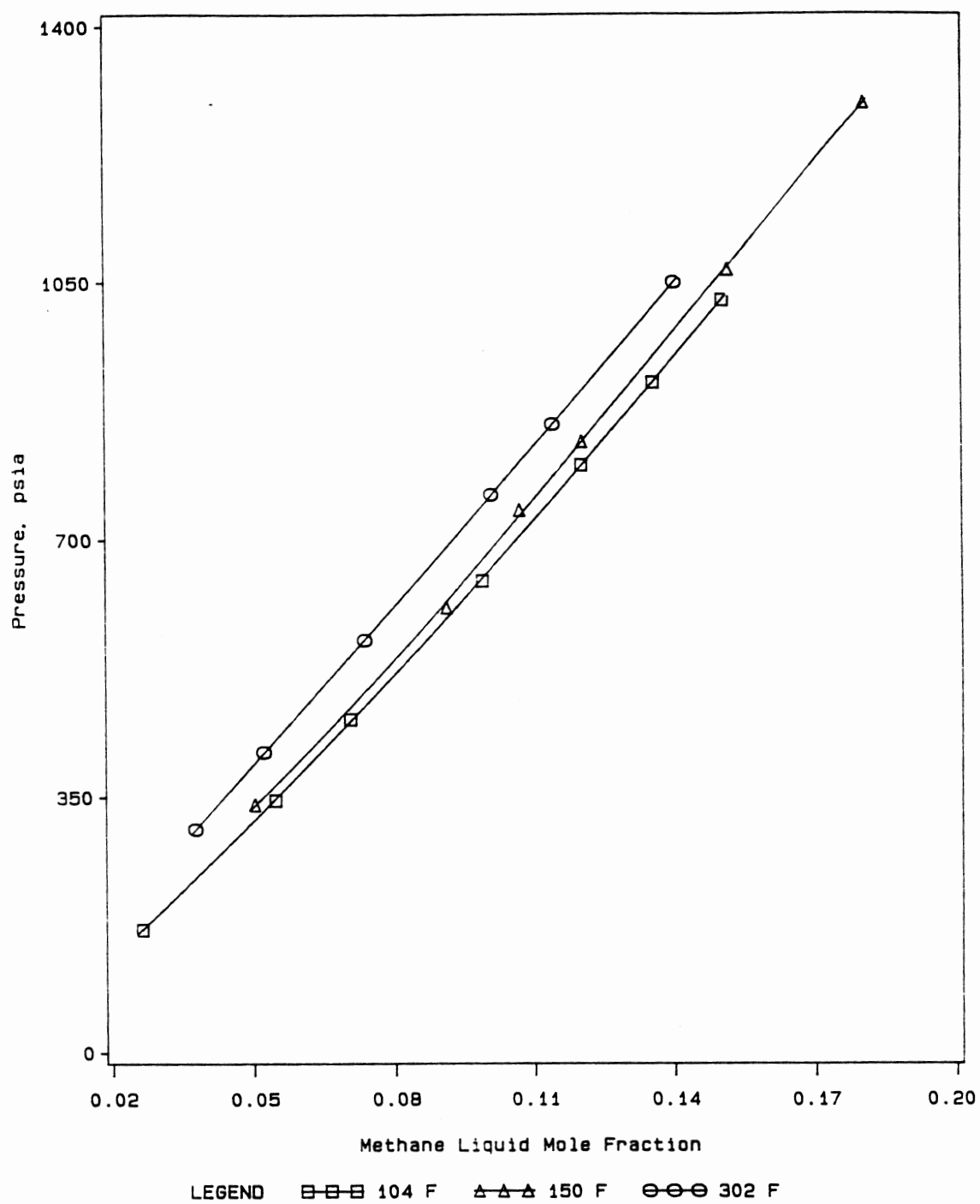


Figure 8. Bubble Point Pressure Data for Methane + Toluene

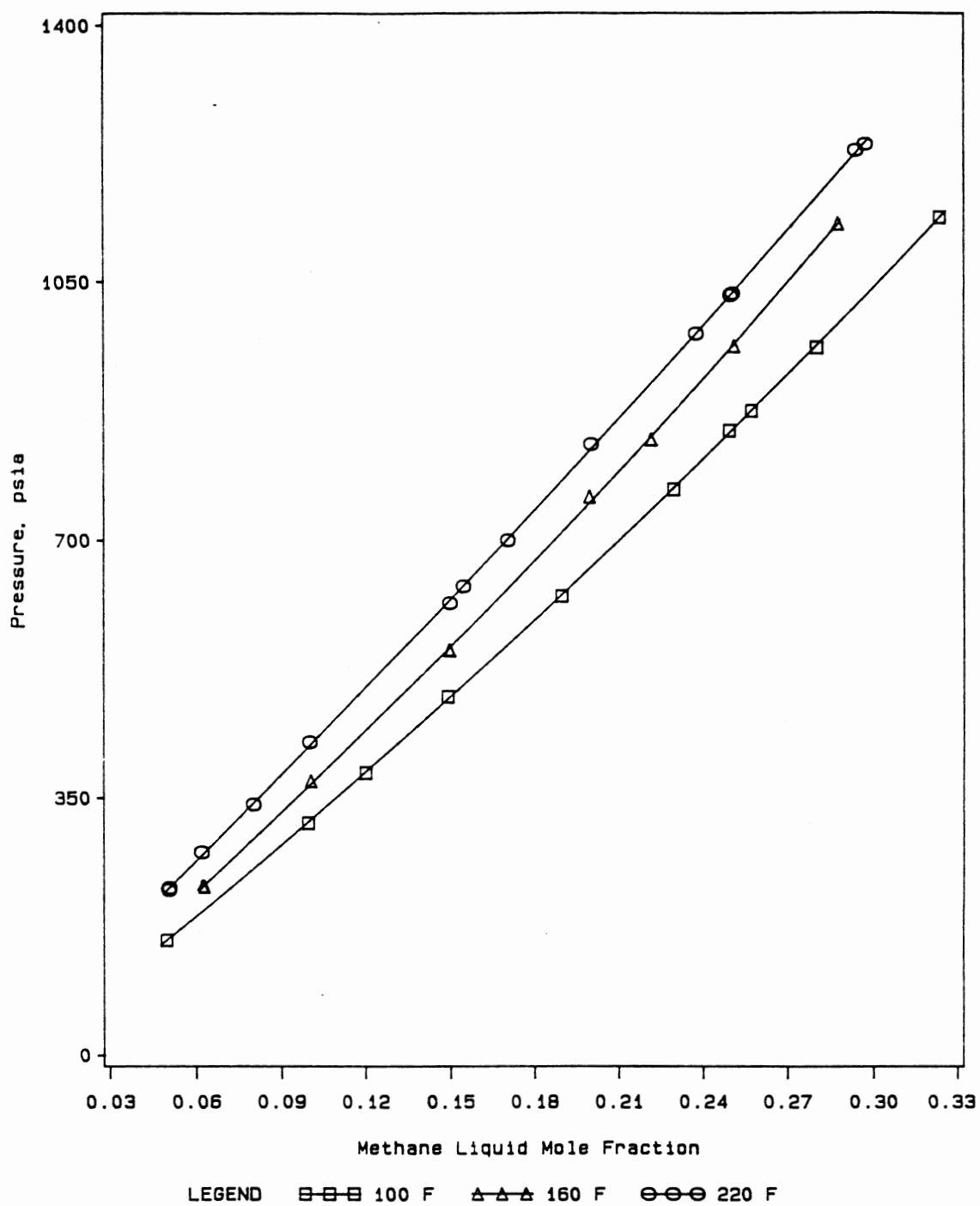


Figure 9. Bubble Point Pressure Data for Methane + n-Hexane

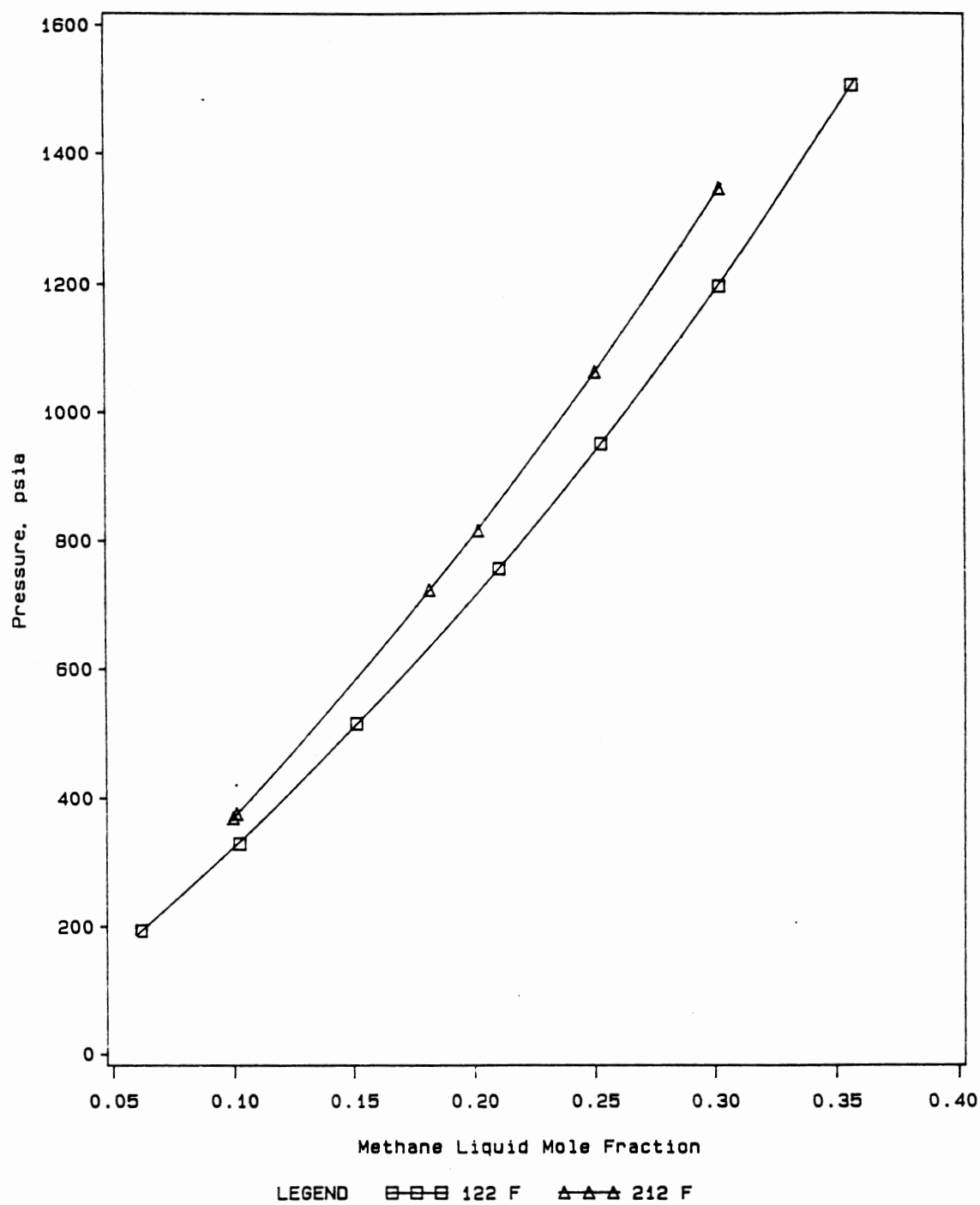


Figure 10. Bubble Point Pressure Data for Methane + n-Dodecane

pressure on the solubility of methane (liquid phase mole fraction of methane) in each of the solvents studied. For a given total pressure, solubility of the gas decreases with increasing temperature. This behavior is the same as observed for  $\text{CO}_2$  and  $\text{CH}_4$  solubilities in heavy normal paraffins [26,49].

The equation of state representation of the solubility for the systems methane + toluene and methane + n-hexane are shown in Tables XI and XII. In general, the SRK and PR equations are capable of describing the data with RMS errors of 0.001 and 0.003 in mole fraction for the two systems, methane + toluene and methane + n-hexane, respectively, when a single interaction parameter,  $C_{ij}$ , is used over the complete temperature range. No significant improvements in equation of state predictions are realized when an additional parameter,  $D_{ij}$ , is used. When one interaction parameter,  $C_{ij}$ , is fitted to each isotherm, the RMS errors are less than 0.001 (0.002 for the methane + n-hexane system at 160 °F) and the two equations of state give comparable representation of data. Using two parameters for each isotherm seems unnecessary, as revealed by the results in Tables XI and XII.

Table XIII shows a similar representation for the system methane + n-dodecane. The SRK equation of state is capable of describing the data with RMS errors of 0.002 when a single pair of interaction parameters,  $C_{ij}$  and  $D_{ij}$ , is used over the complete temperature range. When two

TABLE XI  
SRK AND PR EQUATION OF STATE REPRESENTATIONS  
OF SOLUBILITY OF METHANE IN TOLUENE

Temperature K (°F)	Soave Parameters (PR Parameters) C <sub>ij</sub> D <sub>ij</sub>		Error in Mole Fraction*	
			RMS	IMAXI
313.2 (104.0)	0.0650 (0.0664)	0.0030 (0.0074)	0.0004	0.0008
	0.0715 (0.0813)		0.0004	0.0009
-----				
338.7 (150.0)	0.0560 (0.0581)	0.0043 (0.0082)	0.0008	0.0016
	0.0646 (0.0736)		0.0008	0.0013
-----				
423.2 (302.0)	0.0313 (0.0361)	0.0203 (0.0201)	0.0001	0.0002
	0.0732 (0.0748)		0.0005	0.0008
-----				
313.2, 338.7 423.2	0.0431 (0.0474)	0.0122 (0.0167)	0.0012	0.0030
	0.0684 (0.0775)		0.0013	0.0027

\* The RMS and maximum errors in CH<sub>4</sub> mole fraction are essentially the same for both the SRK and PR equations of state.

TABLE XII  
SRK AND PR EQUATION OF STATE REPRESENTATIONS  
OF SOLUBILITY OF METHANE IN N-HEXANE

Temperature K (°F)	Soave Parameters (PR Parameters)		Error in Mole Fraction*	
	$C_{ij}$	$D_{ij}$	RMS	IMAXI
310.9 (100.0)	0.0280 (0.0299)	-0.0017 (-0.0001)	0.0005	0.0009
	0.0256 (0.0298)		0.0006	0.0008
-----				
344.3 (160.0)	0.0527 (0.0518)	-0.0141 (-0.0131)	0.0011	0.0019
	0.0317 (0.0332)		0.0017	0.0026
-----				
377.6 (220.0)	0.0403 (0.0397)	0.0016 (0.0005)	0.0008	0.0014
	0.0424 (0.0398)		0.0008	0.0015
-----				
310.9, 344.3 377.6	0.0426 (0.0414)	-0.0077 (-0.0058)	0.0031 0.0021	0.0061 0.0043
	0.0317 (0.0334)		0.0033 0.0023	0.0064 0.0046

\* The RMS and maximum errors in CH<sub>4</sub> mole fraction are essentially the same using the SRK and PR equations of state, whenever not mentioned.

TABLE XIII

SRK AND PR EQUATION OF STATE REPRESENTATIONS  
OF SOLUBILITY OF METHANE IN N-DODECANE

Temperature K (°F)	Soave Parameters (PR Parameters)		Error in Mole Fraction*	
	$C_{ij}$	$D_{ij}$	RMS	IMAXI
323.2 (122.0)	0.0663	-0.0130	0.0004	0.0006
	(0.0648)	(-0.0120)		
	0.0343		0.0039	0.0052
	(0.0371)			
-----				
373.3 (212.0)	0.0663	-0.0164	0.0002	0.0004
	(0.0642)	(-0.0167)		
	0.0212		0.0028	0.0034
	(0.0218)			
-----				
323.2, 473.2	0.0730	-0.0167	0.0022	0.0035
	(0.0730)	(-0.0170)	0.0031	0.0049
	0.0304		0.0045	0.0084
	(0.0324)		0.0050	0.0091

\* The RMS and maximum errors in CH<sub>4</sub> mole fraction are essentially the same using the SRK and PR equations of state, whenever not mentioned.

parameters are fitted to each isotherm the RMS errors are less than 0.0004 and the two equations of state give comparable representation of data. However, two interaction parameters are necessary to describe the data for this system, as evident from Table XIII.

From the results in Tables XI-XIII, it is seen that in general the RMS errors in mole fraction are less than the calculated uncertainties for the average mole fractions shown in Table V. The exceptions are the methane + toluene system at 150 °F and methane + n-hexane at 160 °F, which show larger deviations. Since a point-by-point analysis for the uncertainty estimation is not done, the higher values of the RMS errors for these systems are reasonable, especially in light of the fact that the RMS error is used in this comparison. These results illustrate both the ability of the equations of state and the precision of our reported data.

Comparisons of our results with those of other investigators appear in Figures 11-15. The comparisons are shown in terms of deviations of the solubilities from the values predicted using the SRK equation of state. Interaction parameters,  $C_{ij}$  and  $D_{ij}$ , employed in the equation of state predictions were obtained by fitting our data of the isotherm under study.

For the methane + toluene system, significant disagreement between our data and that of Elbishlawi, et al. [35] at 150 °F (solubility differences as high as 0.045) is

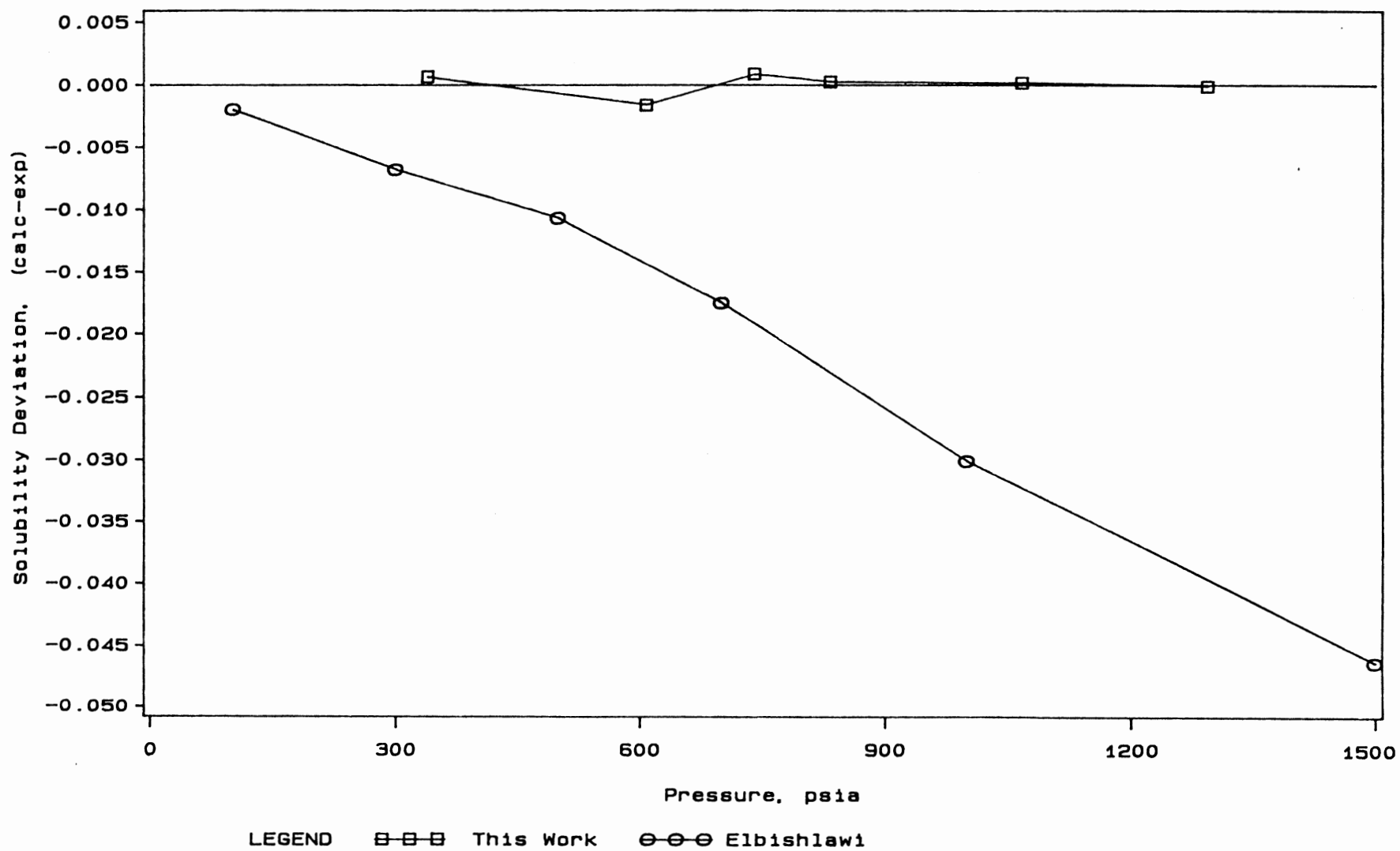


Figure 11. Comparison of Methane Solubilities in Toluene at 150 F

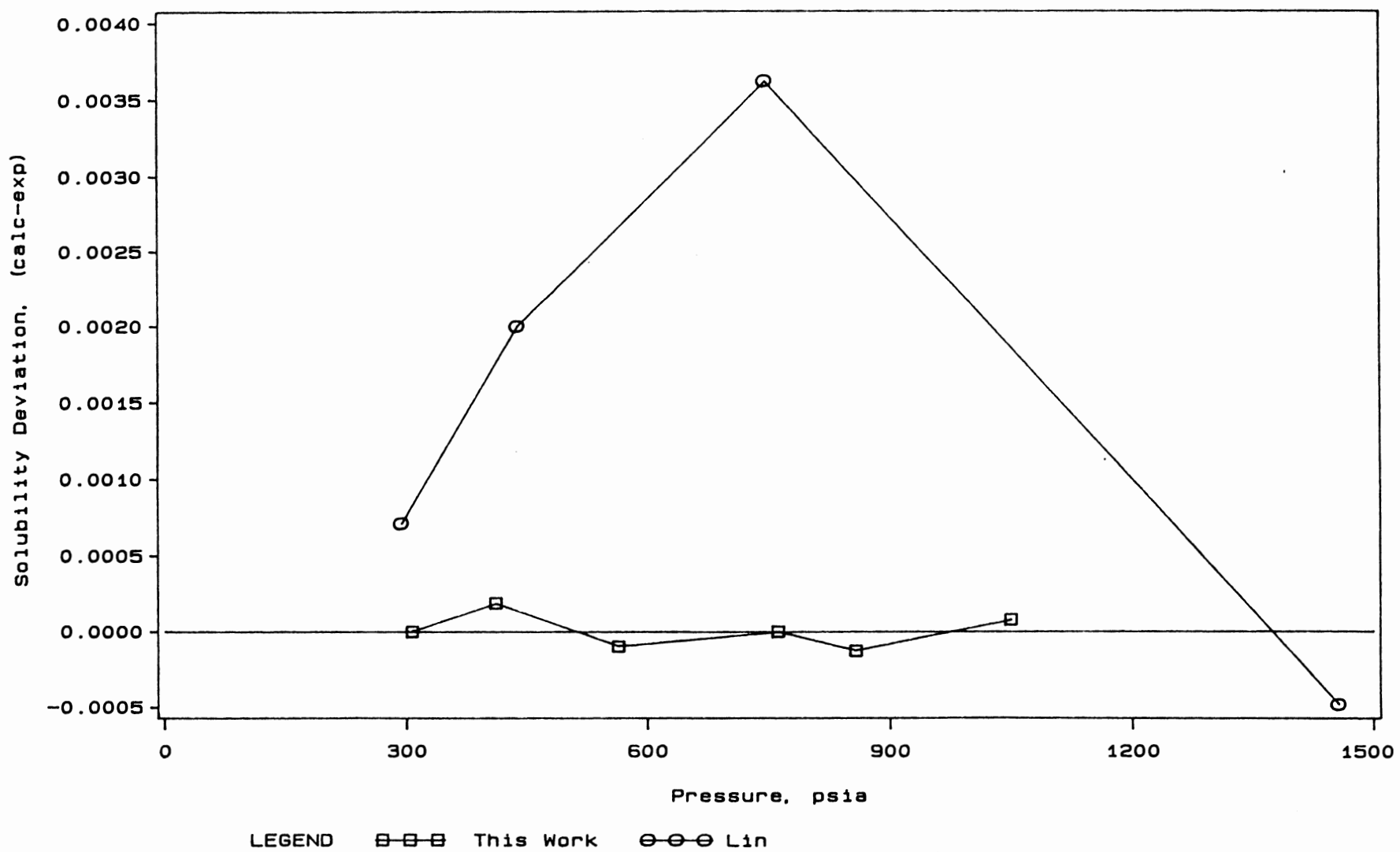


Figure 12. Comparison of Methane Solubilities in Toluene at 302 F

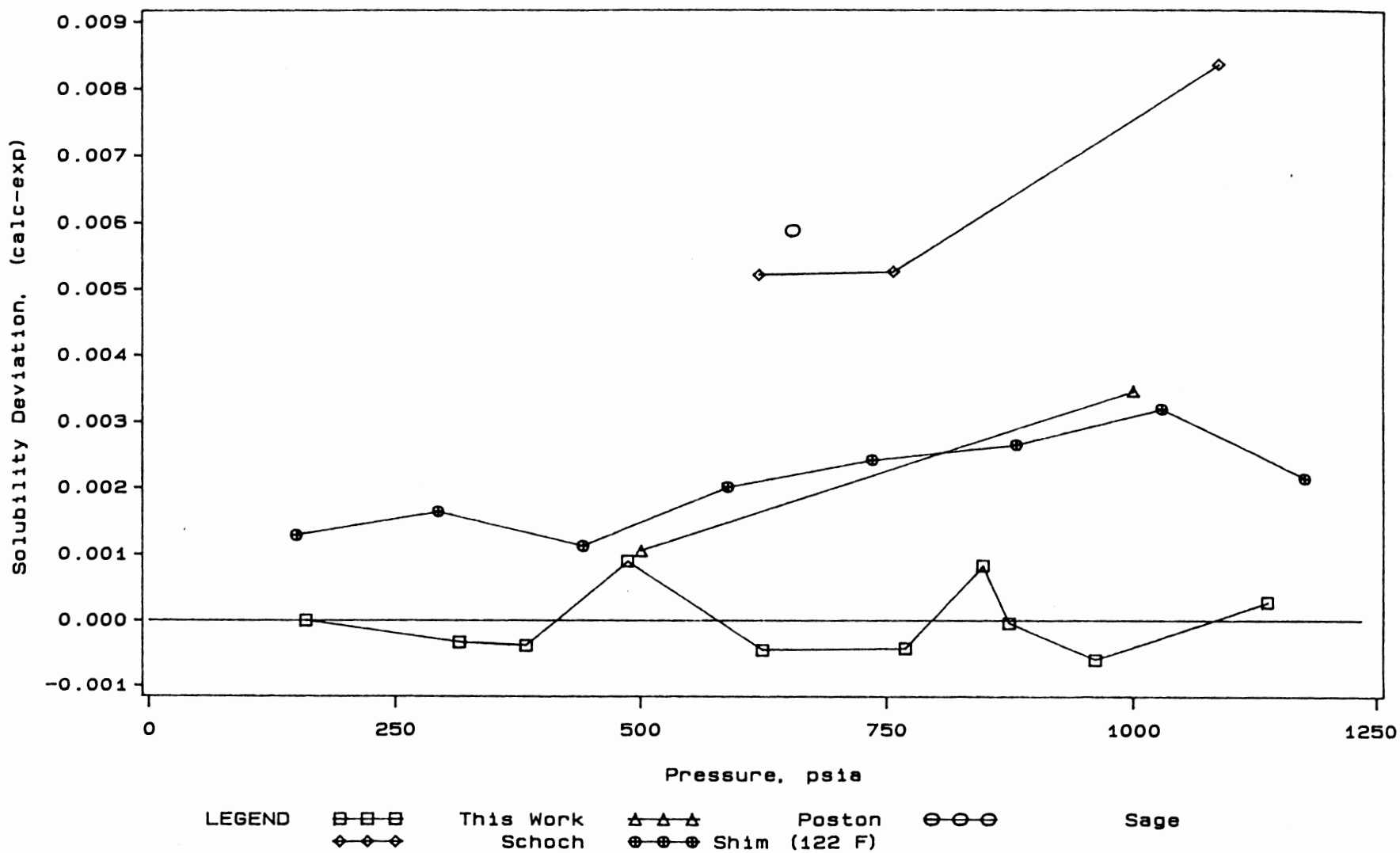


Figure 13. Comparison of Methane Solubilities in n-Hexane at 100 F

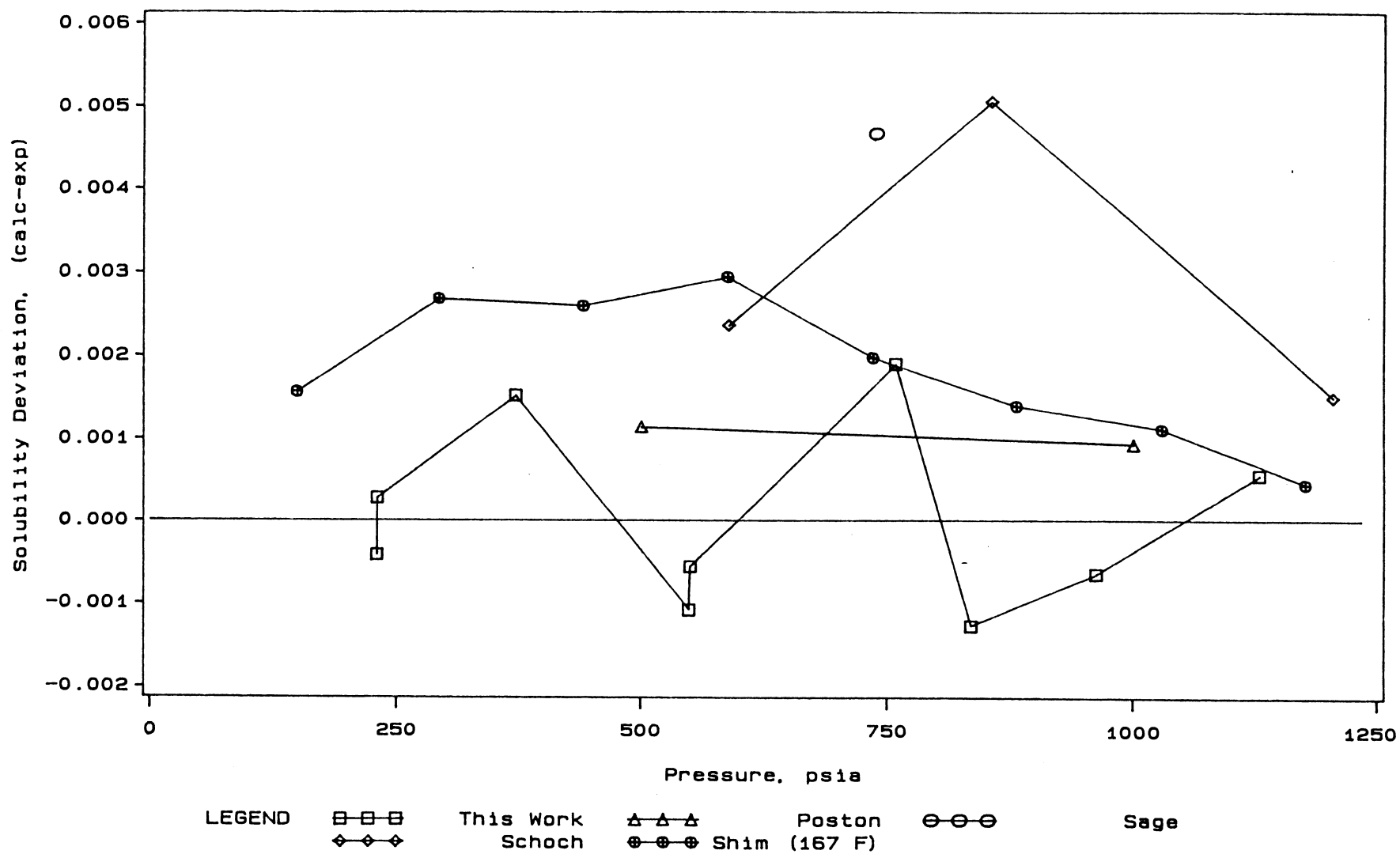


Figure 14. Comparison of Methane Solubilities in n-Hexane at 160 F

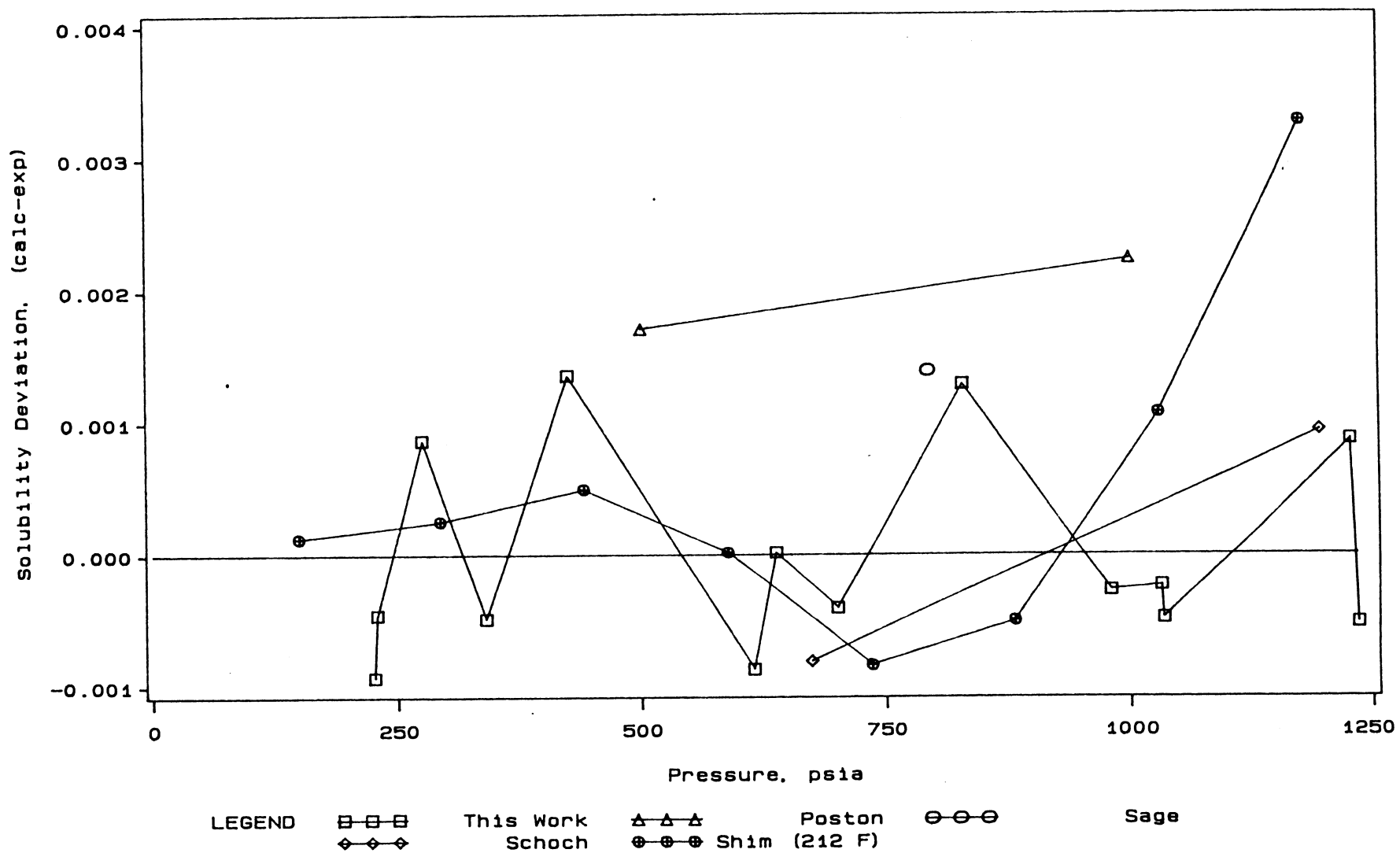


Figure 15. Comparison of Methane Solubilities in n-Hexane at 220 F

evident from Figure 11. The data of this work at 302 °F, however, are in reasonable agreement with the earlier measurements of Lin, et al. [36] (solubility deviations within 0.002 in mole fraction except for one point), as shown in Figure 12.

Figure 13 shows the comparison of our data for the methane + n-hexane system with four other investigators [37-40] at a temperature of 100 °F. The observed deviations in solubility between our data and those by the four other investigators are less than 0.006 except for one point (of Schoch et al [37]). Similarly, Figures 14 and 15 show the results of our comparisons with the same investigators at 160 °F and 220 °F, respectively. In general, the deviations in solubilities between our data and the literature are less than 0.005 for the 160 °F and 0.003 for the 220 °F isotherms. Very good agreement is noted (deviations < 0.003), when our data are compared to those reported by Poston [38] and Shim [39] at all three isotherms of study. In all the above comparisons, interaction parameters,  $C_{ij}$  and  $D_{ij}$ , regressed from our data were used to predict solubility deviations for the data reported by Shim at temperatures slightly different from ours.

No comparisons are available for the methane + n-dodecane system due to the absence of published data. Figure 16 shows solubility deviation of this work at the isotherms of study. The excellent fit of data (deviations < 0.0006) reveal the precision of our measurements.

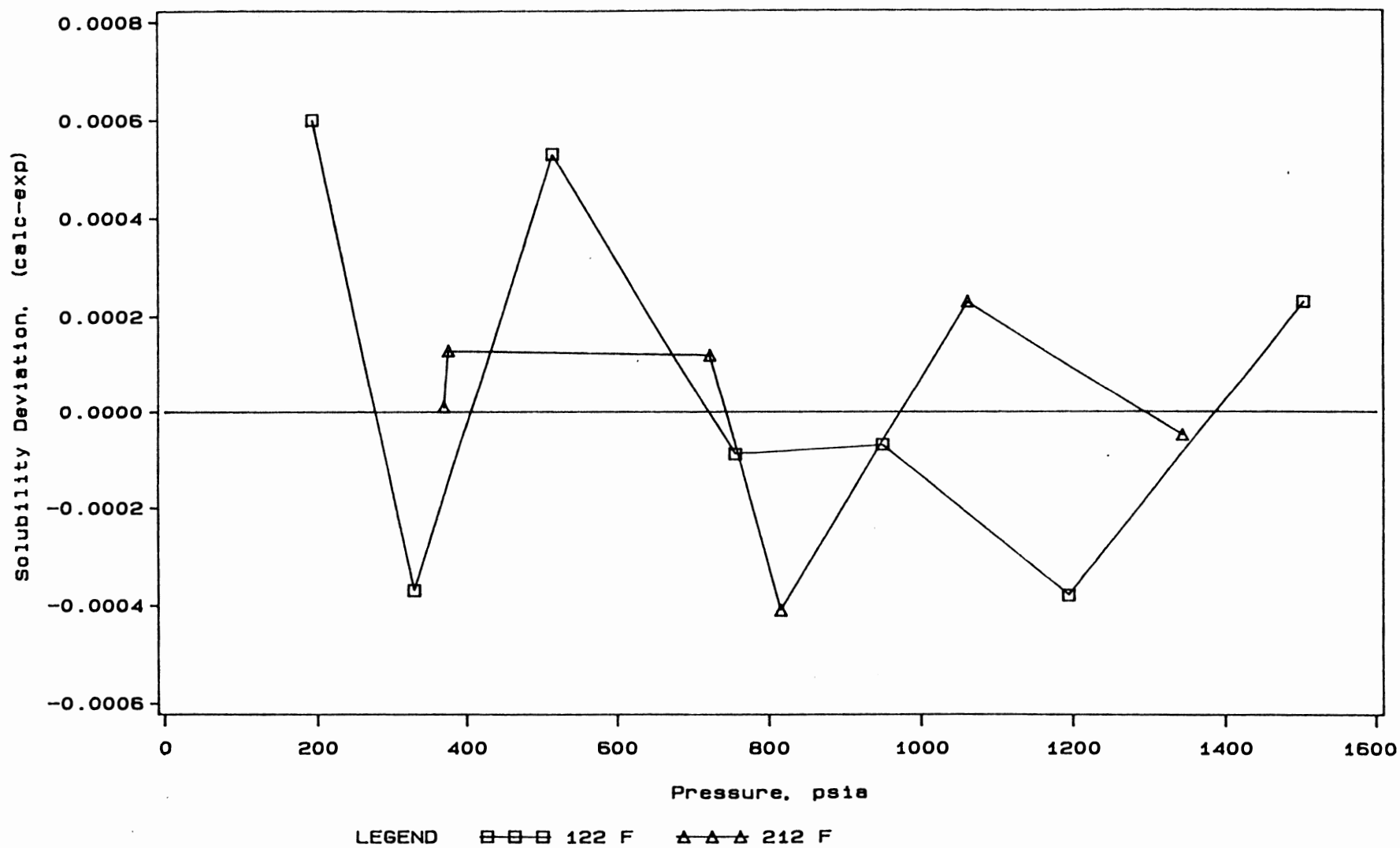


Figure 16. Comparison of Methane Solubilities in n-Dodecane

## CHAPTER VII

### BINARY VAPOR-LIQUID PHASE EQUILIBRIUM FOR CARBON MONOXIDE + HEAVY NORMAL PARAFFINS - RESULTS AND DISCUSSION

Upon completion of the targeted methane solubility measurements, a study of carbon monoxide solubility in heavy hydrocarbons was initiated. n-Eicosane ( $C_{20}$ ), n-octacosane ( $C_{28}$ ), and n-hexatriacontane ( $C_{36}$ ) - all solids at room temperature - were selected from the normal paraffin homologous series for this purpose. Solubilities were measured at temperatures from 323 to 423 K (122 °F to 302 °F) and pressures to 9.10 MPa (1300 psia). The experimental data are presented in Tables XIV-XVI. These data have been correlated using the SRK and PR equations of state and optimum binary interaction parameters obtained by minimizing the objective function given in Chapter III. The input parameters for the pure solvents (acentric factors, critical temperatures and critical pressures) required by the SRK and PR equations of state were estimated using the Asymptotic Behavior Correlation of Gasem and Robinson [26] and are given in Table XVII.

The effects of temperature and pressure on the solubility of carbon monoxide (liquid mole fraction of

TABLE XIV  
SOLUBILITY DATA FOR CARBON MONOXIDE +  
N-EICOSANE

Mole fraction Carbon Monoxide	Bubble Point Pressure	
	bar	(psia)
-----323.2 K (50.0 °C, 122.0 °F)-----		
0.0516	28.0	(407)
0.0645	35.6	(516)
0.0797	45.1	(654)
0.0902	51.6	(749)
0.1024	60.5	(878)
0.1136	67.8	(983)
-----373.2 K (100.0 °C, 212.0 °F)-----		
0.0403	19.9	(289)
0.0516	25.8	(373)
0.0715	36.5	(529)
0.0899	47.2	(684)
0.1107	59.3	(860)
0.1308	72.4	(1049)
-----423.2 K (150.0 °C, 302.0 °F)-----		
0.0616	28.3	(411)
0.0761	35.7	(518)
0.1004	48.3	(700)
0.1187	58.6	(850)
0.1205	59.4	(861)
0.1590	82.4	(1196)
0.1593	82.7	(1200)
0.1614	83.8	(1216)

TABLE XV  
SOLUBILITY DATA FOR CARBON MONOXIDE +  
N-OCTACOSANE

Mole fraction Carbon Monoxide	Bubble Point Pressure bar	(psia)
-----348.2 K (75.0 °C, 167.0 °F)-----		
0.0553	23.3	(338)
0.0604	25.5	(370)
0.0854	38.2	(554)
0.1014	46.2	(671)
0.1320	63.7	(923)
0.1493	75.7	(1097)
-----373.2 K (100.0 °C, 212.0 °F)-----		
0.0519	22.5	(326)
0.0718	31.6	(458)
0.0881	39.7	(576)
0.1042	47.6	(690)
0.1157	53.9	(782)
0.1290	60.2	(873)
-----423.2 K (150.0 °C, 302.0 °F)-----		
0.0522	20.8	(301)
0.0733	31.3	(455)
0.1038	43.3	(629)
0.1257	53.7	(779)
0.1502	66.3	(961)

TABLE XVI  
SOLUBILITY DATA FOR CARBON MONOXIDE +  
N-HEXATRIACONTANE

Mole fraction Carbon Monoxide	Bubble Point bar	Pressure (psia)
-----373.2 K (100.0 °C, 212.0 °F)-----		
0.0494	18.0	(261)
0.0634	23.4	(340)
0.0899	34.4	(499)
0.1192	47.5	(689)
0.1603	67.6	(980)
0.2002	89.5	(1299)
-----423.2 K (150.0 °C, 302.0 °F)-----		
0.0568	18.5	(269)
0.0705	23.7	(344)
0.1040	36.0	(522)
0.1289	46.6	(676)
0.1742	66.1	(958)
0.2099	84.0	(1218)

TABLE XVII  
CRITICAL PROPERTIES AND ACENTRIC FACTORS USED  
IN THE SRK AND PR EQUATIONS OF STATE

Component	Pressure (MPa)	Temperature (K)	Acentric Factor	Reference
Carbon Monoxide	3.494	132.9	0.0491	59,60
n-Eicosane	1.117	770.5	0.8738	26
n-Octacosane	0.826	845.4	1.1073	26
n-Hexatria- contane	0.691	901.1	1.2847	26

carbon monoxide) are shown in Figures 17-19. For a given total pressure, the solubility of carbon monoxide increases with increasing temperature. This is in contrast to the behavior observed for  $\text{CO}_2$  and  $\text{CH}_4$  solubilities in heavy normal paraffins [26,49]. This can be explained using the enthalpy or entropy change of solution. For sparingly soluble gases in essentially nonvolatile solvents, it can be shown that [41]

$$\left( \frac{\partial \ln x_1}{\partial 1/T} \right)_P = - \frac{\Delta \bar{h}_1}{R} \quad (1)$$

$$\left( \frac{\partial \ln x_1}{\partial \ln T} \right)_P = \frac{\Delta \bar{s}_1}{R} \quad (2)$$

where  $x_1$  is the mole fraction of the solute at equilibrium and  $\Delta \bar{h}_1 = \bar{h}_{1L} - h_{1V}$ ,  $\Delta \bar{s}_1 = \bar{s}_{1L} - s_{1V}$ .

From equation (2), it can be inferred that the solubility increases with temperature whenever the partial molar change of the solute is positive. The partial molar entropy change can be written as

$$\Delta \bar{s}_1 = (s_{1L} - s_{1V}) + (\bar{s}_{1L} - s_{1L}) \quad (3)$$

where  $s_{1L}$  is the entropy of the (hypothetical) pure liquid at the temperature of the solution. The first term on the right-hand side of equation (3) is negative since the entropy of the liquid is lower than that of saturated vapor at the same temperature. Assuming ideal entropy of mixing

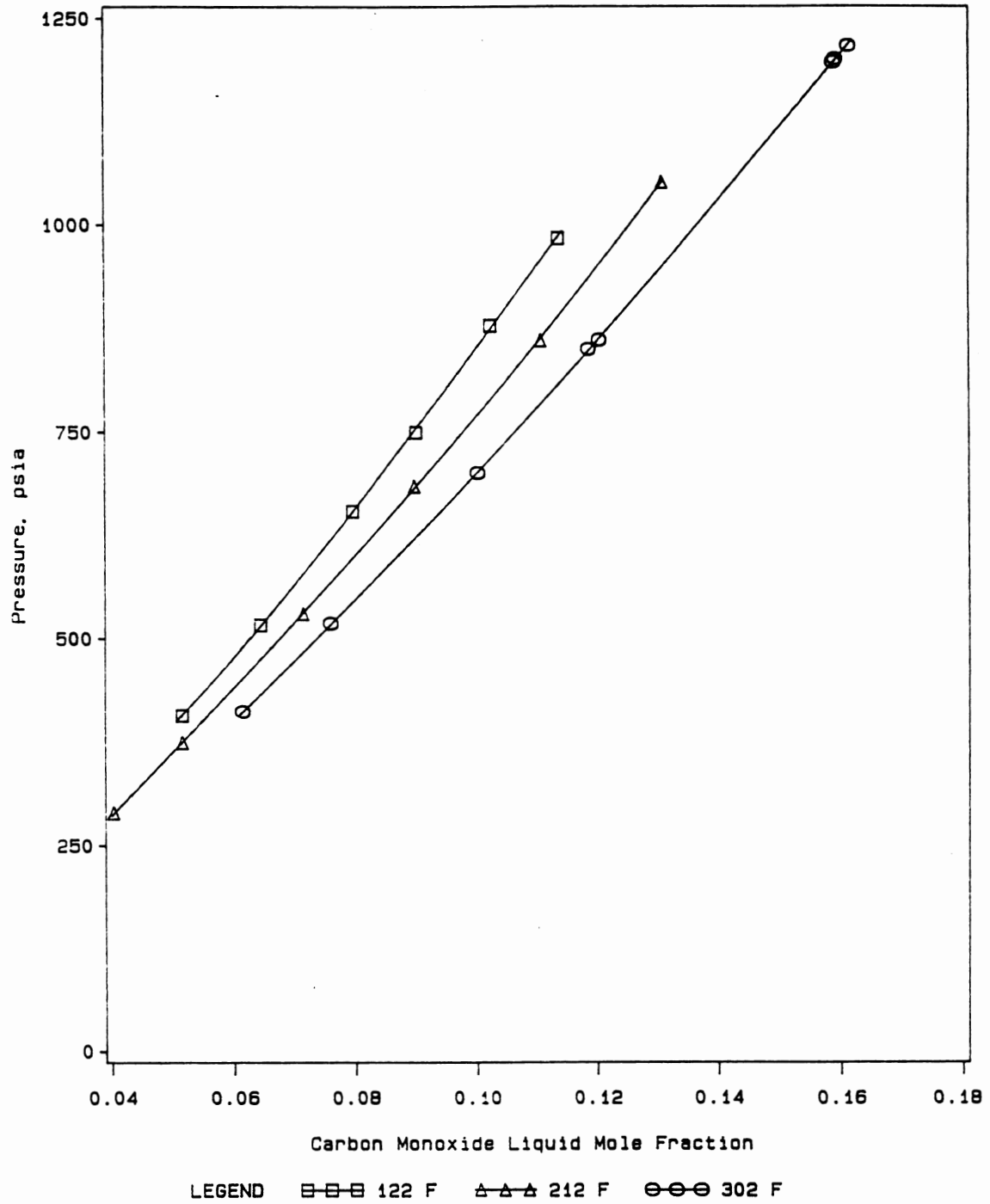


Figure 17. Bubble Point Pressure Data for Carbon Monoxide + n-Eicosane

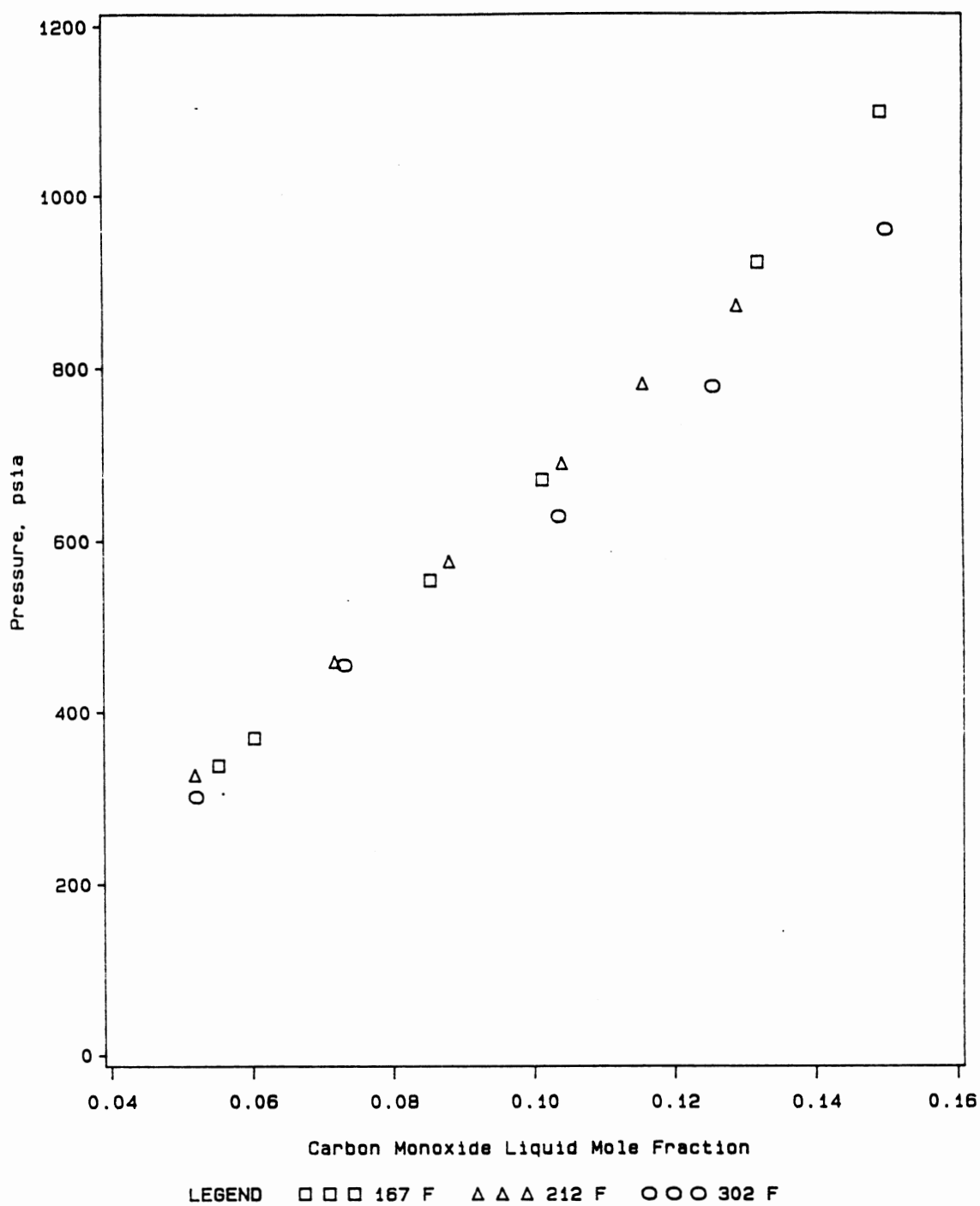


Figure 18. Bubble Point Pressure Data for Carbon Monoxide + n-Octacosane

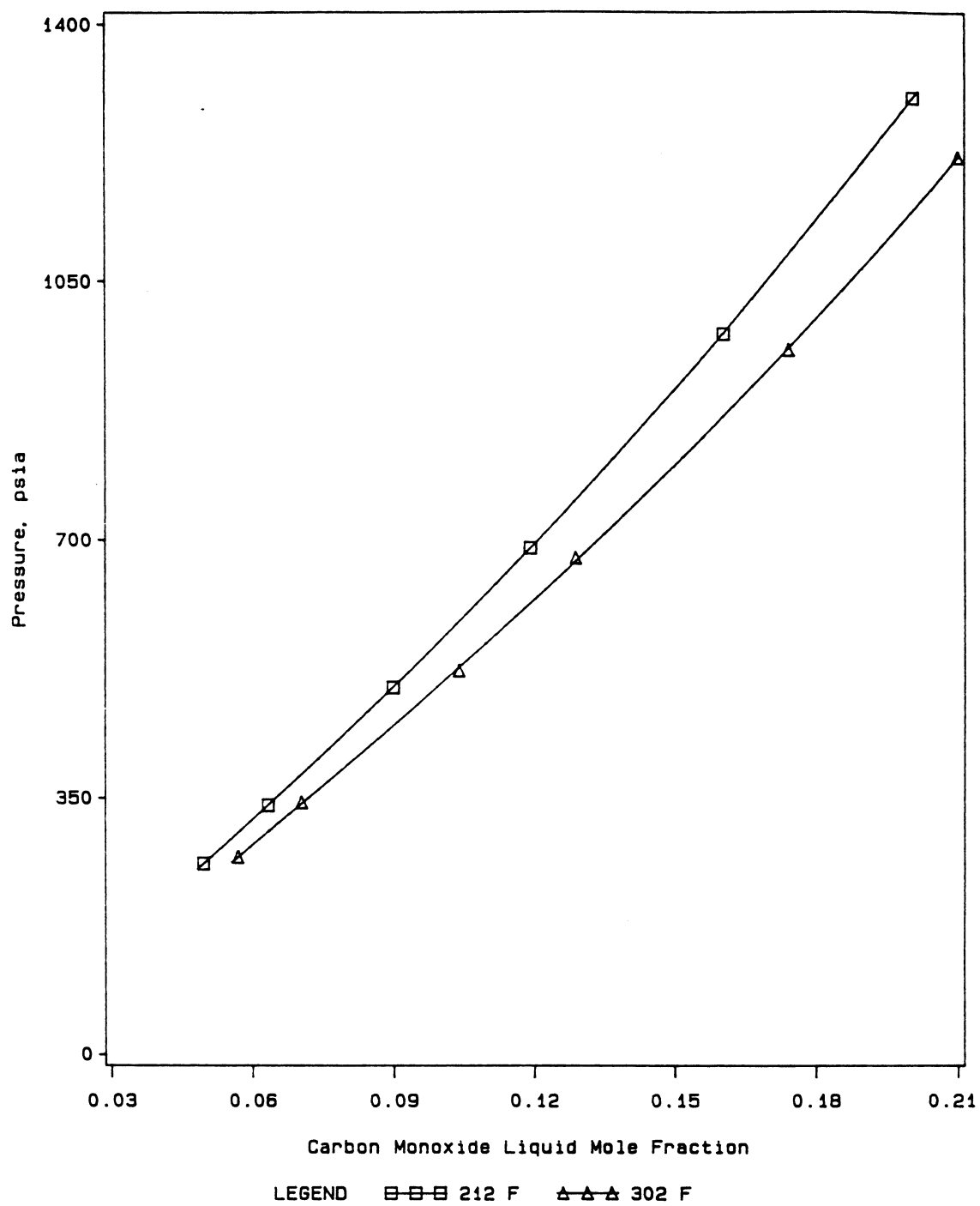


Figure 19. Bubble Point Pressure Data for Carbon Monoxide + n-Hexatriacontane

for the two liquids, the second term in equation (3) can be written as:

$$\bar{s}_{1L} - s_{1L} = -R \ln x_1 \quad (4)$$

From equation (4), it is seen that lower the  $x_1$ , the larger is the term. Thus for very sparingly soluble gases,  $\Delta\bar{s}_1$  is positive and the solubility increases with temperature.

For the n-octacosane system as revealed from Figure 18, the difference in solubility between the isotherms of 167 °F and 212 °F is not very apparent from a p-x plot. Although the difference in temperature is only 25 °C (45 °F), the solubilities vary significantly, as indicated by a closer look at the data in Table XV. For such systems, the solubility differences are magnified when a plot of p/x vs x is made. Further, from Figure 18, the data points at 302 °F isotherm do not appear to be continuous. This is due to the larger deviation in solubility (calc - exp) for the second data point as compared to the other points. The point, however, has not been considered an outlier since the solubility deviation is less than twice the RMSE for the whole data set.

The effect of molecular weight of the solvent (or equivalently the carbon number) is shown in Figure 20. For a given temperature and total pressure, the solubility of the gas (on a molar basis) increases with increasing molecular weight of the solvent. This could be because of

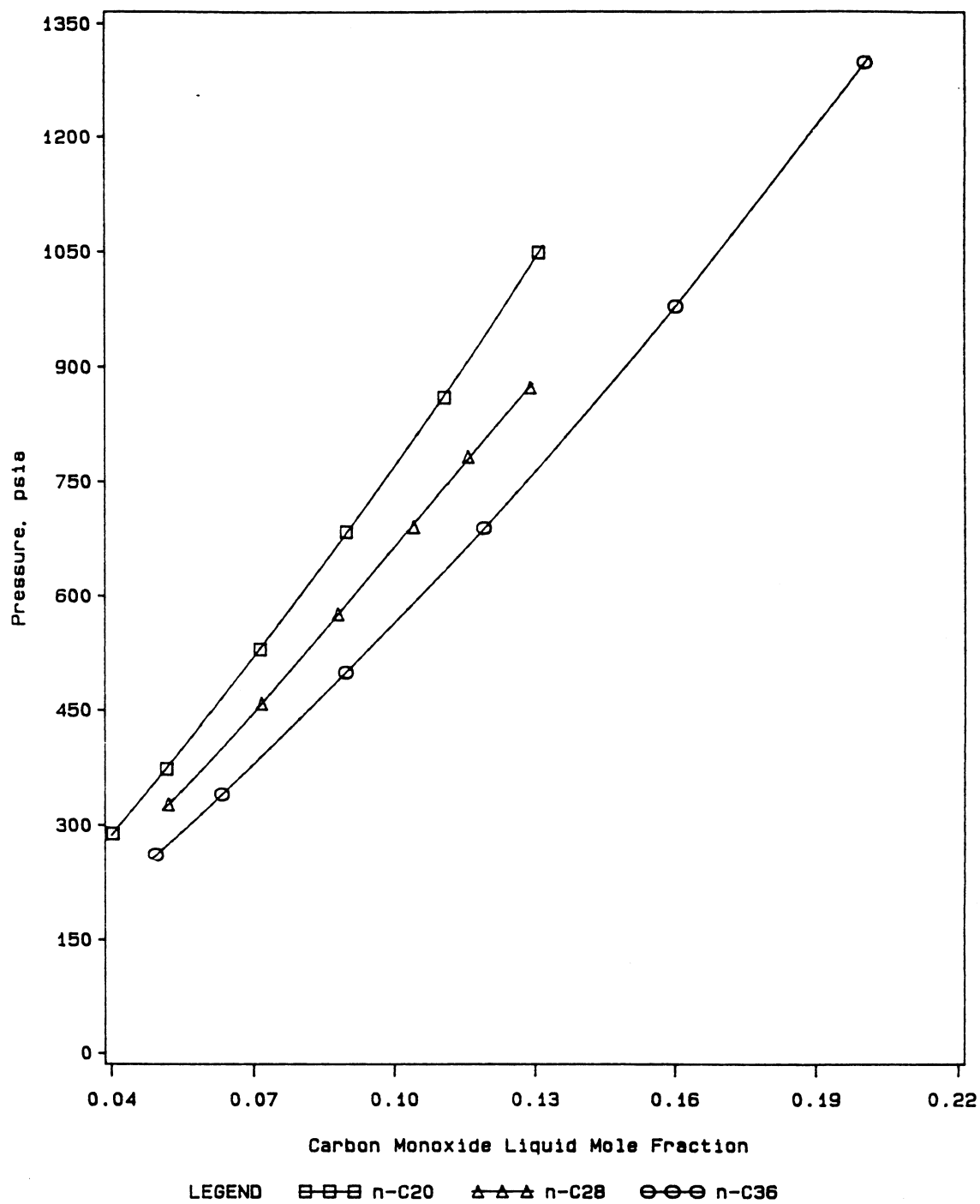


Figure 20. Bubble Point Pressure Data for Carbon Monoxide + n-Paraffins at 212 F

the increased number of sites along the chain of the normal paraffin with which the carbon monoxide molecule can interact, i.e., longer chains (higher carbon number) offer more sites to accommodate the solute molecule than shorter ones.

The equation of state representation of the solubilities for the systems studied are documented in Tables XVIII-XX. The SRK equation of state is capable of describing the data with RMS errors of 0.004 in mole fraction for the two systems, n-C<sub>20</sub> and n-C<sub>28</sub>, when a single interaction parameter,  $C_{ij}$ , is used for each system over the complete temperature range. Only marginal improvements in the equation of state predictions are realized when a second interaction parameter,  $D_{ij}$ , is used over the complete temperature range. However, the use of either one or two interaction parameters, over the complete temperature range does not fit the data as well for the n-C<sub>36</sub> system (RMS errors of 0.007 in mole fraction using two interaction parameters  $C_{ij}$  and  $D_{ij}$ ). From Tables XVIII-XX, it is apparent that the values obtained for the interaction parameters,  $C_{ij}$  and  $D_{ij}$ , when lumped over the complete temperature range lie outside the range of values obtained for the parameters at each isotherm. This is possible since two parameters are used while regressing the data set.

When one interaction parameter,  $C_{ij}$ , is fitted to each isotherm, for the two systems n-C<sub>20</sub> and n-C<sub>28</sub>, the RMS errors are less than 0.0015 in mole fraction (except for the

TABLE XVIII

SRK AND PR EQUATION OF STATE REPRESENTATIONS  
OF CARBON MONOXIDE SOLUBILITY IN N-EICOSANE

Temperature K (°F)	Soave Parameters (P-R Parameters)		Error in Mole Fraction (Using P-R Equation)*	
	C <sub>ij</sub>	D <sub>ij</sub>	RMS	IMAXI
323.2 (122.0)	0.2772 (0.2698)	-0.0113 (-0.0112)	0.0003	0.0006
	0.1602 (0.1686)		0.0006	0.0009
373.2 (212.0)	0.2257 (0.2305)	-0.0105 (-0.0123)	0.0002	0.0004
	0.1166 (0.1214)		0.0006	0.0009
423.2 (302.0)	0.2292 (0.2419)	-0.0140 (-0.0185)	0.0002	0.0002
	0.0873 (0.0862)		0.0008	0.0012
323.2, 373.2 423.2	0.1439 (-0.1557)	-0.0018 (0.0323)	0.0040 (0.0053)	0.0072 (0.0113)
	0.1253 (0.1271)		0.0041 (0.0052)	0.0073 (0.0096)

\* The RMS and maximum errors in CO mole fraction are essentially the same for both the SRK and PR equations of state whenever not mentioned.

TABLE XIX  
SRK AND PR EQUATION OF STATE REPRESENTATIONS  
OF CARBON MONOXIDE SOLUBILITY  
IN N-OCTACOSANE

Temperature K (°F)	Soave Parameters (P-R Parameters)		Error in Mole Fraction (Using P-R Equation)*	
	C <sub>ij</sub>	D <sub>ij</sub>	RMS	IMAXI
348.2 (167.0)	0.4522 (0.4341)	-0.0258 (-0.0270)	0.0005	0.0009
	0.0935 (0.1128)		0.0027	0.0038
373.2 (212.0)	0.0861 (0.1145)	-0.0008 (-0.0019)	0.0004	0.0008
	0.0738 (0.0918)		0.0004	0.0008
423.2 (302.0)	-0.0522 (0.0072)	0.0048 (0.0023)	0.0014	0.0025
	0.0181 (0.0349)		0.0014	0.0029
348.2, 373.2 423.2	0.4495 (0.3541)	-0.0264 (-0.0218)	0.0027 (0.0036)	0.0070 (0.0090)
	0.0743 (0.0916)		0.0036 (0.0042)	0.0079 (0.0089)

\* The RMS and maximum errors in CO mole fraction are essentially the same for both the SRK and PR equations of state whenever not mentioned.

TABLE XX  
SRK AND PR EQUATION OF STATE REPRESENTATIONS  
OF CARBON MONOXIDE SOLUBILITY  
IN N-HEXATRIACONTANE

Temperature K (°F)	Soave Parameters (P-R Parameters)		Error in Mole Fraction (Using P-R Equation)*	
	C <sub>ij</sub>	D <sub>ij</sub>	RMS	IMAXI
373.2 (212.0)	0.1966 (0.2185)	-0.0115 (-0.0127)	0.0001	0.0002
	0.0073 (0.0431)		0.0024	0.0028
423.2 (302.0)	0.1328 (0.1688)	-0.0148 (-0.0172)	0.0005	0.0008
	-0.1154 (-0.0672)		0.0026	0.0034
373.2, 423.2	0.3102 (0.2199)	-0.0212 (-0.0162)	0.0068 (0.0075)	0.0117 (0.0116)
	-0.0409 (-0.0021)		0.0080 (0.0085)	0.0144 (0.0152)

\* The RMS and maximum errors in CO mole fraction are essentially the same for both the SRK and PR equations of state whenever not mentioned.

CO + n-C<sub>28</sub> system at 348.15 K) and the two equations of state give comparable representation of data. No significant improvements are obtained for either CO + n-C<sub>20</sub> or CO + n-C<sub>28</sub>, by using two parameters for each isotherm (except for the CO + n-C<sub>28</sub> system at 348.15 K) as revealed by the results in Tables XVIII and XIX. For the n-C<sub>36</sub> system, however, the use of a second interaction parameter,  $D_{ij}$ , for each isotherm improves the predictions significantly as shown by the results in Table XX. The need for a second parameter could be because of the inadequacy of the mixing rules (for the covolume parameter  $b$ ) or the sensitivity of the interaction parameters to the critical properties and the acentric factors used (as will be explained later). Also evident from Tables XVIII-XX is the fact that the RMS errors in mole fraction, are in general, less than the uncertainty in the calculated mole fractions shown in Table V. These results illustrate both the ability of the equation of state and the precision of our reported data.

Comparison of our results with those reported by Huang, et al. [6] appear in Figures 21-26. The comparisons are shown in terms of deviations of the solubilities from values predicted using the SRK equation of state.

Figures 21, 23 and 25 show comparisons of carbon monoxide solubilities in n-C<sub>20</sub>, n-C<sub>28</sub>, and n-C<sub>36</sub>, respectively, using interaction parameters from our data for the isotherm under study. Reasonable agreement (solubility

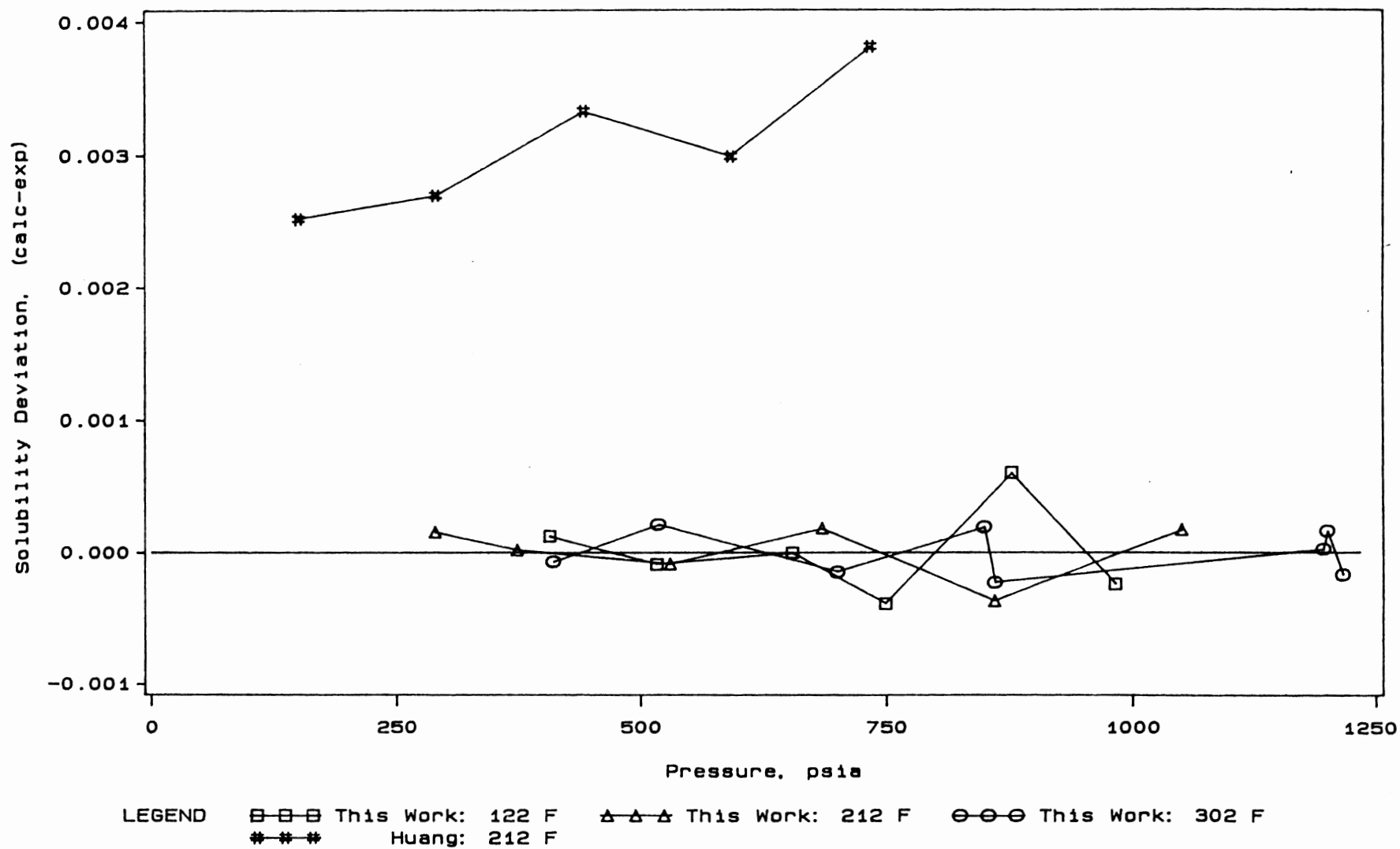


Figure 21. Comparison of Carbon Monoxide Solubilities in n-Eicosane

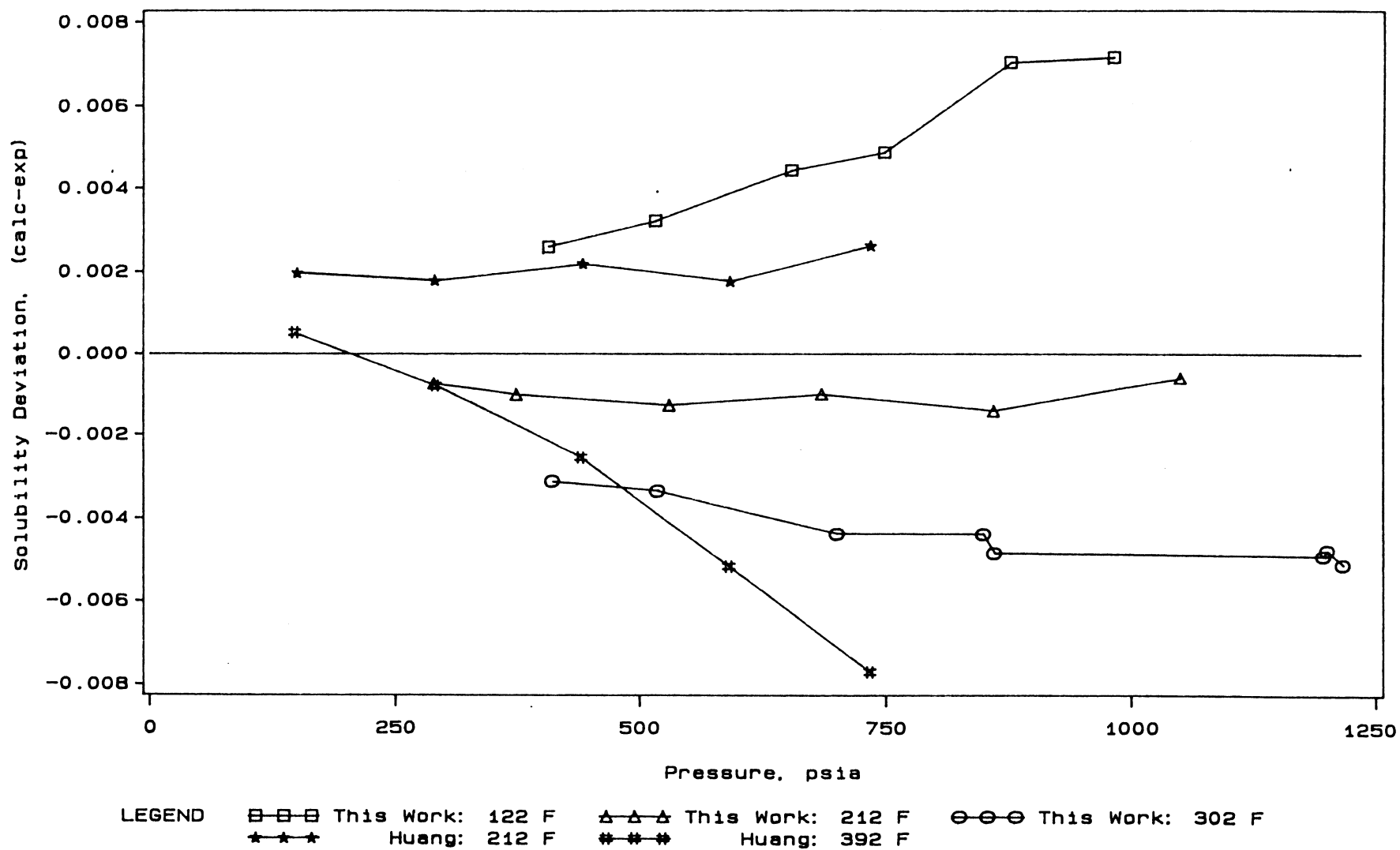


Figure 22. Comparison of Carbon Monoxide Solubilities in n-Eicosane Using Lumped Cij and Dij

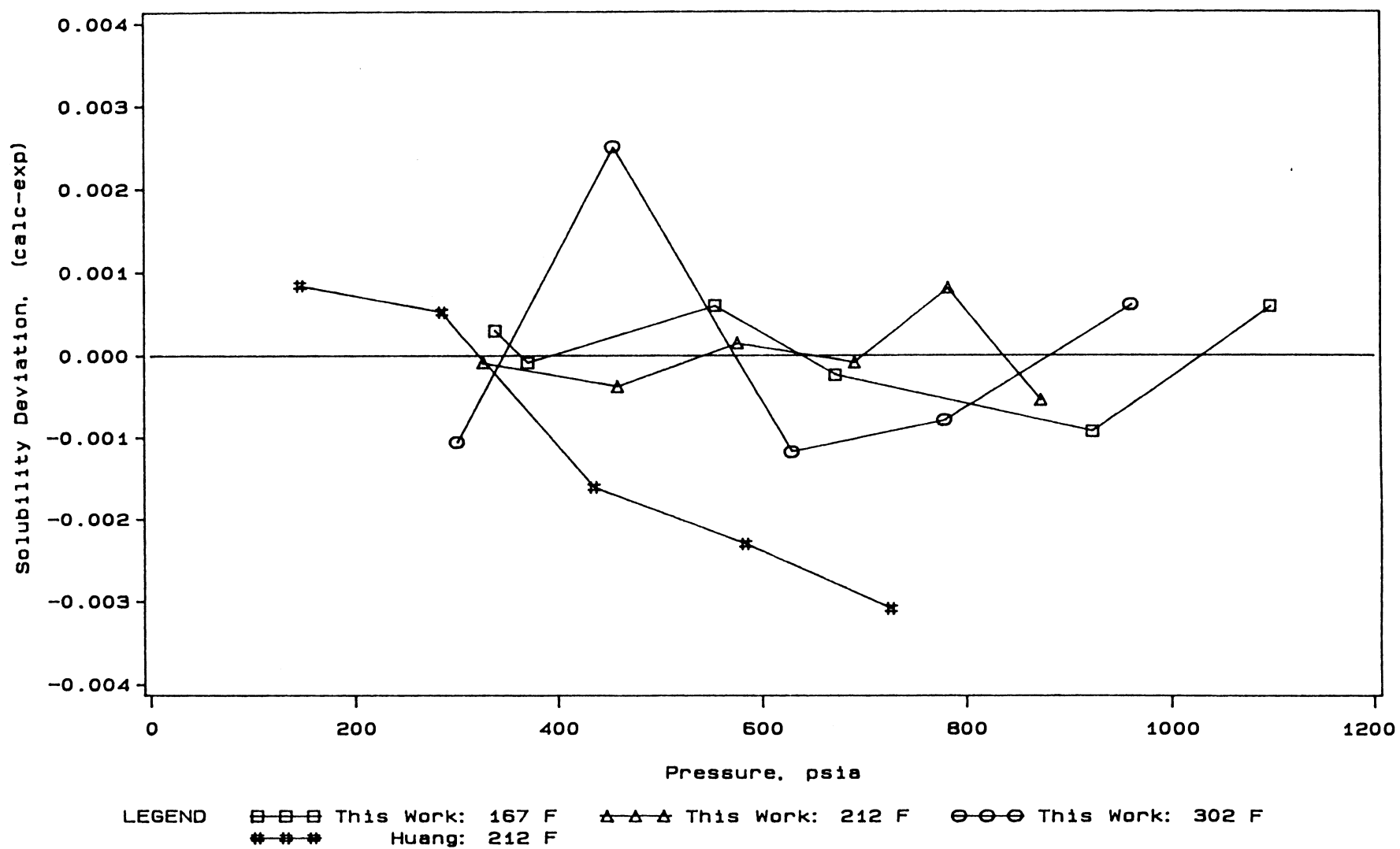


Figure 23. Comparison of Carbon Monoxide Solubilities in n-Octacosane

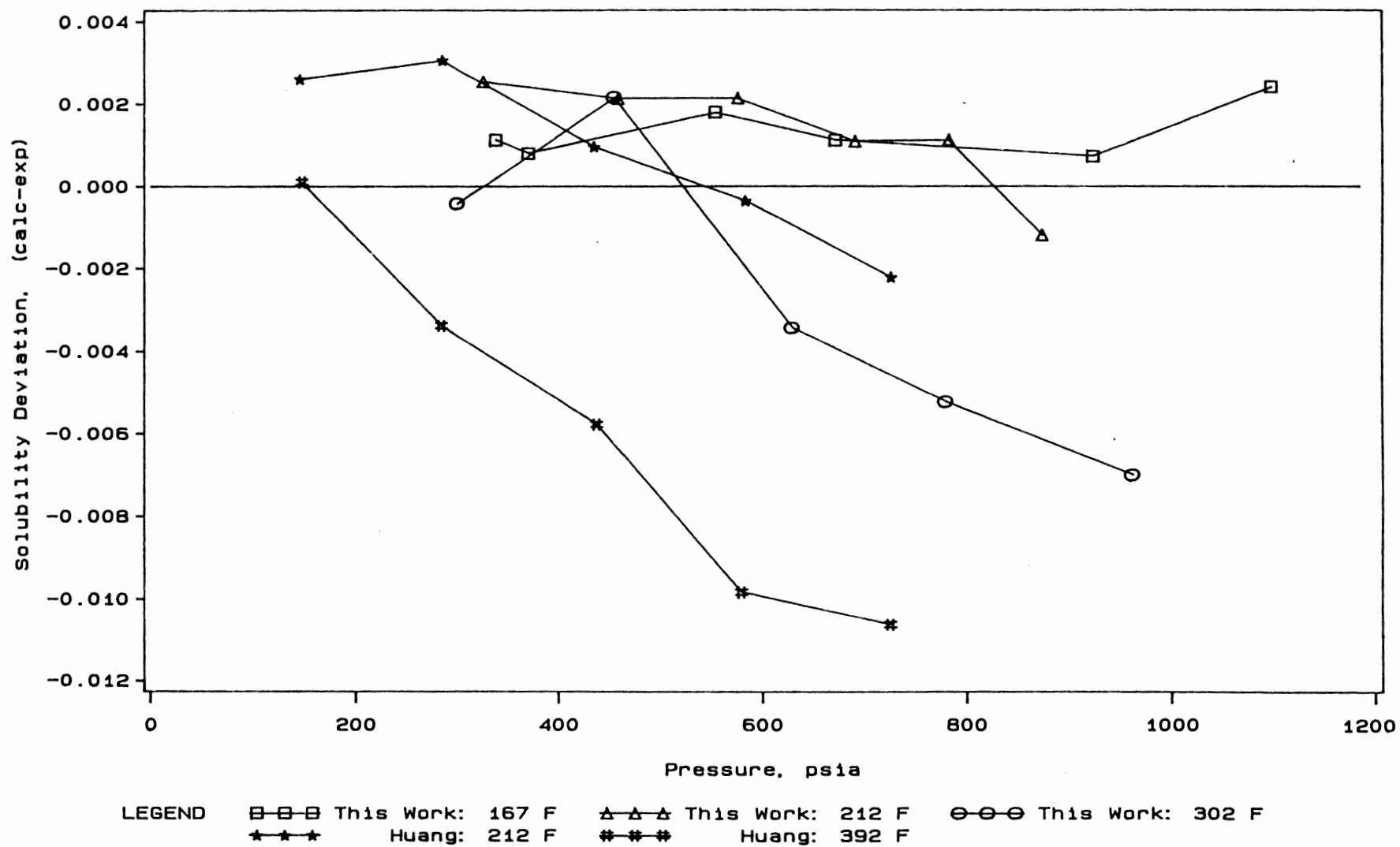


Figure 24. Comparison of Carbon Monoxide Solubilities in n-Octacosane Using Lumped Cij and Dij

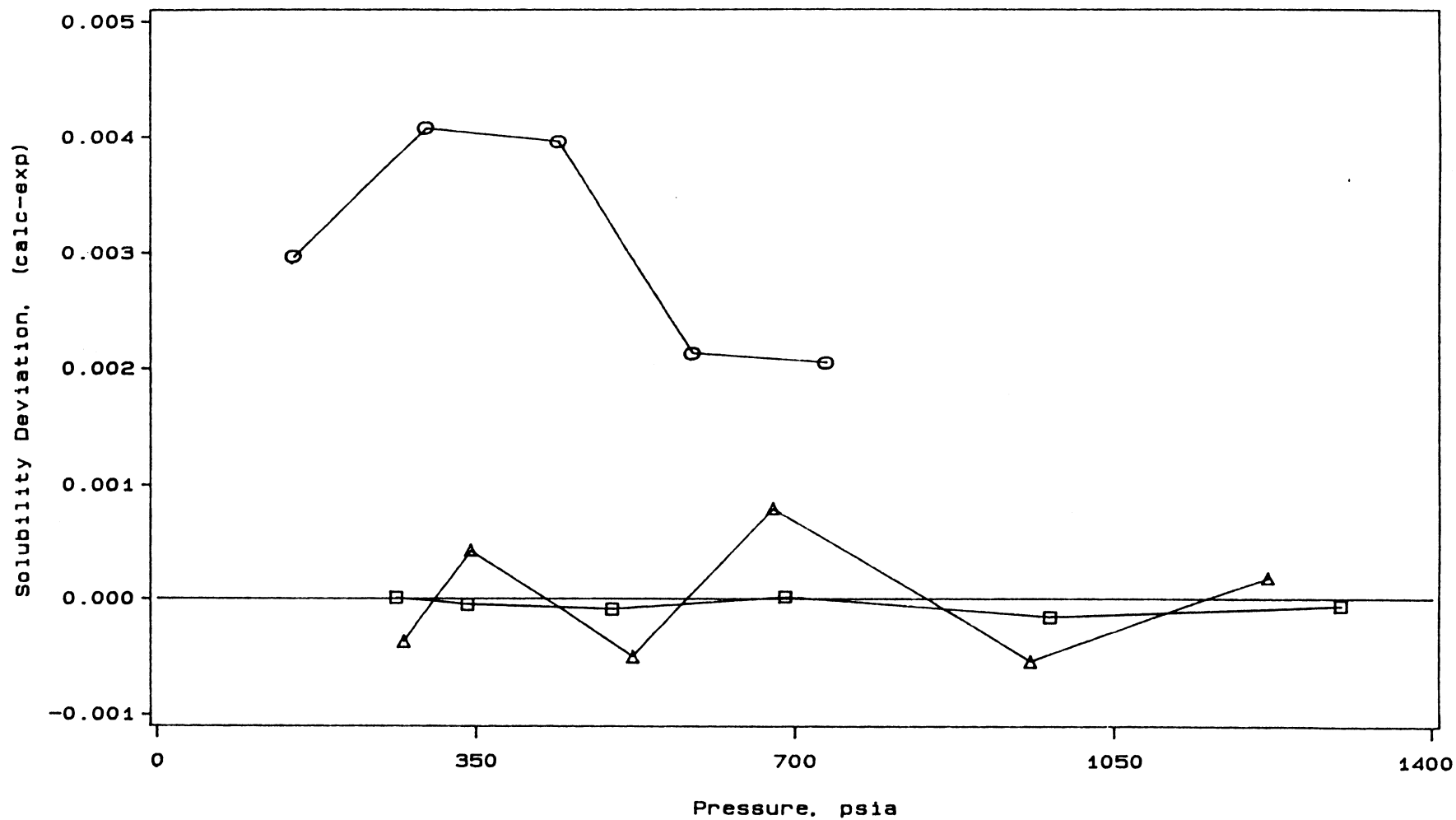


Figure 25. Comparison of Carbon Monoxide Solubilities in n-Hexatriacontane

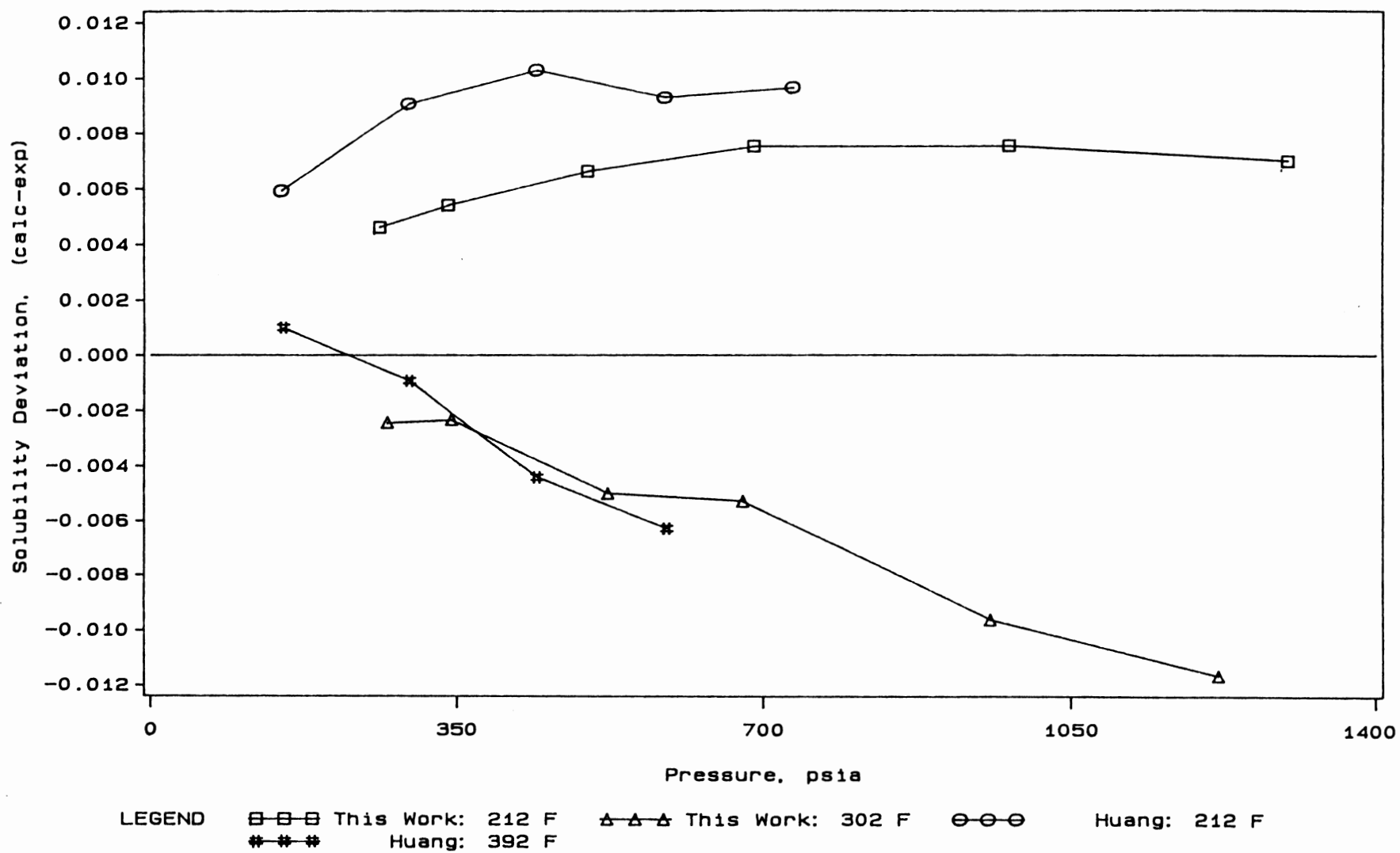


Figure 26. Comparison of Carbon Monoxide Solubilities in n-Hexatriacontane Using Lumped Cij and Dij

deviations  $< 0.004$ ) are obtained for the 212 °F isotherm between this work and that of Huang, et al. for all three systems. Higher bubble point pressures are obtained by Huang for the n-C<sub>28</sub> and n-C<sub>36</sub> systems at 212 °F. To predict the solubility reported by Huang, et al. at 392 °F, interaction parameters from our data lumped over the complete temperature range were used. Figures 22, 24, and 26 show the comparisons for the three systems n-C<sub>20</sub>, n-C<sub>28</sub>, and n-C<sub>36</sub>, respectively, using lumped parameters. While the lumped parameters fit the 212 °F isotherm of Huang, et al. excellently for the two systems n-C<sub>20</sub> and n-C<sub>28</sub> (maximum solubility deviation  $< 0.002$ ), significant deviations (maximum solubility deviation of 0.011) are observed for all three systems at 392 °F. The large deviation in solubility reflects the fact that the binary interaction parameters for these systems are temperature dependent.

#### Effect of Carbon Number on Soave Interaction Parameters

An attempt has been made to generalize the effect of carbon number on the interaction parameters,  $C_{ij}$  and  $D_{ij}$ , using the SRK EOS for the experimental work of this study. Figure 27 shows the variation in the values of the binary interaction parameters,  $C_{ij}$  and  $D_{ij}$ , as a function of the carbon number for the 212 °F isotherm. No clear relationship governing the effect of carbon number on binary interaction parameters can be inferred. The vertical lines

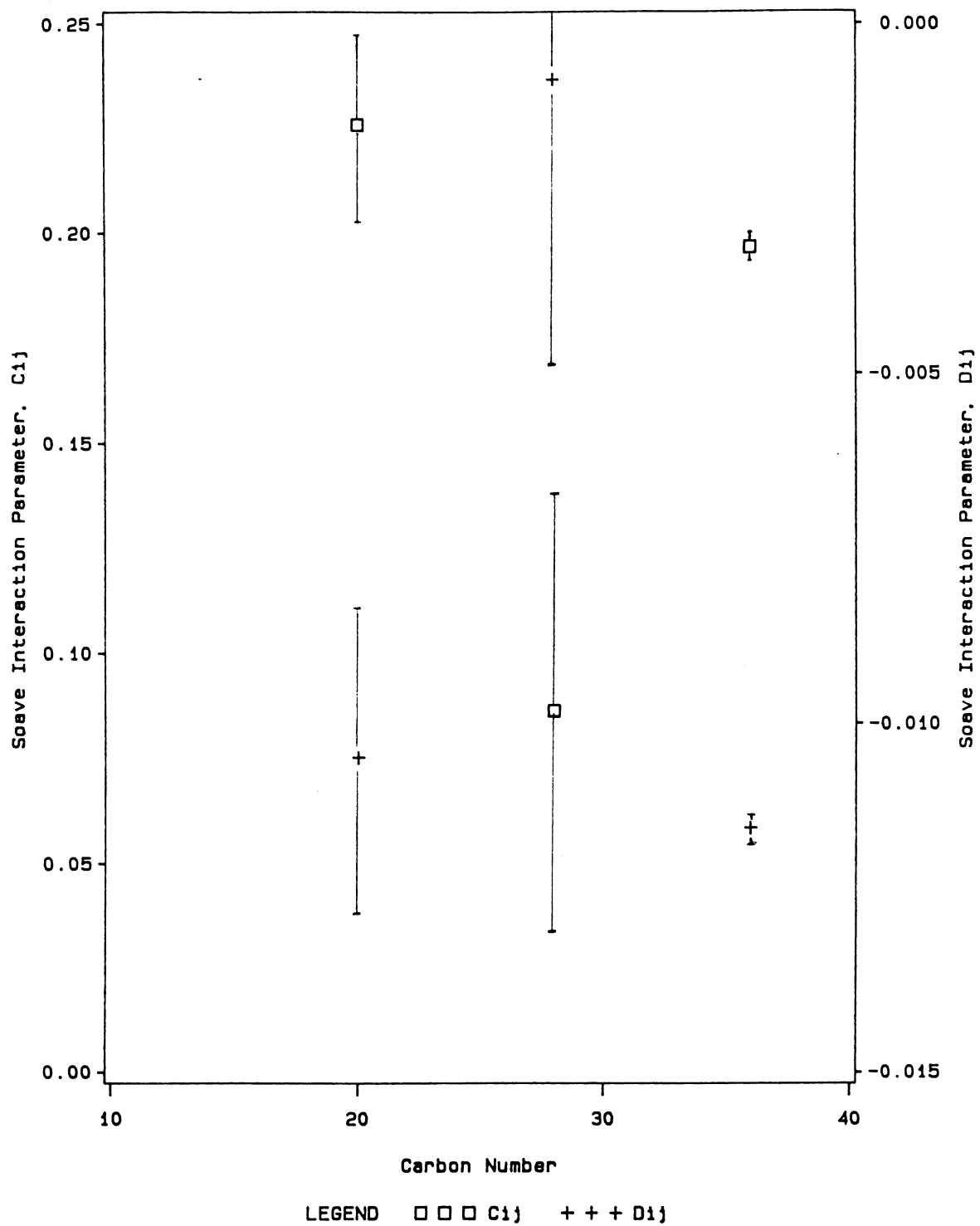


Figure 27. Soave Interaction Parameters  $C_{ij}$  and  $D_{ij}$  for Carbon Monoxide + n-Paraffins at 212 F

in the figure indicate the standard errors (obtained by regression) associated with the value of the interaction parameters. The error bars for the n-C<sub>20</sub> and n-C<sub>28</sub> systems are significant while the interaction parameters for the n-C<sub>36</sub> system show a tight fit. The very high error bars associated with both the interaction parameters,  $C_{ij}$  and  $D_{ij}$ , for the n-C<sub>28</sub> system indicate the possibility of a high degree of correlation between them. This was confirmed by looking at the resultant correlation coefficient (-0.99) from the parameter regression.

To alleviate this problem of parameter correlation, the interaction parameters were then assumed to be linearly dependent on the carbon number ( $C_{ij} = C_1 + C_2 \cdot \text{CN}$ ,  $D_{ij} = D_1 + D_2 \cdot \text{CN}$ ). For  $C_{ij}$ , the slope (constant  $C_2$ ) was kept the same as would be obtained using a linear relation by connecting the  $C_{ij}$  values of n-C<sub>20</sub> and n-C<sub>36</sub> in Figure 27. Thus, only the leading term,  $C_1$ , was regressed. For the second interaction parameter,  $D_{ij}$ , both the constants were found by regression. The plot of the interaction parameters as a function of carbon number using generalized values is shown in Figure 28 for one isotherm. The overall RMS errors in mole fraction using generalized parameters was found to be 0.0009 in mole fraction (as compared to 0.0003 using interaction parameters regressed from experimental data and shown in Figure 27).

Figures 27 and 28 clearly indicate that while a significant difference in the values of the two interaction

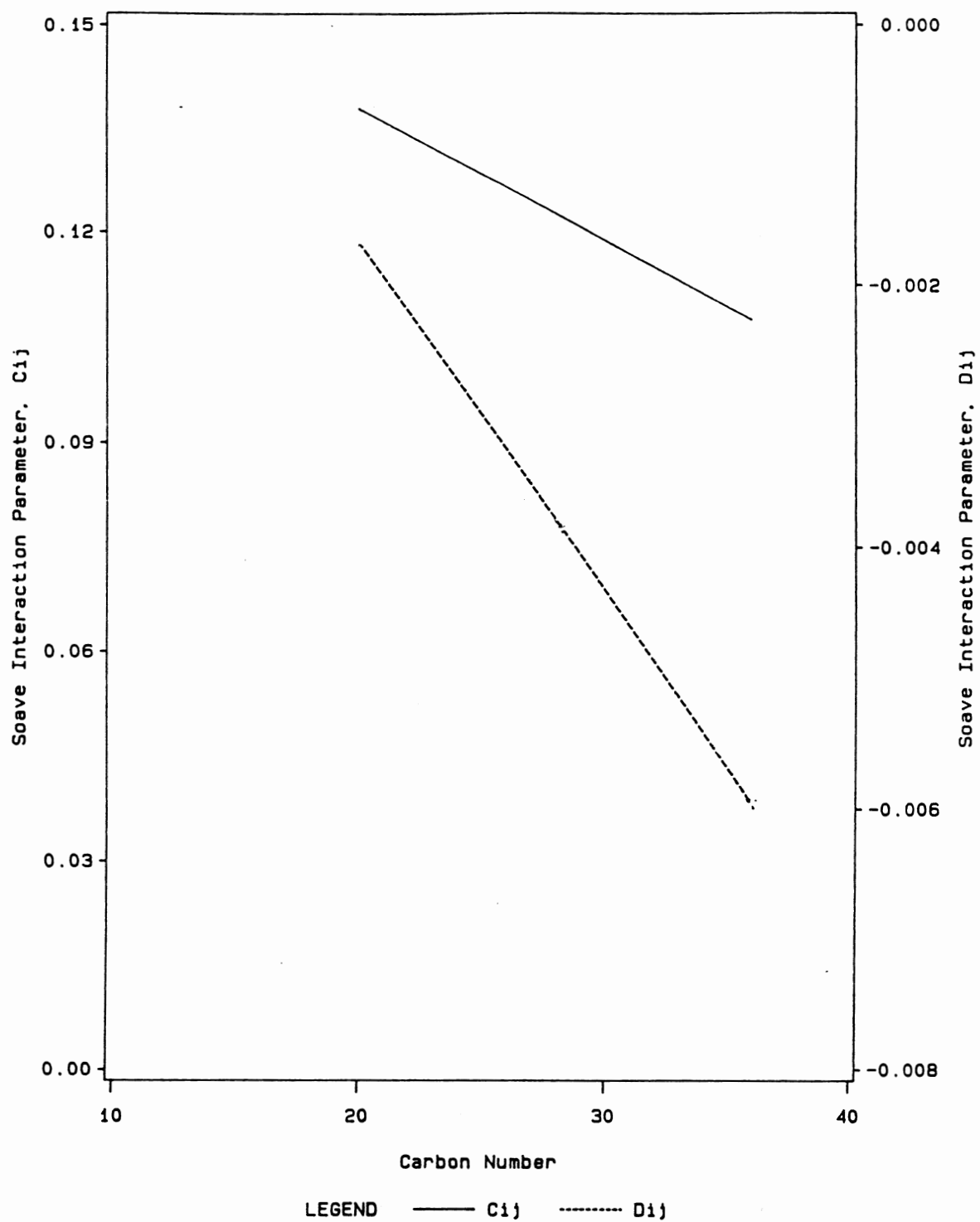


Figure 28. Generalized Soave Interaction Parameters  $C_{ij}$  and  $D_{ij}$  for Carbon Monoxide + n-Paraffins at 212 F

parameters exist, the quality of the fit is not greatly compromised. To explain this, values of  $C_{ij}$  were optimized for various fixed values of  $D_{ij}$  for the n-C<sub>28</sub> system at 212 °F. The plot of the interaction parameters along with the RMS errors in mole fraction is shown in Figure 29. Although the figure does indicate a minimum RMSE (at  $D_{ij} = 0$  and  $C_{ij} = 0.074$ ), it is evident that use of any value of  $D_{ij}$  from -0.015 to 0.010 with the corresponding optimized value of  $C_{ij}$  would lead to a RMS error no larger than 0.0009 in mole fraction. Since this value is about the same as the experimental uncertainty in mole fraction, it follows that a very high degree of correlation exists between the two interaction parameters.

To get a better understanding of the behavior of interaction parameters, the effect of carbon number on only one interaction parameter,  $C_{ij}$ , obtained by regressing the experimental data of this work, was studied at 212 °F by fixing  $D_{ij} = 0$ . The results are shown in Figure 30. A decrease in the value of  $C_{ij}$  with carbon number is indicated and the trend seems to be fairly linear.

#### Effect of Temperature on Soave Interaction Parameters

The effect of temperature on binary interaction parameters was studied for the heavy n-paraffin systems using experimental data of this work. The results are shown in Figures 31 and 32. Figure 31 indicates that the

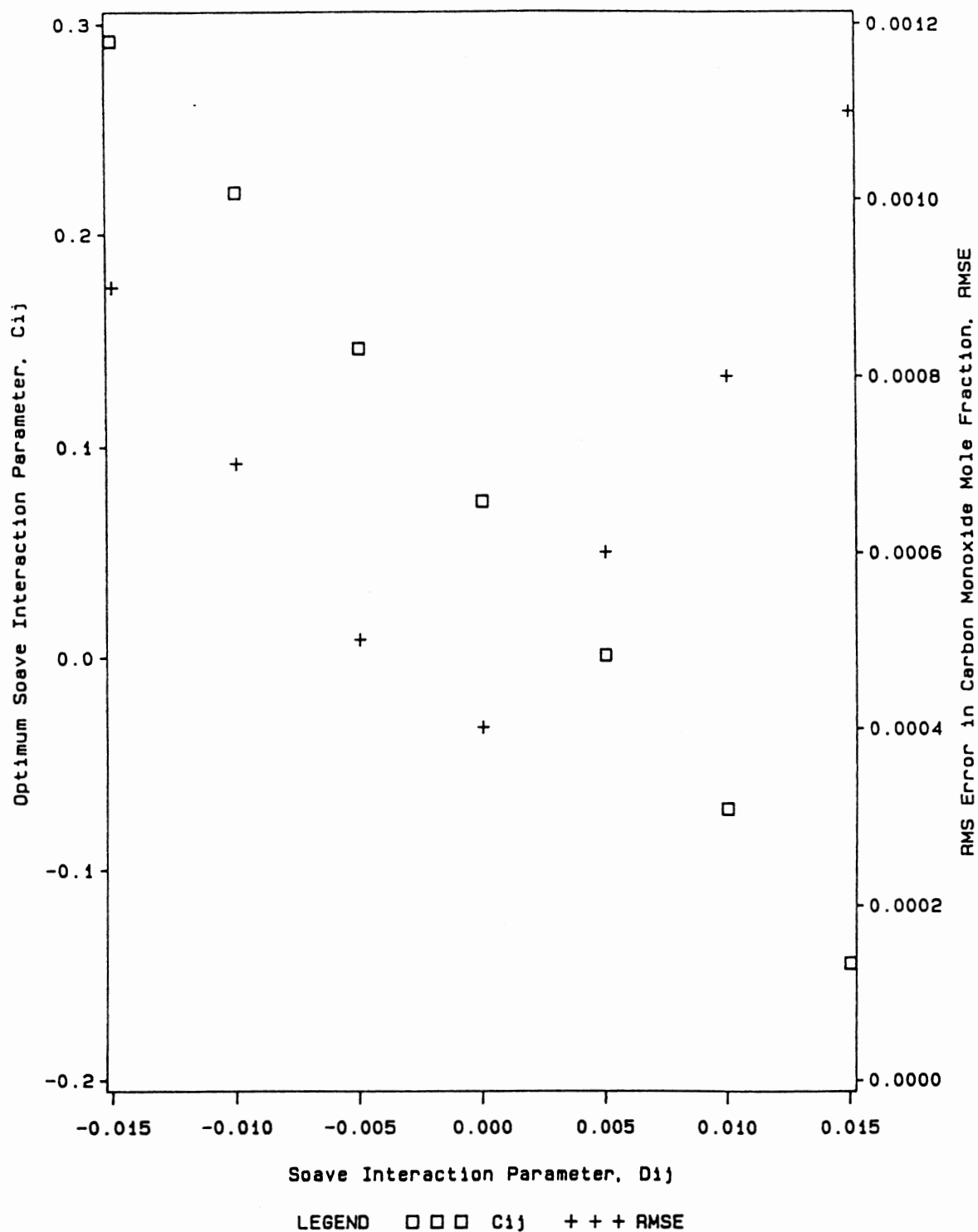


Figure 29. Soave Interaction parameters  $C_{ij}$  and  $D_{ij}$  and Corresponding RMS Errors for Carbon Monoxide + *n*-Octacosane at 212 F

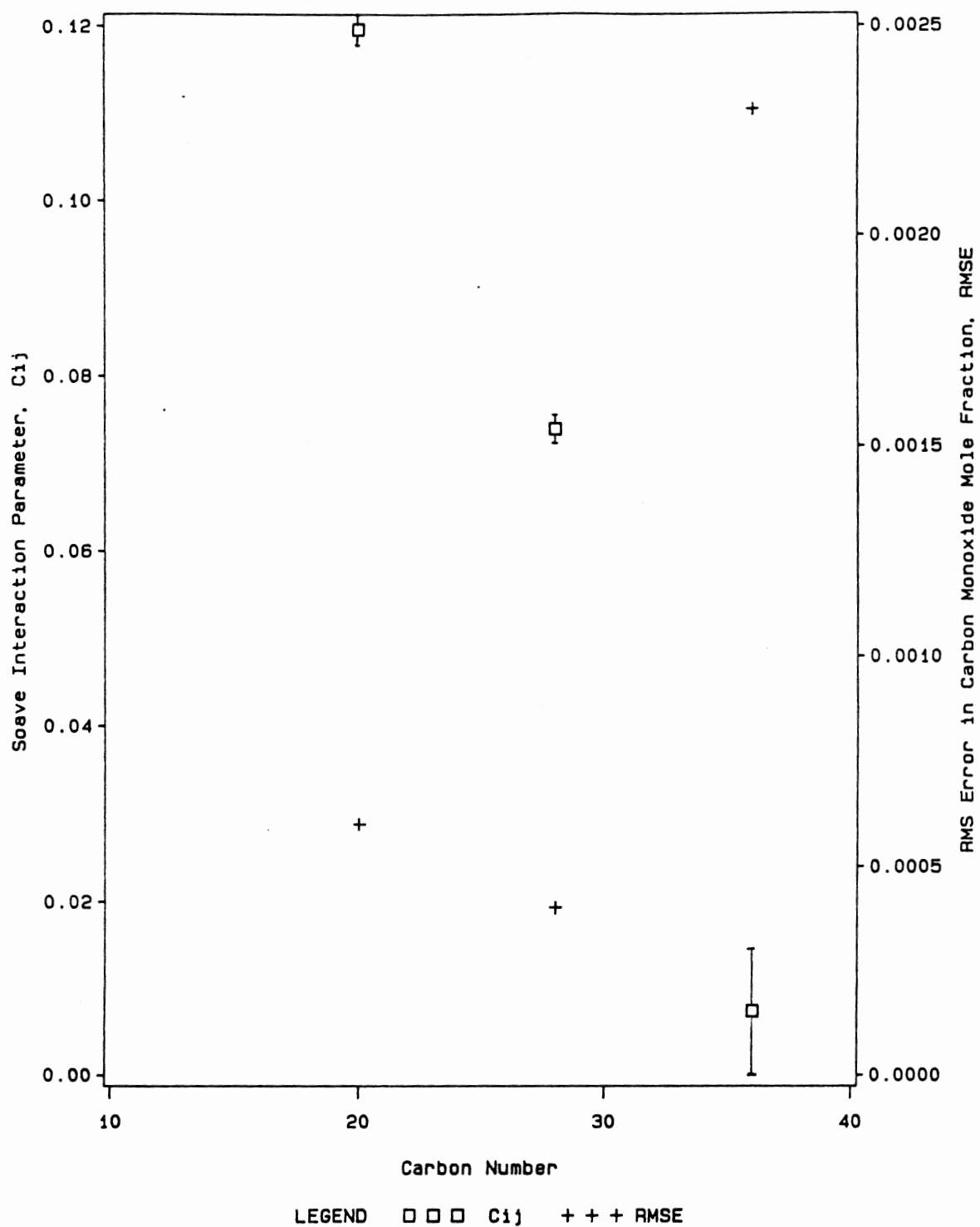


Figure 30. Soave Interaction Parameter,  $C_{ij}$ , and Corresponding RMS Errors for Carbon Monoxide + n-Paraffins at 212 F

temperature dependence on the interaction parameters is most significant for the n-C<sub>28</sub> system. Although, the three systems belong to the same homologous series, the trend exhibited in the variation of the interaction parameters with temperature is widely different. The high degree of correlation between the interaction parameters for the n-C<sub>28</sub> system, as explained in an earlier section, could be the reason for this behavior.

When only one interaction parameter,  $C_{ij}$ , is used, the results are similar for all three systems as shown in Figure 32. The systems show a definite trend with the  $C_{ij}$  values decreasing with temperature.

#### Predictions Using EOS-Specific Critical Properties

Since experimental data for critical properties are not available for n-paraffins with carbon numbers greater than 17, empirical correlations must be used to estimate them. The critical properties used in Table XVII for n-paraffins were developed by extrapolation of the lower paraffin data using the Asymptotic Behavior Correlation [26]. Gasem, et al. [61] found that use of critical properties and acentric factors specific to a given EOS lead to simpler expressions for generalization of the interaction parameters and also yield accurate agreement with pure fluid property correlations. The critical properties of n-paraffins specific to the SRK EOS are given in Appendix C

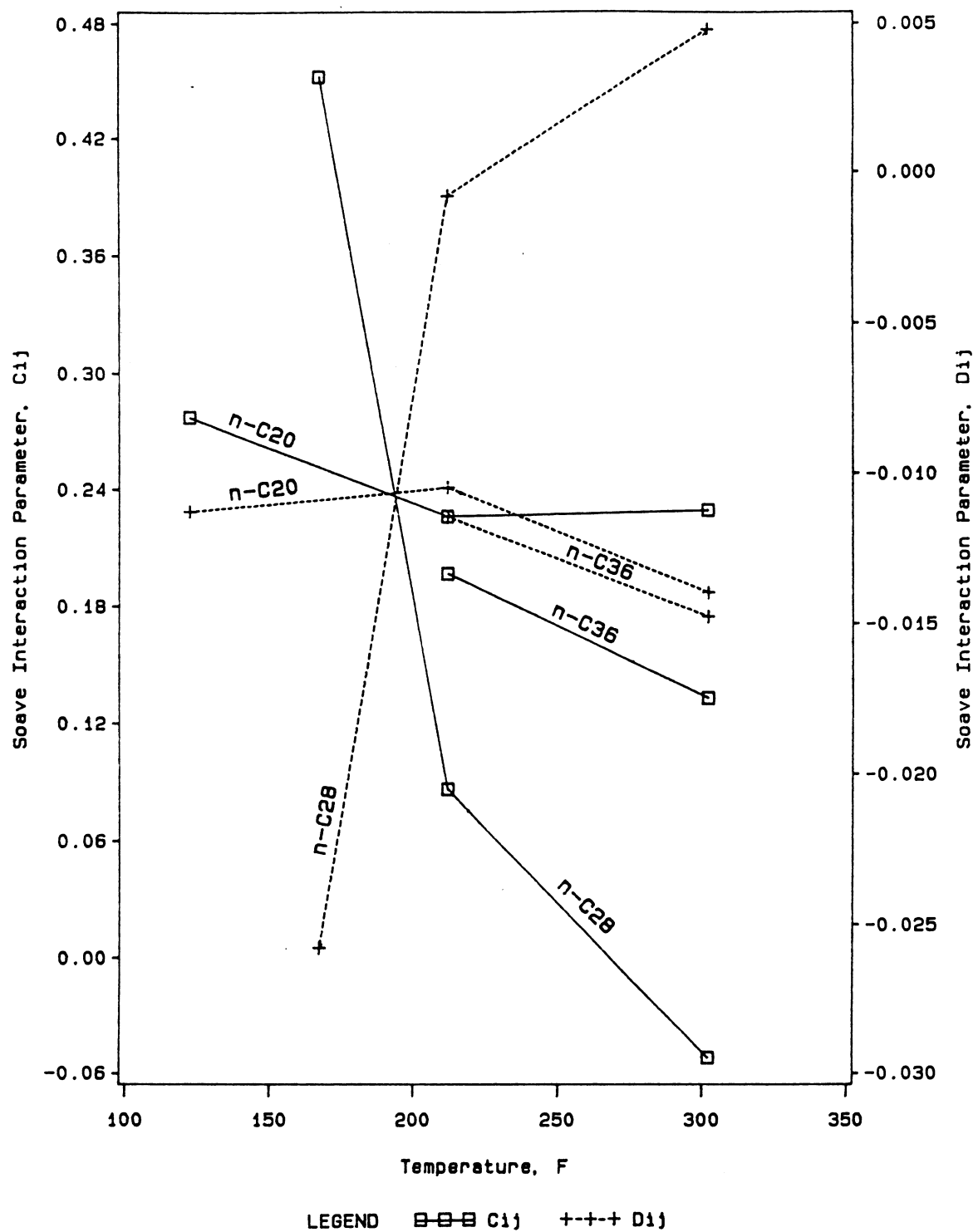


Figure 31. Soave Interaction Parameters,  $C_{ij}$  and  $D_{ij}$ , for Carbon Monoxide + n-Paraffins

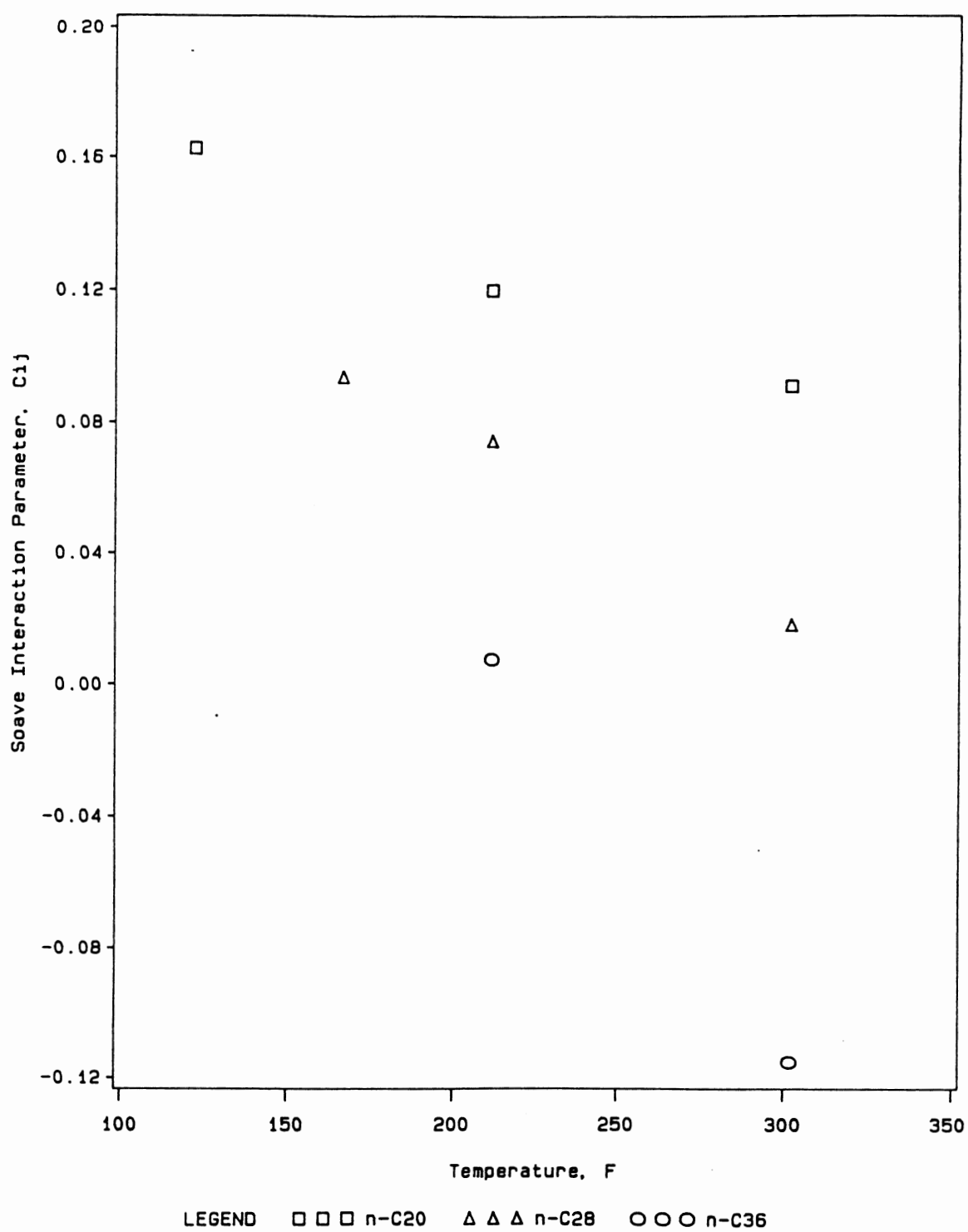


Figure 32. Soave Interaction Parameter,  $C_{ij}$ , for Carbon Monoxide + n-Paraffins

and the SRK representation of the solubility of CO in n-paraffins used in this study is shown in Appendix D.

The results of Appendix D indicate a significant improvement (RMSE in mole fraction) compared to the earlier results (shown in Tables XVIII-XX) for all three systems studied when either one or two interaction parameters are used over the complete temperature range. The results are comparable to the earlier ones when interaction parameters specific to each isotherm are used for the n-C<sub>20</sub> and n-C<sub>28</sub> systems. For the n-C<sub>36</sub> system, however, dramatic improvements in the solubility predictions are obtained when a single interaction parameter either specific to each isotherm or lumped over the whole temperature range is used. The results in Appendix D also indicate that only one interaction parameter,  $C_{ij}$ , with a constant value of 0.45, can be used over the complete temperature range for CO + n-C<sub>36</sub>.

## CHAPTER VIII

### CORRELATION OF CARBON MONOXIDE SOLUBILITIES IN NORMAL PARAFFINS

This chapter presents an evaluation of the ability of the SRK equation of state to represent the phase behavior of binary mixtures of CO + n-paraffins. Binary mixture data for CO + heavy n-paraffins ( $C_{20}$ ,  $C_{28}$  and  $C_{36}$ ) acquired in this work, along with the data from the literature for these systems [6] and for n-octane [63], were employed for the study. The data for carbon monoxide solubilities in propane, although available at 323.2 K [64], were not used since the existing data exhibited significantly larger deviations in comparison with the available data (twice the RMSE of the other data using SRK EOS). The database used in the evaluation is presented in Table XXI. The data considered cover a temperature range from 323.2 K to 473.2 K (122 °F to 392 °F) and pressures to 9.1 MPa (1300 psia). The solvents included vary in carbon number from  $C_8$  to  $C_{36}$ . All data were used as isothermal p-x measurements, i.e., bubble point pressure as a function of solute liquid mole fraction.

TABLE XXI  
EXPERIMENTAL DATA FOR CARBON MONOXIDE +  
N-PARAFFINS USED IN THIS STUDY

Paraffin Carbon Number	Temperature Range, °F	Carbon Monoxide Mole Fraction	Ref.	Number of Points
8	190	0.005 - 0.043	64	5
20	122 - 392	0.023 - 0.161	This Work, 6	30
28	167 - 392	0.028 - 0.149	This Work, 6	27
36	212 - 392	0.026 - 0.210	This Work, 6	22

## Model Evaluation

Eight specific model cases with systematic progression in complexity were examined in this study. Optimum binary interaction parameters were obtained for each of the cases, varying from the use of a single interaction parameter,  $C_{ij}$ , for the whole data set to the use of two interaction parameters,  $C_{ij}$  and  $D_{ij}$ , for each isotherm in each system. Table XXII lists the cases studied. The critical properties for the pure components along with their sources are given in Table XXIII.

Table XXIV presents a summary of the results for the cases described above. The overall model statistics are given for the bubble point pressure and for the RMSE in the predicted mole fraction of solute (evaluated for each case by setting the interaction parameters at their optimum values). The optimum interaction parameters,  $C_{ij}$  and  $D_{ij}$ , using the SRK equation for the various cases outlined in Table XXII are presented in Table XXV.

The "raw ability" of the SRK EOS was first assessed (Case 1) by setting  $C_{ij} = D_{ij} = 0$ . The error in bubble point pressure is substantial (RMSE= 5.4 bar and %AAD= 10.0) when the SRK equation is used without any interaction parameters. When one interaction parameter,  $C_{ij}$ , is used for all the binary systems (Case 2) there is a 20% improvement in the calculated errors. The improvement is significant when two interaction parameters,  $C_{ij}$  and  $D_{ij}$ ,

TABLE XXII  
SPECIFIC CASES USED IN EOS MODEL  
EVALUATION

Case	Description
1 $C_{ij} = 0$ $D_{ij} = 0$	The 'raw' ability of the EOS, using one fluid mixing rules with no interaction parameters; permits prediction from pure component data.
2 $C_{ij}$	A single value of $C_{ij}$ is used for application to all binary systems.
3 $C_{ij}, D_{ij}$	Two interaction parameters are used for application to all binary systems.
4 $C_{ij}(\text{CN})$	A separate value of $C_{ij}$ is determined for each binary system, independent of temperature. Most commonly used EOS representation.
5 $C_{ij}(\text{CN})$ $D_{ij}(\text{CN})$	Two interaction parameters are used for each binary system, independent of temperature.
6 $C_{ij}(\text{CN}, T)$	A separate value of $C_{ij}$ is determined for each system at each temperature.
7 $C_{ij}(\text{CN}, T)$ $D_{ij}(\text{CN}, T)$	Two interaction parameters are determined for each system at each temperature.
8 $C_{ij}(\text{CN}, T)$ $D_{ij} = -0.016$	$D_{ij}$ is kept fixed for all systems at $-0.016$ , while $C_{ij}$ varies with temperature and carbon number.

TABLE XXIII  
CRITICAL PROPERTIES AND ACENTRIC FACTORS USED  
IN MODEL EVALUATION AND GENERALIZATION

Component	Pressure (MPa)	Temperature (K)	Acentric Factor	Reference
Carbon Monoxide	3.494	132.9	0.0491	59, 60
n-Octane	2.531	568.8	0.3995	58
n-Eicosane	1.117	770.5	0.8738	26
n-Octacosane	0.826	845.4	1.1073	26
n-Hexatria- contane	0.691	901.1	1.2847	26

are used for the whole data set (RMSE= 2.60 and %AAD= 5.5). The dramatic improvement in the predictions clearly illustrate the need for using binary interaction parameters to account for unlike molecular interactions. Case 4 represents the use of a single interaction parameter,  $C_{ij}$ , that is specific to each binary system. Significant improvement over Case 2 is realized, emphasizing the effect of carbon number on  $C_{ij}$ . When two interaction parameters are used for each system (Case 5), the results in the model overall statistics are only marginally different. Thus the use of a single interaction parameter,  $C_{ij}$ , for each system seems to be adequate for describing carbon monoxide solubilities in n-paraffins with reasonable accuracy.

Cases 6 and 7 describe the effect of temperature and carbon number on the interaction parameters. Dramatic improvement is seen with the use of a single interaction parameter,  $C_{ij}$ , specific to each isotherm of a given system (RMS error of 0.74 bar in bubble point pressure and 0.002 in mole fraction). The results show further improvement when a second interaction parameter is also used specific to each isotherm and system. The errors are within the experimental uncertainty in this case. These results indicate the heavy temperature dependence of the interaction parameters for the n-paraffin systems. Although the level of complexity may be excessive for routine applications, the precision offered is excellent.

TABLE XXIV  
RESULTS OF MODEL EVALUATION FOR CARBON MONOXIDE  
+ N-PARAFFINS USING THE SRK EOS

Case Number	Bubble RMSE bar	Point BIAS bar	Pressure AAD bar	%AAD	NRMSE <sup>a</sup>	RMSE in $x_{CO}$
1	5.54	-2.39	4.06	10.0	11.1	0.0115
2	4.55	0.34	3.17	8.0	9.1	0.0090
3	2.60	0.00	2.06	5.5	5.2	0.0050
4	2.60	0.45	1.96	4.9	5.2	0.0054
5	2.37	0.07	1.89	5.0	4.7	0.0047
6	0.74	0.06	0.58	2.0	1.5	0.0016
7	0.50	-0.03	0.38	1.3	1.0	0.0010
8	0.73	-0.18	0.53	2.0	1.5	0.0016

a NRMSE =  $RMSE / (RMSE_{\text{case 7}})$  based on bubble point pressure.

TABLE XXV  
SRK EOS OPTIMUM INTERACTION PARAMETERS  
FOR CARBON MONOXIDE + N-PARAFFINS -  
MODEL EVALUATION

Component/ T, °F	Case Number (See Table XXII)						
	4	5		6	7		8
	$C_{ij}$	$C_{ij}$	$D_{ij}$	$C_{ij}$	$C_{ij}$	$D_{ij}$	$C_{ij}$
n-C <sub>8</sub> 374	0.177	0.220	-0.009	0.177	0.220	-0.009	0.250
n-C <sub>20</sub> 122 212 302 392	0.128	0.167	-0.004	0.163 0.128 0.091 0.046	0.279 0.022 0.232 0.566	-0.011 0.010 -0.014 0.055	0.328 0.297 0.252 0.225
n-C <sub>28</sub> 167 212 302 392	0.064	0.585	-0.036	0.094 0.067 0.018 -0.094	0.452 0.086 -0.052 -0.066	-0.026 -0.001 0.005 -0.002	0.316 0.302 0.252 0.154
n-C <sub>36</sub> 212 302 392	-0.042	0.255	-0.017	0.009 -0.115 -0.190	0.099 0.133 -0.324	-0.005 -0.015 0.007	0.278 0.153 0.117
Case 1: $C_{ij} = D_{ij} = 0$ Case 2: $C_{ij} = 0.062$ Case 3: $C_{ij} = 0.371$ ; $D_{ij} = -0.023$ Case 8: $D_{ij} = -0.016$ (fixed)							

Finally, the use of a single  $D_{ij}$  ( $= -0.016$ ) with  $C_{ij}$  varying with temperature and carbon number is shown in Case 8. This case was studied since a high degree of correlation was indicated between the binary interaction parameters during regression. The constant value of  $D_{ij}$  was obtained by regressing the experimental data acquired in this work assuming temperature and carbon number dependence of  $C_{ij}$  and no variation of  $D_{ij}$  with carbon number and temperature. As shown in Table XXIV, results similar to Case 6 are obtained.

#### Generalization of Interaction Parameters

The aim of obtaining experimental measurements on carefully selected binary mixtures is to provide a basis for generalization of the EOS interaction parameters. By generalizing the parameters it is hoped that reliable predictions can be obtained on systems in the same homologous series by interpolation (or even extrapolation in some cases) of the EOS parameters and thus avoid time consuming experimentation.

Three cases of parameter generalization as detailed in Table XXVI were examined using the SRK EOS. The same database documented in Table XXI was used for this purpose. Table XXVII presents a summary of results obtained and the optimum interaction parameters for the various cases are given in Table XXVIII.

Case 1 is the same as that used for model evaluation

TABLE XXVI  
SPECIFIC CASES FOR GENERALIZATION OF  
INTERACTION PARAMETERS USING SRK EOS

Case	Description
1 $C_{ij} = 0$ $D_{ij} = 0$	Same as Case 1, Table XXIII
2 $C_{ij} = f(\text{CN})$	<p><math>C_{ij}</math> is correlated as a function of carbon number using a linear relation of the form</p> $C_{ij} = C_1 + C_2 * \text{CN}$ <p>The values of <math>C_1</math> and <math>C_2</math> are optimized.</p>
3 $C_{ij} = f(\text{CN})$ $D_{ij} = f(\text{CN})$	<p><math>C_{ij}</math> and <math>D_{ij}</math> correlated in terms of carbon number using linear relations as given above.</p>
4 $C_{ij} = f(\text{CN}, T)$ $D_{ij}$	<p><math>C_{ij}</math> correlated as a function of both carbon number and temperature using the relation</p> $C_{ij} = (C_1 + C_2 * \text{CN}) * (1 + C_3 * (T - T_{\text{ref}}))$ $D_{ij} = D_1$ <p>The values of <math>C_1</math>, <math>C_2</math>, <math>C_3</math> and <math>D_1</math> are optimized</p>

(Case 1, Table XXIII) and represents the raw ability of the EOS. Case 2 represents a generalization procedure for  $C_{ij}$ , in terms of the carbon number only. The leading term in the simple linear relation used is the value of  $C_{ij}$  that would be obtained by treating the parameters independent of temperature and carbon number (Case 2, Table XXIII). As indicated by the results of this case, reasonable predictions (RMSE of 2.66 bar in bubble point pressure and %AAD of 5.1) are obtained using a linear correlation for  $C_{ij}(\text{CN})$ . The addition of a second interaction parameter,  $D_{ij}$ , using a linear correlation of  $D_{ij}$  with carbon number (Case 3) gives only a marginal improvement over Case 2 (RMSE of 2.43 in bubble point pressure and %AAD of 5.0). These results support the earlier conclusion that a single interaction parameter for each binary system is enough to represent carbon monoxide solubilities in n-paraffins.

Finally, Case 4, represents a generalization procedure, where a single value of  $D_{ij}$  is obtained for all the systems while the  $C_{ij}$  varies with carbon number and temperature. It is interesting to note that the value of  $D_{ij}$  ( $= -0.017$ ), obtained by regressing the leading term is almost the same that was used in Case 8 of model evaluation. Significant improvement is obtained in this case (RMSE= 1.46 bar and %AAD= 3.3). The results clearly demonstrate the sensitivity of EOS predictions to the interaction parameter values used and the temperature dependence of these parameters for the carbon monoxide - n-paraffin systems.

TABLE XXVII  
RESULTS OF MODEL GENERALIZATION USING SRK EOS  
FOR CARBON MONOXIDE + N-PARAFFINS

Case Number	Bubble RMSE bar	Point BIAS bar	Pressure AAD bar	%AAD	RMSE in $x_{CO}$
1	5.54	-2.39	4.06	10.0	0.0115
2	2.66	0.45	2.03	5.1	0.0055
3	2.43	0.10	1.91	5.0	0.0048
4	1.46	-0.23	1.10	3.3	0.0030

TABLE XXVIII

SRK EOS OPTIMUM INTERACTION PARAMETERS  
FOR CARBON MONOXIDE + N-PARAFFINS -  
MODEL GENERALIZATION

Component/ T, °F	Case Number (See Table XXVI)				
	2	3		4	
	$C_{ij}$	$C_{ij}$	$D_{ij}$	$C_{ij}$	$D_{ij}$
n-C <sub>8</sub>	0.255	0.086	0.005		
374				0.221	-0.017
n-C <sub>20</sub>	0.132	0.202	-0.007		
122				0.351	-0.017
212				0.301	-0.017
302				0.250	-0.017
392				0.199	-0.017
n-C <sub>28</sub>	0.050	0.279	-0.015		
167				0.314	-0.017
212				0.290	-0.017
302				0.241	-0.017
392				0.192	-0.017
n-C <sub>36</sub>	-0.033	0.356	-0.023		
212				0.279	-0.017
302				0.232	-0.017
392				0.185	-0.017
Case 1: $C_{ij} = D_{ij} = 0$					

Although simple generalization schemes (interaction parameters varying linearly with carbon number) do produce reasonable results (Table XXVII), the values of the interaction parameters vary widely as one goes from  $n\text{-C}_8$  to  $n\text{-C}_{36}$ . Moreover, the quality of representation deteriorates for the larger carbon number. This indicates that caution should be exercised when extrapolating using such simple generalization schemes.

The significant dependence of the interaction parameters of  $\text{CO} + n\text{-paraffin}$  systems on carbon number and temperature combined with the accuracy associated with extrapolation, suggests the value of evaluating alternate equations of state which are theoretically more rigorous. Previous studies [65] involving ethane +  $n\text{-paraffin}$  systems suggest that the simplified-perturbed-hard-chain-theory (SPHCT) EOS offers clear advantages in this regard. Simple generalization schemes using temperature independent interaction parameters may be expected using the SPHCT EOS.

## CHAPTER IX

### CONCLUSIONS AND RECOMMENDATIONS

This work has dealt with measuring the solubility of methane and carbon monoxide in selected hydrocarbons. From the experimental data, binary interaction parameters have been determined for all systems studied. The ability of the cubic equations of state to represent data has been evaluated and simple generalization schemes proposed for a priori predictions of interaction parameters. In general, solubilities obtained are within the experimental uncertainties for all systems studied. The pertinent conclusions and recommendations from the study are detailed below.

#### Conclusions

1. Except for  $\text{CH}_4 + n\text{-C}_{12}$  and  $\text{CO} + n\text{-C}_{36}$ , a single interaction parameter,  $C_{ij}$ , over the complete temperature range is sufficient to represent solubility data using the Soave and Peng-Robinson equations of state with maximum RMS errors of 0.004 in mole fraction.
2. For  $\text{CH}_4 + n\text{-C}_{12}$ , a single pair of interaction parameters,  $C_{ij}$  and  $D_{ij}$ , over the complete temperature range is needed to describe the solubility data with RMS errors of

0.003 in mole fraction.

3. For CO + n-C<sub>36</sub>, the RMS errors in mole fraction, are within 0.003 using one interaction parameter,  $C_{ij}$ , fitted to each isotherm.

4. For carbon monoxide in n-paraffins, the temperature dependence of the interaction parameters is significant, especially for the larger solvents.

5. At a given temperature, the solubility of carbon monoxide in n-paraffins is substantially lower than the solubility of methane or carbon dioxide.

6. While the solubility of methane in n-paraffins decreases with increase in temperature, an opposite trend is observed for carbon monoxide solubilities.

7. The solubilities calculated using the cubic equations of state are very sensitive to the input parameters (critical properties and acentric factors) used.

#### Recommendations

1. Further studies are needed on carbon monoxide solubilities in n-paraffins, aromatics and naphthenes.

2. Modifications in cubic EOS mixing rules are needed to improve the representation of solubility data for systems involving carbon monoxide.

3. Development and testing of an equation of state based on the perturbed-hard-chain-theory is recommended to explore its potential for providing more accurate representation of equilibrium phase compositions.

## BIBLIOGRAPHY

1. Wichterle, I.; Linek, J.; Hala, E., Vapor Liquid Equilibrium Data Bibliography, Elsevier, New York, (1973, 1976, 1979, 1982, 1985).
2. Che, S., Vapor Liquid Equilibrium Data at High Pressures, Elsevier, Japan (1990).
3. Mohindra, S., M.S. Thesis, University of Oklahoma, Norman, Oklahoma (1987).
4. Fornari, R.E.; Alessi, P.; Kikic, I., Fluid Phase Equilibria, 57, 1-33 (1990).
5. Hala, E.; Pick, J.; Fried, V.; Vilim, O., Vapor Liquid Equilibrium, Pergamon Press (1967).
6. Huang, S.H.; Lin, H-M.; Tsai, F-N.; Chao, K-C., Ind. Eng. Chem. Res., 27, 162-169 (1988).
7. Eubank, P.T.; Hall, K.R.; Holste, J.C., 2nd Int. Conf. on Phase Equilibria and Fluid Properties in Chemical Industry. Knapp, H. and Sandler, S.I. (Editors), DECHEMA, Frankfurt, Part II, 675-687 (1980).
8. Deiters, U.K.; Schneider, G.M., Fluid Phase Equilibria, 29, 145-160 (1986).
9. Richon, D.; Renon, H., Fluid Phase Equilibria, 14, 235-243 (1983).
10. Legret, D.; Richon, D.; Renon, H., AIChE J., 27, 203-207 (1981).
11. Legret, D.; Richon, D.; Renon, H., Ind. Eng. Chem. Fundam., 19, 122-126 (1980).
12. Figuiere, P.; Hom, J.F.; Laugier, S.; Renon, H.; Richon, D.; Szwarc, H., AIChE J., 26, 872-875 (1980).
13. Hong, J.H.; Malone, P.V.; Jett, M.D.; Kobayashi, R., Fluid Phase Equilibria, 38, 83-96 (1987).
14. Charoensombut-amon, T.; Martin, R.J.; Kobayashi, R., Fluid Phase Equilibria, 31, 89-104 (1986).

15. Kragas, T.K.; Pollin, J.; Martin, R.J.; Kobayashi, R., Fluid Phase Equilibria, 16, 205-213 (1984).
16. Nasir, P.; Martin, R.J.; Kobayashi, R., Fluid Phase Equilibria, 5, 279-288 (1980/1981).
17. Mohamed, R. S.; Holder, G.D., Fluid Phase Equilibria, 32, 295-317 (1987).
18. Gilbert, M.L.; Paulaitis, M.E., J. Chem. Eng. Data, 31, 296-298 (1986).
19. Lin, H.M.; Kim, H.; Leet, W.A.; Chao, K-C., Ind. Eng. Chem. Fundam., 24, 260-262 (1985).
20. Huang, S.H.; Lin, H.M.; Chao, K-C., Fluid Phase Equilibria, 36, 141-148 (1987).
21. Huang, S.S.S.; Leu, A.D.; Ng, H.J.; Robinson, D.B., Fluid Phase equilibria, 19, 21-32 (1985).
22. Freitag, N.P.; Robinson, D.B., Fluid Phase Equilibria, 31, 183-201 (1986).
23. Ng, H.J.; Robinson, D.B., Leu, A.D., Fluid Phase Equilibria, 19, 273-286 (1985).
24. Ng, H.J.; Robinson, D.B., Fluid Phase Equilibria, 2, 283-292 (1979).
25. Gasem, K.A.M.; Robinson, Jr., R.L., J. Chem. Eng. Data, 30, 53-56 (1985).
26. Gasem, K.A.M., Ph.D. Dissertation, Oklahoma State University, Stillwater, Oklahoma (1986).
27. Fontalba, F.D.; Richon, D.; Renon, H., Rev. Sci. Instrum., 55(6) (1984).
28. Rousseaux, P.; Richon, D.; Renon, H., Fluid Phase Equilibria, 11, 153-168 (1983).
29. Meskel-Lesavre, M.; Richon, D.; Renon, H., Ind. Eng. Chem. Fundam., 20, 284-289 (1981).
30. Glaser, M.; Peters, C, J.; Van der Kooi, H.J.; Lichtenthaler, R.N., J. Chem. Thermodynamics, 17, 803-815, (1985).
31. Enick, R.; Holder, G.D.; Morsi, B.I., Fluid Phase Equilibria, 22, 209-224 (1985).

32. DiAndreth, J.R.; Ritter, J.M.; Paulaitis, M.E., *Ind. Eng. Chem. Res.*, 26, 337-343 (1987).
33. Kim, C.H.; Vimalchand, P.; Donohue, M.D., *Fluid Phase Equilibria*, 31, 299-311 (1986).
34. Hsu, J.J-C.; Nagarajan, N.; Robinson, Jr., R.L., *J. Chem. Eng. Data*, 30, 485-491 (1985).
35. Elbishlawi, M.; Spencer, J.R., *Ind. Eng. Chem.*, 43, 1811-1815 (1951).
36. Lin, H-M.; Sebastian, H.M.; Simnick, J.J.; Chao, K-C., *J. Chem. Eng. Data*, 24, 146-149 (1979).
37. Schoch, E.P.; Hoffman, A.E.; Mayfield, F.D., *Ind. Eng. Chem.*, 33, 688-691 (1941).
38. Poston, R.S.; McKetta, J.J., *J. Chem. Eng. Data*, 11, 362-363 (1966).
39. Shim, J.; Kohn, J.P.; *J. Chem. Eng. Data*, 7, 3-8 (1962).
40. Sage, B.H.; Webster, D.C.; Lacey, W.N., *Ind. Eng. Chem.*, 28, 1045-1047 (1936).
41. Prausnitz, J.M., "Molecular Thermodynamics of Fluid Phase Equilibria", Prentice-Hall, Englewood Cliffs, New Jersey (1969).
42. Prausnitz, J.M.; Anderson, T.; Grens, E.; Eckert, C.; Hsieh, R.; O'Connell, J.P., "Computer Calculations for Multicomponent Vapor-Liquid and Liquid-Liquid Equilibria", Prentice-Hall, Englewood Cliffs, New Jersey (1980).
43. Van Ness, H.C.; Abbott, M.M., "Classical Thermodynamics of Nonelectrolyte Solutions with Applications to Phase Equilibria", McGraw-Hill, New York (1982).
44. Chao, K-C.; Robinson, Jr., R.L., (Editors), "Equations of State in Engineering and Research", American Chemical Society, Washington, D.C (1986).
45. Chao, K-C.; Robinson, Jr., R.L., (Editors), "Equations of State, Theories and Applications", American Chemical Society, Washington, D.C (1986).
46. Walas, S.M., "Phase Equilibria in Chemical Engineering", Butterworth Publishers, Massachusetts (1985).

47. Soave, G., Chem. Eng. Sci., 27, 1197-1203 (1972).
48. Peng, Y.D.; Robinson, D.B., Ind. Eng. Chem. Fundam., 15, 59-64 (1976).
49. Darwish, N.A., Ph.D. Dissertation, Oklahoma State University, Stillwater, Oklahoma (1991).
50. ASHRAE Handbook 1981 Fundamentals, American Society of Heating, Refrigerating, and Air Conditioning Engineers, Inc., Atlanta, Georgia (1981).
51. Gupta, M.K.; Li, Y-H.; Hulsey, B.J.; Robinson, Jr., R.L., J. Chem. Eng. Data, 27, 55-57 (1982).
52. Anderson, J.M., M.S. Thesis, Oklahoma State University, Stillwater, Oklahoma (1985).
53. Reamer, H.H.; Olds, R.H.; Sage, B.H.; Lacey, W.N., Ind. Eng. Chem., 34, 1526-1531 (1942).
54. Barrick, M.W., M.S. Thesis, Oklahoma State University, Stillwater, Oklahoma (1985).
55. Bufkin, B., M.S. Thesis, Oklahoma State University, Stillwater, Oklahoma (1986).
56. Young, H., "Statistical Treatment of Experimental Data", McGraw Hill, New York (1962).
57. Goodwin, R.D., "The Thermophysical Properties of Methane from 90 to 500 K at Pressures to 700 Bar", NBS Technical Note, 653, 22 (1974).
58. Ely, J.F.; Hanley, H.J.M., NBS Technical Note, 1039 (1981).
59. Goodwin, R.D., J. Phys. Chem. Ref. Data, 14, 849 (1985).
60. Reid, R.C.; Prausnitz, J.M.; Sherwood, T.K., "The Properties of Gases and Liquids", 2nd Edition, McGraw Hill, New York (1977).
61. ESDU Engineering Series Data, Physical Data, Chemical Engineering Sub-series, Volume 3 (1987, 1989, 1990).
62. Gasem, K.A.M.; Ross, C.H.; Robinson, Jr., R.L., "Prediction of Phase Behavior of Ethane + Heavy Normal Paraffins Using Generalized Parameter Soave and Peng-Robinson Equations of State", Paper Presented at the AIChE Annual Meeting, Washington, D.C (1988).

63. Trust, D.B.; Kurata, F., *AIChE J.*, 17, 415-419 (1971).
64. Connolly, J.F.; Kandilac, G.A., *J. Chem. Thermodynamics*, 16, 1129-1139 (1984).
65. Gasem, K.A.M.; Robinson, Jr., R.L., *Fluid Phase Equilibria*, 58, 13-33, (1990).

## APPENDIXES

# APPENDIX A

## DENSITIES OF SOLVENTS USED IN THIS STUDY

Solvent	Temperature (°F)	Density (g/cc)	Reference
Toluene	104	0.8491	61
	150	0.8245	61
	302	0.7364	61
n-Hexane	100	0.6429	61
	160	0.6106	61
	220	0.5756	61
n-Dodecane	122	0.7268	61
	212	0.6895	61
n-Eicosane	122	0.7693	49
	212	0.7347	49
	302	0.7040	49
n-Octacosane	167	0.7716	49
	212	0.7555	49
	302	0.7235	49
n-Hexatria- contane	212	0.7666	49
	302	0.7357	49

# APPENDIX B

## TYPICAL OUTPUT OF PRESSURE CALIBRATION TEST

DATE 1/07/91

TRANSDUCER PRESSURE	DEAD WEIGHT PRESSURE	TRANSDUCER CORRECTION
64.90	49.94	-0.46
94.90	79.90	-0.50
144.90	129.84	-0.56
194.80	179.77	-0.53
244.70	229.71	-0.49
264.70	249.68	-0.52
294.60	279.65	-0.45
394.50	379.52	-0.48
444.30	429.46	-0.34
544.40	529.33	-0.57
644.20	629.21	-0.49
744.10	729.08	-0.52
844.00	829.03	-0.47
943.90	928.83	-0.57
1043.70	1028.70	-0.50
1143.50	1128.58	-0.42
1243.40	1228.42	-0.48
1343.30	1328.30	-0.50
1443.10	1428.17	-0.43
1542.90	1528.04	-0.36

# APPENDIX C

## CRITICAL PROPERTIES AND ACENTRIC FACTORS OF NORMAL PARAFFINS SPECIFIC TO SRK EOS

Component	Pressure (MPa)	Temperature (K)	Acentric Factor	Reference
n-C <sub>20</sub>	1.083	766.6	0.8791	62
n-C <sub>28</sub>	0.670	827.4	1.1617	62
n-C <sub>36</sub>	0.434	864.0	1.4228	62

# APPENDIX D

## SRK EOS REPRESENTATION OF CARBON MONOXIDE SOLUBILITY IN N-PARAFFINS USING EOS SPECIFIC CRITICAL PROPERTIES

Temperature K (°F)	Soave Parameters		Error in Mole Fraction	
	C <sub>ij</sub>	D <sub>ij</sub>	RMS	MAX
-----Carbon Monoxide + n-Eicosane-----				
323.2 (122.0)	0.3039 0.1975	-0.0102	0.0003 0.0006	0.0006 0.0008
373.2 (212.0)	0.2565 0.1641	-0.0087	0.0002 0.0005	0.0004 0.0007
423.2 (302.0)	0.2652 0.1475	-0.0115	0.0002 0.0007	0.0004 0.0010
323.2, 373.2 423.2	0.2032 0.1732	-0.0029	0.0027 0.0028	0.0049 0.0050
-----Carbon Monoxide + n-Octacosane-----				
348.2 (167.0)	0.6142 0.2791	-0.0218	0.0005 0.0021	0.0009 0.0030
373.2 (212.0)	0.1959 0.2894	0.0058	0.0004 0.0005	0.0008 0.0009
423.2 (302.0)	0.0632 0.2976	0.0145	0.0014 0.0017	0.0025 0.0037
348.2, 373.2 423.2	0.3390 0.2850	-0.0034	0.0018 0.0018	0.0048 0.0044

# APPENDIX D (continued)

Temperature K (°F)	Soave Parameters		Error in Mole Fraction	
	C <sub>ij</sub>	D <sub>ij</sub>	RMS	MAX
-----Carbon Monoxide + n-Hexatriacontane-----				
373.2 (212.0)	0.4541	-0.0004	0.0001	0.0001
	0.4458		0.0001	0.0002
423.2 (302.0)	0.4535	-0.0001	0.0005	0.0009
	0.4523		0.0005	0.0009
373.2, 423.2	0.4473	0.0000	0.0005	0.0012
	0.4480		0.0005	0.0012

VITA

SRINIVASA SRIVATSAN

Candidate for the Degree of  
Master of Science

Thesis: BINARY VAPOR-LIQUID PHASE EQUILIBRIUM FOR METHANE  
AND CARBON MONOXIDE IN SELECTED HYDROCARBONS

Major Field: Chemical Engineering

Biographical:

Personal Data: Born in New Delhi, India, August 8,  
1963, the son of Parthasarathy S. and Indira  
Chari. Married to Snehalata Vedaraman on January  
29, 1989.

Education: Graduated from D.T.E.A Senior Secondary  
School, New Delhi, India, in May 1980; recieved  
Bachelor of Engineering (Honors) Degree in  
Chemical Engineering from Birla Institute of  
Technology and Science, Pilani, India, in  
April, 1985. completed requirements for the  
Master of Science degree at Oklahoma State  
University in December, 1991.

Professional Experience: Research Scientist, R & D  
Center, Oil India Limited, Assam, India, 1985 to  
1988. Assistant Engineer, Chemical Division, Tata  
Consulting Engineers, Bombay, India, February,  
1989 to December, 1989. Research Assistant, School  
of Chemical Engineering, Oklahoma State  
University, June, 1990 to August, 1991.  
Member of American Institute of Chemical  
Engineers, Phi Kappa Phi and Omega Chi Epsilon.